

**FEASIBILITY ASSESSMENT OF PALM OIL CLINKER POWDER AS  
SUPPLEMENTARY CEMENTITIOUS MATERIAL**

**MOHAMMAD RAZAUL KARIM**

**FACULTY OF ENGINEERING  
UNIVERSITY OF MALAYA  
KUALA LUMPUR**

**2017**

**FEASIBILITY ASSESSMENT OF PALM OIL CLINKER  
POWDER AS SUPPLEMENTARY CEMENTITIOUS  
MATERIAL**

**MOHAMMAD RAZAUL KARIM**

**THESIS SUBMITTED IN FULFILMENT OF THE  
REQUIREMENTS FOR THE DEGREE OF DOCTOR OF  
PHILOSOPHY**

**FACULTY OF ENGINEERING  
UNIVERSITY OF MALAYA  
KUALA LUMPUR**

**2017**

**UNIVERSITY OF MALAYA**  
**ORIGINAL LITERARY WORK DECLARATION**

Name of Candidate: Mohammad Razaul Karim,

Registration/Matric No: KHA 130069

Name of Degree: Doctor of Philosophy (Ph.D.)

Title of Thesis (“this Work”): **Feasibility Assessment of Palm Oil Clinker Powder as  
Supplementary Cementitious Material**

Field of Study: **Structural Engineering & Materials**

I do solemnly and sincerely declare that:

- (1) I am the sole author/writer of this Work;
- (2) This Work is original;
- (3) Any use of any work in which copyright exists was done by way of fair dealing and for permitted purposes and any excerpt or extract from, or reference to or reproduction of any copyright work has been disclosed expressly and sufficiently and the title of the Work and its authorship have been acknowledged in this Work;
- (4) I do not have any actual knowledge nor do I ought reasonably to know that the making of this work constitutes an infringement of any copyright work;
- (5) I hereby assign all and every right in the copyright to this Work to the University of Malaya (“UM”), who henceforth shall be owner of the copyright in this Work and that any reproduction or use in any form or by any means whatsoever is prohibited without the written consent of UM having been first had and obtained;
- (6) I am fully aware that if in the course of making this Work, I have infringed any copyright whether intentionally or otherwise, I may be subject to legal action or any other action as may be determined by UM.

Candidate’s Signature

Date:

Subscribed and solemnly declared before,

Witness’s Signature

Date:

Name:

Designation:

## ABSTRACT

Palm oil clinker (POC) is a waste material produced from palm oil shells and mesocarp fibres as fuel to run steam turbines in palm oil mills. The current practice is to dump the waste in the open lands or landfills, which leads to environmental pollution. The current research addresses the question of feasibility of palm oil clinker powder (POCP) as a supplementary cementitious material in cement-based applications. The characterization, chemical interaction, i.e. organic carbon effects and pozzolanic activity of POCP and its influences on fresh and hardened properties of cement were determined for confirmation of the technical suitability as supplementary cementitious material. The greenhouse gas (GHG) reduction and natural resource conservation, radiological hazards and heavy metal leaching toxicity were evaluated for confirming the environmental feasibility of POCP. The characterization and chemical interaction of POCP in cement-based applications were carried out using particle size analyzer, scanning electron microscopy (SEM), ICP-MS, X-ray fluorescence (XRF), field emission scanning electron microscopy and energy-dispersive X-ray (FESEM-EDX), thermogravimetric analysis (TGA), total organic carbon (TOC) analyzer, X-ray diffraction (XRD) and Fourier transform infrared spectroscopy (FTIR). The influence of organic carbon free POCP in strength development was observed at 30% replacement of OPC. The pozzolanic activity was determined by using aforementioned apparatus and through the strength activity measurement. The effect of POCP on the fresh and hardened properties of cement has been determined according to ASTM standard methods. The level of radionuclides and radiological hazard indices were measured using a gamma ray spectrophotometer. The leachability of heavy metals was carried out according to EPA standard method. The characterization results of POCP confirmed that POCP is composed of a mixture of inorganic oxides with a portion of organic carbon. The XRD pattern and the crystallinity index of POCP confirmed that quartz was

partially disordered in the matrix of POCP. Moreover, the right condition for removal of organic carbon from POCP was found to be at 580°C for 3 hours, where the compressive strength of mortar was significantly increased. The microstructure properties investigation and strength activity index confirmed that POCP is a pozzolanic material. The water for normal consistency, setting time and soundness was found within ATSM standard limit up to 60% replacement level. The compressive strength was found to decrease. The incorporation of POCP in cement reduces the cost and the emission of carbon dioxide, and saves the natural resources. The radiological hazard indices of POCP were below the standard limit. However, the value of radium equivalent activity of POCP was found significantly lower than fly ash and was comparable with palm oil fuel ash. Heavy metals were present, but did not leach out from the matrix of POCP more than standard limit. It is safer in terms of radiological and heavy metal leaching risk when used as an ingredient of building material. The POCP is feasible to be used as a supplementary cementitious material in cement-based applications which ultimately leads to lower carbon footprint concrete, cleaner environment and convert waste into a resource.

## ABSTRAK

Klinker kelapa sawit (POC) adalah bahan buangan yang dihasilkan akibat daripada menggunakan bom minyak sawit dan gentian mesokarpa sebagai bahan api untuk menjalankan turbin wap di kilang-kilang minyak sawit. Amalan semasa adalah untuk membuang sisa di dalam tanah atau tapak pelupusan laman terbuka, yang membawa kepada pencemaran alam sekitar. Penyelidikan semasa menangani persoalan kemungkinan serbuk klinker kelapa sawit (POCP) sebagai bahan bersimen tambahan dalam aplikasi berasaskan simen. Pencirian dan kimia interaksi iaitu kesan karbon organik dan aktiviti pozzolanic daripada POCP dan pengaruh ke atas sifat-sifat segar dan mengeras simen dicampur ditentukan bagi pengesahan kesesuaian teknikal sebagai bahan bersimen tambahan. Pengurangan gas rumah hijau dan pemuliharaan sumber asli, bahaya radiologi dan ketoksikan larut lesap logam berat telah dinilai untuk mengesahkan kelayakan alam sekitar POCP menjadi menggabungkan dalam aplikasi berasaskan simen. Pencirian dan kimia interaksi POCP telah dijalankan menggunakan saiz zarah penganalisis, imbasan mikroskop elektron (SEM), ICP-MS, X-ray pendarfluor (XRF), bidang pelepasan mikroskop imbasan elektron dan tenaga serakan sinar-X (FESEM - EDX), analisis Termogravimetri (TGA), jumlah karbon organik (TOC) analyzer, X-ray pembelauan (XRD) dan Fourier mengubah teknik spektroskopi inframerah (FTIR). Pengaruh karbon percuma POCP organik untuk pembangunan kekuatan diperhatikan pada penggantian 30% daripada OPC. Aktiviti pozzolanic telah ditentukan dengan menggunakan alat yang dinyatakan di atas dan melalui pengukuran aktiviti kekuatan. Kesan POCP kepada sifat-sifat segar dan mengeras simen dicampur telah dipilih mengikut ASTM kaedah standard. Tahap radionuklid dan bahaya radiologi telah diukur menggunakan spektrofotometer gamma ray. The leachability logam berat telah dijalankan mengikut EPA kaedah standard. Keputusan pencirian POCP disahkan bahawa POCP terdiri dalam campuran oksida bukan organik dengan sebahagian karbon

organik. Pola XRD dan indeks penghabluran daripada POCP disahkan bahawa kuarza sebahagiannya bercelaru dalam matriks POCP. Selain itu, keadaan yang sesuai untuk penyingkiran karbon organik dari POCP didapati di 580 ° C selama 3 jam, di mana kekuatan mampatan mortar telah meningkat dengan ketara. Hasil siasatan sifat mikrostruktur dan aktiviti kekuatan indeks disahkan bahawa POCP adalah bahan pozzolanic. Air untuk konsisten normal, menetapkan masa dan kekukuhan ditemui dalam ATSM had standard sehingga 60% tahap penggantian, tetapi telah menurun kekuatan mampatan. Pemerbadanan POCP dalam simen dikurangkan kos dan pelepasan karbon dioksida, dan juga disimpan sumber semula jadi. The radium aktiviti bersamaan POCP didapati jauh lebih rendah daripada abu terbang arang batu, dan setanding dengan abu bahan api minyak sawit yang memastikan persekitaran dalaman selamat. Logam berat yang hadir di dalamnya, tetapi tidak Meluluhkan ketara daripada matriks POCP. Adalah lebih selamat dari segi risiko larut lesap logam radiologi dan berat untuk digunakan sebagai bahan binaan. The POCP boleh dilaksanakan untuk digunakan sebagai bahan bersimen tambahan dalam aplikasi berasaskan simen yang akhirnya membawa kepada menurunkan konkrit jejak karbon, persekitaran yang lebih bersih dan menukar sisa kepada sumber.

## ACKNOWLEDGEMENTS

First of all, I would like to express my gratitude to the Almighty Allah who has created the whole universe, taught by pen and taught man that he knew not. I would like to extend my gratefulness to my supervisors Prof. Dr. Hashim Abdul Razak as well as Associate Professor Dr. Sumiani Yusoff for their continuous support during my Ph.D. study and research, for their patience, enthusiasm, motivation and immense knowledge. I am especially grateful to my beloved wife Mahbuba Rashid, my parents and my little angel Rushda Mahjabeen who has encouraged and supported me with continuous help throughout the study.

Finally, I would like to acknowledge gratefully the University of Malaya for providing me the financial support through HIR project: UM.C/625/1/HIR/MOHE/ENG/56 and PG256-2015B to accomplish this work. I gratefully acknowledge the privileges and opportunities offered by the University of Malaya. I also express my gratitude to the staff and friends who helped me directly or indirectly to carry out my research work.



## TABLE OF CONTENTS

Abstract .....	iii
Abstrak .....	v
Acknowledgements .....	vii
Table of Contents .....	viii
List of Figures .....	xv
List of Tables.....	xviii
List of Symbols and Abbreviations.....	xix
<b>CHAPTER 1: INTRODUCTION.....</b>	<b>1</b>
1.1 Background .....	1
1.2 Problem Statement .....	4
1.3 Research Objectives .....	5
1.4 Scopes and Limitations .....	5
1.5 Significance of the Study .....	7
1.6 Outline of the Thesis .....	8
<b>CHAPTER 2: LITERATURE REVIEW.....</b>	<b>10</b>
2.1 Introduction .....	10
2.2 Characterization of Palm Oil Clinker.....	11
2.2.1 Chemical Composition.....	11
2.2.2 Mineralogical Composition.....	14
2.2.3 Thermal Stability .....	15
2.2.4 Organic Carbon .....	16
2.2.5 Microstructure and Morphology .....	17
2.2.6 FTIR Analysis and Crystallinity .....	18

2.3 Effect of Thermal Activation .....	19
2.3.1 Thermal Activation Process .....	20
2.3.2 Chemical Composition.....	20
2.3.3 Structure of Minerals .....	21
2.3.4 Microstructure and Morphology .....	22
2.3.5 Organic Carbon.....	24
2.3.6 Compressive Strength .....	24
2.4 Pozzolanic Activity .....	27
2.4.1 Chemical Composition.....	27
2.4.2 Amorphisity .....	29
2.4.3 Micro Analytical Studies .....	29
2.4.4 Strength Activity Index.....	30
2.5 Fresh and Hardened Properties .....	31
2.5.1 Water Consistency and Setting Time.....	31
2.5.2 Volume Stability .....	34
2.5.3 Rheological Properties .....	35
2.5.4 Mechanical Properties.....	35
2.5.5 Sustainability and Resource Conservation.....	36
2.6 Potential Radiological Hazards .....	38
2.6.1 Radioactivity in Earth Materials .....	39
2.6.2 Health Hazards.....	40
2.6.3 Radiological Hazards Investigation .....	41
2.7 Heavy Metal Levels and Leaching Toxicity .....	42
2.7.1 Possibility of Heavy Metals in POC .....	42
2.7.2 Heavy Metals Characterization.....	43
2.7.3 Pervious Concrete and Leaching Possibility.....	44

2.7.4 Mobility and Bioavailability .....	45
2.8 Research Gaps .....	45
<b>CHAPTER 3: MATERIALS AND METHODS .....</b>	<b>47</b>
3.1 Introduction .....	47
3.2 Characterization Procedures .....	47
3.2.1 Material .....	47
3.2.2 Physical Properties .....	49
3.2.3 Chemical Composition .....	49
3.2.4 Minerals .....	50
3.2.5 Crystallinity .....	50
3.2.6 Thermal Stability .....	50
3.2.7 Organic Carbon .....	51
3.2.8 Morphology .....	51
3.3 Effect of Thermal Activation and Compressive Strength Measurement .....	51
3.3.1 Materials and Methods .....	51
3.3.2 Thermogravimetric Analysis .....	52
3.3.3 Thermal Activation Process .....	53
3.3.4 Micro Analytical Techniques .....	54
3.3.5 Mix Proportion and Curing .....	54
3.3.6 Test of Hardened Mortar .....	55
3.4 Pozzolanic Reactivity Measurement .....	55
3.4.1 Properties Investigation .....	56
3.4.2 Paste Preparation .....	56
3.4.3 Micro Analytical Characterization of Paste .....	57
3.4.4 Strength Activity Index Measurement .....	57
3.5 Fresh and Hardened Properties Determination .....	57

3.5.1 Properties of POCP .....	57
3.5.2 Blended Cement Composition .....	58
3.5.3 Physical Properties of Blended Cement .....	58
3.5.4 Viscosity Measurement.....	59
3.5.5 Preparation and Test of Cement Mortar.....	59
3.6 Radiological Hazards Determination .....	60
3.6.1 Sample Preparation .....	60
3.6.2 Characteristics of POC and POFA.....	61
3.6.3 Measurement of Radioactivity .....	62
3.6.4 Radiological Hazard Indices Calculations .....	65
3.6.4.1 Radium equivalent activity (Raeq).....	65
3.6.4.2 Absorbed $\gamma$ -dose rate .....	66
3.6.4.3 Annual effective dose.....	66
3.6.4.4 Gamma index.....	67
3.6.4.5 Alpha index.....	67
3.6.4.6 Health hazard indices .....	68
3.7 Heavy Metal Leaching Risk Assessment.....	69
3.7.1 Sample Preparation .....	69
3.7.2 Chemical Reagents.....	70
3.7.3 Digestion of POC .....	71
3.7.4 Speciation Analysis.....	72
3.7.5 Leaching Toxicity Measurement .....	73
<b>CHAPTER 4: RESULTS AND DISCUSSIONS .....</b>	<b>75</b>
4.1 Introduction.....	75
4.2 Characterization of Palm Oil Clinker Powder .....	75

4.2.1 Physical Properties .....	75
4.2.2 Chemical Characteristics .....	78
4.2.3 TGA and Organic Carbon .....	81
4.2.4 Mineralogical Characteristics .....	84
4.2.5 Crystallinity of POCP .....	85
4.3 Effect of Thermal Activation and Compressive Strength .....	88
4.3.1 Chemical Composition.....	88
4.3.2 Total Organic Carbon .....	90
4.3.3 Crystalline Structure of Minerals .....	92
4.3.4 Morphology.....	93
4.3.5 Compressive Strength Development.....	94
4.4 Pozzolanic Reactivity of POCP .....	98
4.4.1 Properties of POCP .....	98
4.4.2 XRD Studies of Pastes .....	101
4.4.3 Thermogravimetric Analysis .....	105
4.4.4 FTIR Analysis.....	108
4.4.5 Microstructure Analysis.....	108
4.4.6 Strength Activity Index (SAI).....	109
4.5 Fresh and Hardened Properties .....	111
4.5.1 Characteristics of Materials .....	111
4.5.2 Rheological Properties .....	114
4.5.2.1 Consistency.....	114
4.5.2.2 Setting time of cement paste .....	115
4.5.2.3 Viscosity of cement paste.....	117
4.5.3 Volume Stability .....	118
4.5.4 Compressive Strength .....	119

4.5.5 Flexural Strength.....	121
4.5.6 Cost and Compressive Strength .....	122
4.5.7 Greenhouse Gas Reduction and Compressive Strength.....	123
4.5.8 Natural Resource Conservation .....	125
4.6 Radiological Hazards .....	127
4.6.1 Radionuclide in POC and POFA .....	127
4.6.2 Potential Radiological Hazard .....	129
4.6.3 Comparison of Radiological Hazard.....	133
4.7 Heavy Metal Levels and Potential Leaching Risk.....	134
4.7.1 Characterization of Heavy Metal .....	135
4.7.1.1 FESEM-EDX studies .....	135
4.7.1.2 Mineral analysis.....	136
4.7.1.3 ICP-MS studies.....	138
4.7.2 Potential Leaching Risk .....	141
4.7.2.1 Leaching behaviour studies .....	141
4.7.2.2 Speciation studies .....	142
4.7.2.3 Potential risk studies.....	144
<b>CHAPTER 5: CONCLUSIONS AND RECOMMENDATIONS.....</b>	<b>146</b>
5.1 Introduction.....	146
5.2 Characterization of POCP .....	146
5.3 Chemical Interaction of POCP in Cement-Based Applications.....	147
5.4 Effect of POCP Characteristics on Fresh and Hardened Properties of Cement.....	149
5.5 Radiological Hazard and Heavy Metal Leaching Risk .....	150
5.6 Conclusions .....	151
5.7 Recommendations .....	152
References .....	154

List of Publications ..... 172

University of Malaya

## LIST OF FIGURES

<b>Figure 2.1:</b> Solid biomass produced in Malaysia.....	10
<b>Figure 2.2:</b> Elemental composition .....	14
<b>Figure 2.3:</b> X-ray diffraction patterns of POCP .....	15
<b>Figure 2.4:</b> XRD pattern of GPOFA and TPOFA.....	22
<b>Figure 2.5:</b> Micrographs of GPOFA and TPOFA.....	23
<b>Figure 2.6:</b> Cross section of pervious concrete .....	44
<b>Figure 3.1:</b> Selection and sampling area of POC (Dengkil, Malaysia).....	48
<b>Figure 3.2:</b> Photographs of (A) POC, (B) big chunk and (C) POCP .....	49
<b>Figure 3.3:</b> Thermal analysis of POCP under nitrogen atmosphere .....	53
<b>Figure 3.4:</b> Heating patterns.....	54
<b>Figure 3.5:</b> Schematic diagram of POC & POFA production.....	61
<b>Figure 3.6:</b> Characteristic $\gamma$ -ray spectrum of POC .....	64
<b>Figure 3.7:</b> Characteristic $\gamma$ -ray spectrum of POFA .....	64
<b>Figure 3.8:</b> Micrograph of POC sample.....	70
<b>Figure 3.9:</b> Particle size of POCP .....	71
<b>Figure 3.10:</b> Particle size of materials used in leaching test .....	74
<b>Figure 4.1:</b> Photographs of (a) bulk quantity and (b) a big chunk of POC.....	76
<b>Figure 4.2:</b> Particle size of POCP .....	77
<b>Figure 4.3:</b> Morphological differences of (a) POCP and (b) FA .....	78
<b>Figure 4.4:</b> FESEM-EDX micrograph of POCP.....	79
<b>Figure 4.5:</b> TGA analysis pattern of POCP.....	82
<b>Figure 4.6:</b> Colour change, (a) raw and (b) heated at 800°C for 1 hour .....	83
<b>Figure 4.7:</b> X-ray diffraction pattern.....	84
<b>Figure 4.8:</b> FTIR spectra of POCP .....	86
<b>Figure 4.9:</b> Color change due to thermal activation.....	91



<b>Figure 4.10:</b> XRD patterns of (A) POCP and (B) TPOCP <sub>580</sub> .....	93
<b>Figure 4.11:</b> SEM micrographs of (a) POCP and (b) TPOCP <sub>580</sub> .....	94
<b>Figure 4.12:</b> Effect of thermal activation on compressive strength .....	95
<b>Figure 4.13:</b> Comparison of relative compressive strength of TPOCP.....	95
<b>Figure 4.14:</b> Relative compressive strength and air content of mortars.....	97
<b>Figure 4.15:</b> X-ray diffraction pattern of POCP .....	99
<b>Figure 4.16:</b> Particle size distribution of POCP and OPC .....	100
<b>Figure 4.17:</b> Micrograph of POCP .....	101
<b>Figure 4.18:</b> XRD patterns for (a) OPC and (b) POCPC paste cured in 3 days .....	102
<b>Figure 4.19:</b> XRD patterns of OPC and POCPC paste of curing age in 28 days.....	103
<b>Figure 4.20:</b> XRD patterns for OPC and POCPC paste cured in 90 days.....	104
<b>Figure 4.21:</b> TGA curve of OPC and POCPC paste cured in 3 days.....	106
<b>Figure 4.22:</b> TGA for OPC and POCPC paste cured in 90 days .....	107
<b>Figure 4.23:</b> FTIR analysis of (a) OPC and (b) POCPC paste cured in 90 days .....	108
<b>Figure 4.24:</b> Micrographs of (a) OPC and (b) POCPC pastes cured in 90 days.....	109
<b>Figure 4.25:</b> Strength activity indexes (28 days) of waste materials .....	110
<b>Figure 4.26:</b> Particle size of OPC and POCP.....	113
<b>Figure 4.27:</b> Micrograph of POCP .....	114
<b>Figure 4.28:</b> Relative water demand in POCP blended cements .....	115
<b>Figure 4.29:</b> Effect of POCP on setting behaviour .....	116
<b>Figure 4.30:</b> Viscosity related with shear rate (running time-60 seconds) .....	117
<b>Figure 4.31:</b> Shear stress related to shear rate (running time 60 seconds).....	118
<b>Figure 4.32:</b> Volume expansion of POCP blended cements.....	119
<b>Figure 4.33:</b> Effect of POCP on compressive strength .....	120
<b>Figure 4.34:</b> Relative compressive strength of cements .....	120
<b>Figure 4.35:</b> Effect of POCP on flexural strength.....	122

<b>Figure 4.36:</b> Cost and compressive strength of cements.....	123
<b>Figure 4.37:</b> CO <sub>2</sub> reduction and compressive strength of cements .....	124
<b>Figure 4.38:</b> Natural resource conservation at different replacement levels.....	126
<b>Figure 4.39:</b> Relative contributions of <sup>226</sup> Ra, <sup>232</sup> Th & <sup>40</sup> K to Ra <sub>eq</sub> in POC & POFA .	130
<b>Figure 4.40:</b> FESEM-EDX of POC .....	136
<b>Figure 4.41:</b> Mineral analysis of POC .....	137
<b>Figure 4.42:</b> Speciation of targeted metals of POC .....	143
<b>Figure 4.43:</b> Potential heavy metal leaching risk of POC.....	145

University of Malaya

## LIST OF TABLES

<b>Table 2.1:</b> Chemical composition of POCP .....	13
<b>Table 2.2:</b> FTIR analysis report of some agricultural wastes.....	18
<b>Table 2.3:</b> Thermal activation effect on compressive strength .....	26
<b>Table 2.4:</b> Pozzolanicity of POCP based on chemical composition .....	28
<b>Table 2.5:</b> Radioactivity in soil and water of Malaysia .....	40
<b>Table 3.1:</b> Thermal activation applied to POCP .....	53
<b>Table 3.2:</b> Mixing ratio of blended cement .....	58
<b>Table 3.3:</b> Properties of POC and POFA .....	62
<b>Table 3.4:</b> Sequential extraction.....	72
<b>Table 3.5:</b> Leaching test parameters.....	74
<b>Table 4.1:</b> FESEM-EDX results of POCP .....	80
<b>Table 4.2:</b> Chemical compositions of POCP and commonly used waste materials.....	81
<b>Table 4.3:</b> Total carbon analysis report of POCP.....	84
<b>Table 4.4:</b> Minerals in POCP and common waste material .....	85
<b>Table 4.5:</b> Chemical compositions of OPC, POCP and TPOCP.....	89
<b>Table 4.6:</b> Change in chemical composition through thermal activation.....	89
<b>Table 4.7:</b> Total carbon in POCP and TPOCP .....	91
<b>Table 4.8:</b> Chemical composition of POCP .....	98
<b>Table 4.9:</b> Properties of OPC and POCP .....	112
<b>Table 4.10:</b> Radioactivity of $^{226}\text{Ra}$ , $^{232}\text{Th}$ and $^{40}\text{K}$ in POC and POFA.....	129
<b>Table 4.11:</b> Indicators of radiological hazard of POC and POFA .....	132
<b>Table 4.12:</b> Radioactivity of $^{226}\text{Ra}$ , $^{232}\text{Th}$ , $^{40}\text{K}$ in POC, POFA and Fly Ash.....	134
<b>Table 4.13:</b> Total concentration of targeted metals of POC.....	139
<b>Table 4.14:</b> Comparison of heavy metals among different ashes .....	140

## LIST OF SYMBOLS AND ABBREVIATIONS

BLA	:	Bamboo Leaf Ash
BA	:	Bottom Ash
C-S-H	:	Calcium Silicate Hydrate
CH	:	Portlandite
FA	:	Fly Ash
FFB	:	Fresh Fruit Bunch
FESEM-EDX	:	Field Emission Scanning Electron Microscopy & Energy-Dispersive X-Ray Analysis
FTIR	:	Fourier Transform Infrared Spectroscopy
GBFS	:	Granulated Blast Furnaces Slag
GPOFA	:	Grounded Palm Oil Fuel Ash
GHG	:	Greenhouse Gases
IC	:	Inorganic Carbon
ICP-MS	:	Inductively Coupled Plasma Mass Spectrometry
LOI	:	Loss of Ignition
MF	:	Mesocarp Fibre
MSD	:	Municipal Solid Waste
NORM	:	Naturally Occurring Radioactive Materials
OPS	:	Oil Palm Shell
PC	:	Pervious Concrete
POC	:	Palm Oil Clinker
POCP	:	Palm Oil Clinker Powder
POCPC	:	Palm Oil Clinker Powder Cement
POFA	:	Palm Oil Fuel Ash
TPOFA	:	Thermally Activated Palm Oil Fuel Ash
RHA	:	Rich Husk Ash
SIA	:	Strength Activity Index
SEM	:	Scanning Electron Microscopy
SCM	:	Supplementary Cementitious Material
SBA	:	Sugarcane Bagasse Ash
SF	:	Silica Fume
TPOCP	:	Thermally Activated Palm Oil Clinker Powder
TPOCPC	:	Thermally Activated Palm Oil Clinker Powder Cement
TGA	:	Thermogravimetric Analysis
TOC	:	Total Organic Carbon
TCLP	:	Toxicity Characteristic Leaching Procedure
XRF	:	X-ray Fluorescence
XRD	:	X-ray Diffraction

## CHAPTER 1: INTRODUCTION

### 1.1 Background

This research is applicable to the present situation and future trend for the sustainable utilization of waste materials in low carbon footprint concrete production. Although a number of researches have been done to seek an alternative binder to cement, up till date the main binding material of concrete is ordinary Portland cement (OPC). The challenge for modern cement manufacturing is to increase the production without increasing the environmental pollution. Considering these issues in mind, this chapter describes the general facts which are related to the management of palm oil mill wastes as well as the production of OPC. It highlights the environmental problems associated with the disposal of local palm oil wastes, the utilization of the traditional supplementary materials and Portland cement production. The possibility of heavy metals and radionuclide in palm oil mill waste will be ascertained. Additionally, the limitation on the utilization of traditional wastes or by-product of industries, i.e. slag, fly ash (FA), silica fume (SF) etc. as supplementary cementitious materials (SCMs) in cement-based applications will also be discussed. The significance of the newly introduced SCM, i.e. palm oil mill powder (POCP) which is locally available in Malaysia in cement-based applications will be exemplified. Finally, this chapter is concluded with the outline of this study.

The production of concrete and cement has increased rapidly in the last ten years in order to meet the infrastructure and housing demand for the rise in the world's population. This fact ultimately leads to increase in cement factories, the consumption of raw materials and fossil fuel for cement production, and the emission of greenhouse gases. Additionally, the Kyoto Protocol and the United Nations Framework Convention on climate change was intended at reducing the emission of CO<sub>2</sub> for cement production,

since the cement industries are accountable for 5% of the total global CO<sub>2</sub> emission. This was the main catalyst for accelerating the rate of development in technology and cement itself in recent years (Ludwig & Zhang, 2015). Furthermore, the concrete industries have adhered to sustainable utilization of the materials. A promising way to solve the aforementioned problems is to blend the clinker with the by-products or wastes of other industries such as SCMs. The traditional supplementary materials, i.e. FA, SF and ground granulated blast furnace slag (GBFS) is being used in many countries, according to the standard of the CEM II, EN 197-1 and type IS, IP and IT of ASTM C595/C595M. However, a number of difficulties are associated with the typical SCMs because of their inadequate availability or unapproachable location and expenditure due to importation (Alam et al, 2015). The radiological hazard and heavy metal leaching risk are important issues for using fly ashes as SCMs in concrete (Hvistendahl et al., 2007a, 2007b; Pöykiö et al., 2016; Tiwari et al., 2015).

Conversely, the solid biomass production of palm oil industries has rapidly increased, due to the rising demand of palm oil. Previous research predicted that the biomass production will be 85-110 million tonnes at 2020 (Shuit et al., 2009). Statistics show that 85.5% biomass originated from palm oil in Malaysia (Shuit et al., 2009). Palm oil clinker (POC) is a waste material which is produced as a result of using palm oil shell and mesocarp fibres (MF) as fuel to run steam turbines in palm oil mills. In current practice, POC waste is dumped in the open land or landfill sites which lead to environmental pollution. The palm oil mill wastes are also increasing proportionally with the demand of palm oil worldwide. This emphasizes the critical need to establish a proper palm oil mill waste management system. As contemporary practice, the utilization of these wastes is used to cover the potholes on the roads within premises of the plantation areas (Kanadasan & Abdul Razak, 2015).

Meanwhile, the naturally occurring radioactive materials (NORMs) in soil, in water and/or in the earth borne materials show heterogeneous distribution. Thus, several authors studied the levels of natural radioactivity in soil, water, building materials as well as plants in different regions of Malaysia, and found a wide variation with respect to the geographical and geological origin (Ahmad et al., 2015). Radionuclide which is available in soil (Ahmad et al., 2015; Asaduzzaman et al., 2015; Saleh et al., 2013), natural coal (Amin et al., 2013; Đurašević et al., 2014) and water (Ramli et al., 2005) are taken up by plant tissue in the similar way to the uptake of minerals by the plant-root system. Like other environmental materials, fresh fruit bunch (FFB), shell, nut fibre have natural radionuclide's of uranium, thorium and potassium in minimal levels that do not cause severe problems to the human being (Ramli et al., 2005). Furthermore, although the majority of the uranium and thorium and their progenies are not liberated from the original oil palm shell (OPS) and fibre via the burning process, they rather end to become enriched in the residue materials such as POC and POFA as inorganic oxides (Peppas et al., 2010).

The excessive soil erosion, high rainfall, overflowing flood, fertilizer used for cultivation are very common ways to transfer heavy metals in the soil-plant system. Research studies have found that the soil is contaminated with the magnesium (Mg), nickel (Ni), chromium (Cr), cobalt (Co), and manganese (Mn) metals which come from rock such as serpentinite due to soil erosion, high rain to fall, overflowing flood (Aziz et al., 2015). The long term utilization of phosphate rock fertilizer in soil for oil palm plantations increases Zn and Cd content in soil as well accumulated in the palm oil fronds and fruit lets. A study in Malaysia found that Zn is concentrated in fronds and soil. The Cd and Zn in soil and soil solution influences the uptake by the oil palm trees (Azura et al., 2012).

The utilization of palm oil clinker powder (POCP) as a SCM in cement-based applications are feasible and more logical rather than dumping in open land which could be harmful to the environment. Moreover, the determination of the radiological hazards and the heavy metal leaching behaviour is mandatory for the safe incorporation of palm oil mill waste as ingredient in building materials. The aim of this study is to evaluate the feasibility of POCP to be used as a SCM in cement-based applications.

## **1.2 Problem Statement**

The magnitude of environmental contamination can be related to the increase in OPC production. OPC is responsible for the emission of greenhouse gas (CHG) and the depletion of natural resources. The solid waste generated in palm oil mills are produced in bulk quantity and it is used for covering potholes on the road or disposed without treatment by land filling. This will cause contamination of water and deterioration of the soil anality (Kanadasan & Abdul Razak, 2015). The waste biomass production from the palm oil mill increase potentially due to uprising demands for palm oil. A management system is essential to minimize severe environmental pollution. Proper solid waste management is a challenge in Malaysia. The many health and environmental problems are associated with the solid wastes which are not properly managed.

Although, FA have been used as SCM in cement-based applications, it has some disadvantages. The coal fly ash composes of the radionuclide (radium, thorium and potassium) and the corresponding radiological hazards are more than the international standard. The incorporation of the radionuclide containing fly ash as building material can cause various health problems such as the effect on respiratory system, lung disease, leukopenia, and anemia, necrosis of the jaw, damage bone, head, and nasal passage tumors in excessive exposure than the world recommended values (Almayahi et al., 2012a, Kovler, 2011, 2012; Omar, 2002; Trevisi et al., 2012; Rosabianca Trevisi et



al., 2013). The heavy metals in fly ashes cause several health problems such as kidney damage, bone effects and fractures, neurological damage, cancer, hyperkeratosis and pigmentation changes (Shaheen & Rinklebe, 2015). Moreover, the traditional SCMs are not available in Malaysia. They are imported from other countries and are expensive for use in cement-based applications.

### **1.3 Research Objectives**

This study is conducted to evaluate the feasibility of palm oil clinker powder to be used as a supplementary cementitious material in cement-based applications. This research also attempts to quantify the radiological and leaching toxicity risk for the incorporation of POCP in cement-based applications. Detailed objectives are as follows:

- (1) Characterization of POCP for utilization in cement-based applications;
- (2) Evaluation of the chemical interaction, i.e. the effect of organic carbon of POCP on strength development and also the pozzolanic reactivity of POCP;
- (3) Effect of POCP on the fresh and hardened properties of cement mortar at different replacement level;
- (4) Evaluation of the radiological hazard and heavy metals leaching toxicity aspect for the incorporation of POCP as ingredients of building materials.

### **1.4 Scopes and Limitations**

This research focused on the feasibility assessment of palm oil clinker powder as supplementary cementitious materials in cement-based applications based on the following scope and limitations:

- (1) The palm oil clinker sample was collected from a selected area of Dengkil in Malaysia. The technical suitability of POCP is analyzed by blending with OPC at different replacement levels.
- (2) The characterization of POCP is performed using XRF, XRD, TGA, FTIR, particle size analyzer, FESEM-EDX, TOC analyzer and Blaine apparatus.
- (3) The effect of heat energy on the characteristics of POCP are determined by aforementioned apparatus and the compressive strength of OPC mortar with only 30% replacement of OPC by POCP using 50mm cubes are measured at a water/binder (W/B) and binder/sand (B/S) ratios of 0.40, 0.50, respectively.
- (4) The participation of SiO<sub>2</sub> of POCP in pozzolanic reaction is determined using micro analytical apparatus mentioned before, and the strength activity index is measured according to ASTM standard. The micro structural properties is measured and 30% POCP blended cement paste mortar cured in 3, 28 and 90 days.
- (5) The effect of POCP characteristics on the setting time and hardened properties cement paste and mortar are measured according to ASTM standards.
- (6) The economic benefit, greenhouse gas reduction and natural resource conservation are observed through a pilot scale experiment using the mini ball in the laboratory.
- (7) The radio nuclide in POCP is determined using Gamma-ray spectrophotometer and the radiological hazard indices is compared with POFA and fly ash. The heavy metal are characterized with ICP-MS apparatus and the digestion of POCP is confirmed at microwave condition. The leaching toxicity are analyzed according to EPA method.

- (8) The radiological and leaching toxicity risk of palm oil clinker powder for the incorporation in cement-based applications are measured in the samples with POCP collected from a specific area in Malaysia.

### **1.5 Significance of the Study**

Based on the related literature review, there is insufficient research work on the for utilization of palm oil clinker as a supplementary cementitious material (SCM), the radiological hazards and heavy metal leaching risk for the incorporation of POCP in cement-based applications. Palm oil clinker powder is thus proposed as a new SCM. It should be noted that there is not sufficient research work on the characterization of palm oil clinker powder for use as SCM. Moreover, the assessment of the effect of organic carbon of POCP on strength development of cement mortar and the pozzolanic activity is rarely studied. In addition, leaching toxicity & radiological hazards were also evaluated for the utilization of POCP in cement-based applications. The analyses of the aforementioned objectives lead to the safe incorporation of POCP as a supplementary cementitious material for low carbon footprint concrete production with a significant reduction in cost. Furthermore, the sustainability of the cement industry can also be conserved with the introduction of POCP as an alternative source of supplementary cementitious material. The natural resource such as limestone, clay, and quartz and iron ore will also be saved significantly. This is a way to convert the waste material into a resource. The utilization of POCP instead of fly ash (FA) as SCM in cement-based applications will reduce the various health problems which are associated with the radionuclide and heavy metals of fly ash.

## 1.6 Outline of the Thesis

This thesis is arranged in such a way that the reader can easily understand the scope and goals of the research and it divided into five chapters. First chapter explained the introduction of this study, which comprised the subjects in palm oil clinker solid waste from the palm oil mill, environmental issues in the Portland cement industry, problem statement, objectives, scopes and limitations, and the importance of this work.

Chapter 2 presented the literature reviews of past researches related to the background information on palm oil clinker as well as similar waste materials to research areas in SCMs. The characteristics of waste materials are discussed at the first step in the literature review chapter. The chemical interactions of waste materials in cement-based applications are also reviewed in this work. In addition, the effects of the heat energy on mineralogy, chemical composition, morphology, organic carbon of waste material are discussed and their influences on compressive strength development deliberated. At the last part of the Chapter 2 discuss about the contamination possibility of heavy metal and natural radionuclide for the incorporation of POCP as an ingredient of concrete.

The third chapter presents the methodology, including the section of the experiments for justifying the research gap which was found in the literature review chapter. The used materials, methods and apparatus used in performing the test parameters are described clearly. The micro analytical methods are used to investigate the characterization and chemical interaction, and the ASTM standard methods are used to determinate the compressive strength as well as water consistency and setting time. Radioactivity levels and radiological hazards are evaluated using a gamma ray spectrophotometer. Also, the ICP-MC apparatus used to assess the heavy metal content as well as leaching properties according to standard methods are discussed.

The fourth chapter represents the results and discussions which was designed from the sequence of experiments, which can be separated into six sections, characterization, chemical interaction, i.e. organic carbon effect and pozzolanic activity, the fresh and harden properties of POCP blended cement, and the radiological hazards and heavy metal leaching toxicity for incorporation of POC in building materials which were explained and discussed.

The fifth chapter summarized the overall findings of this study. The feasibility assessment of palm oil clinker use as a supplementary cementitious material as stated at the end of objectives in chapter 1. Recommendations were also made further work in the related area.

## CHAPTER 2: LITERATURE REVIEW

### 2.1 Introduction

The background information of palm oil mill waste and environmental issues will be discussed in the introduction of the literature review chapter. The high demand for the palm oil waste is the main catalyst for increasing the solid biomass of palm oil mills from eighty million tonnes in 2010 to an estimated amount of 85-110 million tonnes in 2020 (Shuit et al., 2009). **Figure 2.1** shows the biomass produced by different industries in Malaysia.

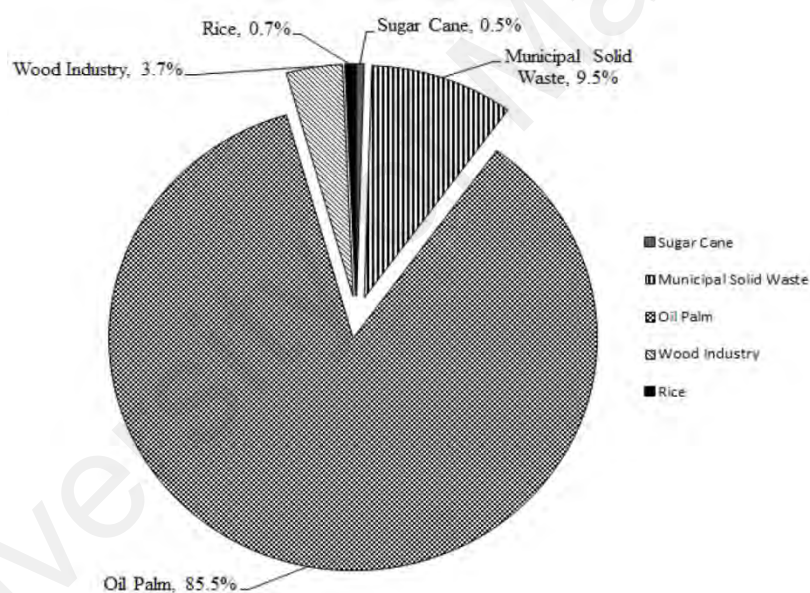


**Figure 2.1:** Solid biomass produced in Malaysia (Shuit et al., 2009).

A proper waste management system is essential to overcome the serious environmental problems due to palm oil mill wastes. This chapter will review the previous works that have been carried out for the utilization of palm oil mill wastes as ingredient of building material. Moreover, the discussion about the traditional supplementary cementitious waste materials, i.e. slag, FA, SF and other similar materials for utilization in cement-based applications is also included in this chapter.

The first section of the literature review chapter presents the characteristic properties of palm oil mill wastes as well as other traditional supplementary materials. Generally, every section is arranged according to the introduction, body of the section and conclusion. The second and third sections discuss the effect of heat energy on the properties of waste materials and their influences on the development of compressive strength and the pozzolanic activity, respectively. The subsequent sections of the literature review chapter will describe the effect of supplementary cementitious materials on fresh and hardened properties of cement. The last two sections of the literature review chapter illustrate the possibility of the radionuclide and heavy metals in POCP, and their effect on health and environment when incorporated as supplementary materials in concrete construction. Finally, the overall findings of the literature review along with research gaps have been summarized in the research gap section. These findings are the motivation of the experimental work of this study.

## **2.2 Characterization of Palm Oil Clinker**

In-depth knowledge of POCP properties is important for its application as SCM in cement-based applications. The characteristics such as chemical composition, mineralogical composition, organic matter presence, thermal stability, morphology and crystalline nature of palm oil mill wastes as well as other similar waste materials which are already being used as cementitious materials will be discussed in this section. The methodology and apparatus which was used in previous researches will also be detailed with a brief conclusion on the findings in characterization.

### **2.2.1 Chemical Composition**

The chemical composition of POCP is tabulated in **Table 2.1** with a standard deviation (SD) from the data available in the literatures. Most of the researchers used the XRF technique for determination of the chemical composition (Gao et al., 2015;

Kanadasan et al., 2015). The chemical composition is an important parameter to assess the variability of a material in terms of oxide ingredients; particularly, when the waste materials are used as a mineral addition in cement-based applications. The chemical composition of POCP is a mixture of inorganic oxides. The XRF observation reveals that the major component of POCP are  $\text{SiO}_2$ ,  $\text{Al}_2\text{O}_3$ ,  $\text{Fe}_2\text{O}_3$ , alkali oxides and low content of calcium oxide. In addition, low concentrations of several transition metals and alkali oxides are also present in POCP (Kanadasan & Razak, 2015). The results of the chemical composition were not consistent, having variation with standard deviation. These variations were observed for POCP samples which were obtained from the different locations in Malaysia. The variation in the chemical composition in POCP depends on the feeding ratio to the boiler, the burning temperature and operating conditions of a boiler, and the geological condition of the respective area where the palm oil tree are planted (Kanadasan et al., 2015).



**Table 2.1:** Chemical composition of POCP

Samples	Chemical Composition (by weight %)						
	SiO <sub>2</sub>	Al <sub>2</sub> O <sub>3</sub>	Fe <sub>2</sub> O <sub>3</sub>	K <sub>2</sub> O	CaO	MgO	P <sub>2</sub> O <sub>5</sub>
<sup>a</sup> POCP	59.63	3.7	4.62	11.56	8.16	5.01	5.37
<sup>k</sup> POCP	59.90	3.89	6.93	15.10	6.37	3.30	3.47
<sup>b</sup> POCP	81.8	3.5	5.18	4.66	2.3	1.24	0.76
<sup>kd</sup> POCP	65.10	3.28	6.34	9.23	3.89	2.34	3.06
<sup>kd</sup> POCP	73.31	6.00	6.13	8.78	4.01	2.83	1.43
<sup>kd</sup> POCP	72.64	5.18	3.89	9.65	4.42	2.56	3.96
<sup>kd</sup> POCP	69.91	4.15	5.15	9.24	8.56	3.92	3.24
<sup>kd</sup> POCP	74.29	3.11	2.09	6.22	5.10	1.72	2.79
<sup>kd</sup> POCP	60.79	7.27	15.64	5.17	10.48	2.23	1.61
<sup>kd</sup> POCP	65.64	7.56	14.41	7.26	4.11	2.64	1.73
<sup>kd</sup> POCP	64.84	3.42	4.19	12.82	5.96	5.01	3.37
<sup>kd</sup> POCP	57.41	4.95	10.11	11.32	6.95	4.01	4.90
<sup>kd</sup> POCP	69.05	4.73	3.71	11.09	5.70	2.27	3.22
<sup>kd</sup> POCP	62.05	1.42	2.20	13.48	9.51	6.09	7.33
<sup>kd</sup> POCP	62.52	0.82	1.10	8.44	16.74	3.43	4.75
Max	81.8	7.56	15.64	15.1	16.74	6.09	7.33
Min	57.41	0.82	1.10	4.66	2.3	1.24	0.76
Mean	66.27	4.16	5.74	9.67	6.83	3.25	3.2
SD	6.40	1.74	4.07	2.83	3.34	1.26	1.65

**Note:** <sup>a</sup>POCP (Ahmmad et al., 2014), <sup>k</sup>POCP (Kanadasan & Razak, 2014), <sup>b</sup>POCP (Binti Robani & Chan, 2009) and <sup>kd</sup>POCP (Kanadasan et al., 2015).

The elemental composition and micrograph of POCP is presented in **Figure 2.2**. By FESEM-EDX analysis, the predominant elements in the POCP sample are oxygen, silicon, potassium, calcium, magnesium, whereas there exists smaller amount of sodium, manganese, aluminium, sulfur, phosphorous and iron (Kanadasan & Abdul Razak, 2015).

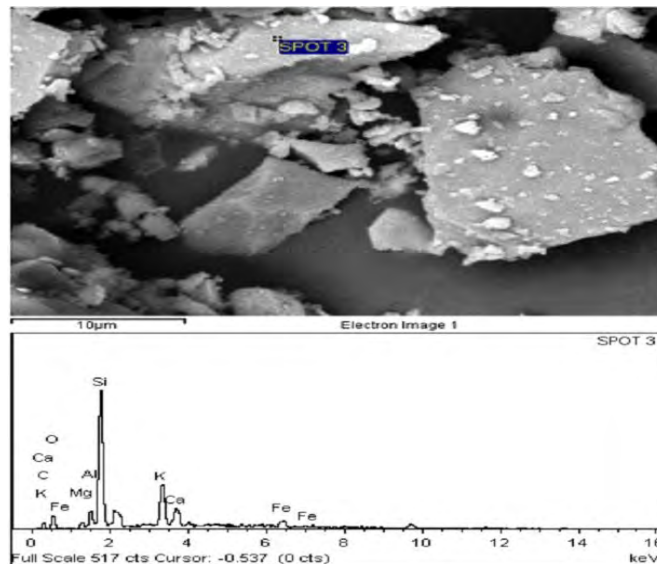


**Figure 2.2:** Elemental composition (Kanadasan & Abdul Razak, 2015)

### 2.2.2 Mineralogical Composition

The mineralogical composition of POCP is rarely reported in the literature. The XRD pattern of POCP which was collected from the different states of Malaysia are shown in **Figure 2.3**. The major peaks of the quartz and cristobalite minerals were found in the  $2\theta$  angles of  $26.87^\circ$  and  $20.45^\circ$ , respectively. The XRD plots also illustrated that the minor quartz peaks were shown at the  $2\theta$  of  $20.83^\circ$ ,  $26.61^\circ$ ,  $50.11^\circ$  and  $59.93^\circ$ . In addition, the crystalline phase of cristobalite can also be detected through the presence of a peak at  $2\theta$  of  $21.92^\circ$ . Despite of having a variation of intensity levels, similar minerals can be found in the XRD patterns for the different POC samples (Kanadasan et al., 2015). The variation of the intensity of quartz peak at  $2\theta$  angles of  $26.87^\circ$  ensures that there is variation on the crystallinity of the samples of the different estates. The amorphisity of POCP is not clear from the XRD patterns which are available in literature.

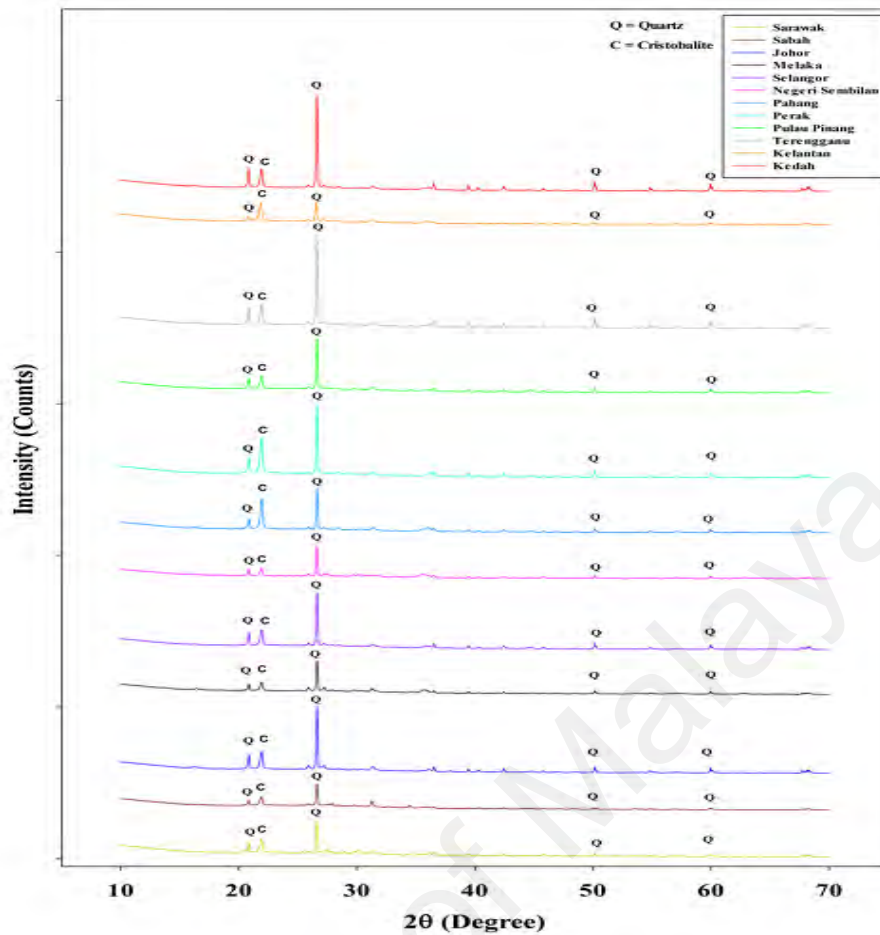


**Figure 2.3:** X-ray diffraction patterns of POCP (Kanadasan et al., 2015)

The mineralogy of POCP is similar with other form of waste, such as. POFA which also reported by Chandara et al. (2010).

### 2.2.3 Thermal Stability

The interaction of the heat energy with waste material properties depends on the internal bonding energy of the material. The effect of this interaction can be observed by measuring the weight loss with respect to temperature using TGA apparatus. In literature, it was found that the crystalline lattice of clay minerals becomes disordered through the application of heat energy and this increase the pozzolanic activity (Alam et al., 2015). Some waste materials such as POFA contain organic matter that decomposes easily due to application of heat. Generally, the unburned carbon is

removed from the waste in the operation temperature of TGA apparatus from 30°C to 800°C. The unburned carbon is a significant factor to be considered (Bartoňová et al., 2015), since the water requirement for normal consistency and also dosage of super plasticizer (SP) increase due to absorption by the carbon particles (Chandara et al., 2010). In addition, the compressive strength was also found to increase significantly when the unburned carbon free wastes are incorporated as SCMs (Chandara et al., 2011; Chandara et al., 2010). Previous studies show that oil palm kernel shell has been used as raw feed of the boiler which composes of the hemicelluloses (1.2%), cellulose (38.6%) and lignin (39.0%), and some extractives (Ninduangdee & Kuprianov, 2013). The lignin of shell becomes moderately stable at higher temperatures due to its highly aromatic backbone. A major mass loss (about 40%) of Kraft lignin usually between 200°C and 600°C (Sen et al., 2015a). TGA analysis of POFA shows that the major mass loss is observed when the temperature range is 400°C to 600°C. Researchers suggest that this mass loss might be due to the decomposition of CaCO<sub>3</sub> which was presented in POFA (Lim et al., 2015).

#### **2.2.4 Organic Carbon**

Extensive information about the organic carbon content are important aspects for the utilization of new waste or by-products as SCMs in cement-based applications (Gardner et al., 2015; Sow et al., 2015). POFA is one of the forms of palm oil mill waste which is produced as a result of incomplete burning of palm shells, fibres and nuts as fuel in a boiler. The organic carbon in POFA comes from the palm oil fruit bunches and shells. The variation of organic carbon in POFA is due to the feeding ratio of palm shells, fibres and nuts into the boiler as well as burning condition. These wastes are composed mainly of sugar based polymer like cellulose and hemicelluloses combined with lignin, protein, starch and inorganic phases (Hesas et al., 2013). The

composition of fruit bunch and shell consist of cellulose, hemicelluloses, lignin and extractives at 32.6%, 22.1%, 42.3% and 3.0% by weight, respectively (Lahijani et al., 2012). Factors such as the type and age of the plant, climatic condition and processing methods affect the content of carbon-based materials in the palm oil plant. In literature it was found that the 6.01% unburned carbon was present in POFA. However, the unburned carbon of waste materials posed a negative effect on the compressive development (Chandara et al., 2012).

### **2.2.5 Microstructure and Morphology**

The performances of waste materials as SCM are associated with its' microstructure. In general, fly ash particles are smooth spheres with rounded shape. The micro structure and morphology of fly ashes collected from Sarawak, Malaysia and Gladstone, Australia are found to have different shape, size and porosity. The morphology of ultrafine and fine particles are present as smooth spheres with rounded shape (Linak et al., 2002). Higher ultra fine particles was found in fly ash of Gladstone, which has more spherical and regular shape than the fly ash of Sarawak. The irregular shapes are due to the incomplete burning of organic matters of coal (Smith et al., 1979). Additionally, the fly ash collected from Sarawak are more agglomerated compared to the fly ash of Gladstone. The particles of fly ash which are in irregular in shape are responsible for excess water required to maintain same workability. Previous studies show that the irregular shape of wastes creates the void in mortar matrix that ultimately leads to the reduction in compressive strength (Leong et al., 2016). A number of researchers found that the palm oil mill waste, i.e. POFA are irregular in size and shape, and highly porous in nature (Khankhaje et al., 2016; Noorvand et al., 2013). POC chunk is another form of waste of palm oil mill which is a blackish color solid waste material. A few observations had been done for the investigation of the micro structures and

morphology of palm oil clinker powder particles, which was found to be irregular in shape and size. Some of the POC particles were cuboidal in shape with sharp edges while others were flaky (Kanadasan & Abdul Razak, 2015). The impact of the morphology and micro structures of POCP on the properties of cement is rarely identified.

## 2.2.6 FTIR Analysis and Crystallinity

The bonding information of the chemical ingredients and crystallinity of waste materials can be analyzed using FTIR. The mineralogical phases of waste can also be identified from FTIR spectrum. The FTIR results of some common agriculture wastes which have been used as a supplementary cementitious material presented in **Table 2.2**.

**Table 2.2:** FTIR analysis report of some agricultural wastes

Wastes	Major Peaks	Main Finding
POFA (Lim et al., 2015; Salih et al., 2015)	Si-O asymmetric stretching band at 1040 $\text{cm}^{-1}$ , O-H stretching bands of $\text{H}_2\text{O}$ at 3465 $\text{cm}^{-1}$ , H-O-H stretching bands of chemically combined $\text{H}_2\text{O}$ at 1650 $\text{cm}^{-1}$ .	The Si-O asymmetric stretching vibration is the highest intensity of peaks.
SBA (Pereira et al., 2015)	Si-O-Si stretching bands 3036 $\text{cm}^{-1}$ , Organic mater 694 $\text{cm}^{-1}$ , Quartz peaks ( $\text{SiO}_2$ ) at 775 $\text{cm}^{-1}$ , 447 $\text{cm}^{-1}$ .	Organic carbon present at 694 $\text{cm}^{-1}$
BLA (Moisés Frías et al., 2012)	O-H absorption vibration bands 3436 $\text{cm}^{-1}$ , H-O-H deformation- 1635 $\text{cm}^{-1}$ , C-O typical calcite bands at 1100 $\text{cm}^{-1}$ , Si-O Stretching vibration bands-1100 $\text{cm}^{-1}$ bending vibration bands-469 $\text{cm}^{-1}$ .	Crystalline mineralogical phases such as quartz, cristobalite and mainly amorphous silica present.
RHA (Seddighi et al., 2015)	Si-O-H stretching-3450 $\text{cm}^{-1}$ , Absorbed $\text{H}_2\text{O}$ banding 1635 $\text{cm}^{-1}$ , $\text{SiO}_2$ strong asymmetric-1100 $\text{cm}^{-1}$ , symmetric-800 $\text{cm}^{-1}$ , bending 467 $\text{cm}^{-1}$ .	The strong peaks at 1100,800 and 467 $\text{cm}^{-1}$ assign to the asymmetric stretching, the symmetric stretching and bending mode of $\text{SiO}_2$ , respectively.

**Note:** SBA - sugarcane bagasse ash; BLA - bamboo leaf ash; RHA - rice husk ash

The main intense peak of Si-O stretching band is observed to be in the range of 1000 to 1100  $\text{cm}^{-1}$  in the most of the agricultural waste. The absorbing or deforming water bands which are common in agricultural waste is to found to occur at 1650  $\text{cm}^{-1}$ . The organic matter of SBA shows a band at 694  $\text{cm}^{-1}$  (Pereira et al., 2015). Studies on FTIR spectrum of POCP is limited. FTIR data provides the information of the crystallinity of waste materials. The crystallinity can be defined as the fraction of crystalline materials in a mixture of crystalline and non-crystalline materials. However, the amorphosity is inversely proportional to crystallinity of materials. The degree of crystallinity has a significant effect on pozzolanic activity because only amorphous materials can take part in the pozzolanic reaction (Wang et al., 2014). The crystallinity cannot be evaluated directly, it is determined from the crystallinity index. Previous research shows that FTIR spectra can provide a useful assessment of the crystalline state of quartz. The crystallinity index of quartz calculated by comparing the intensity of the characterization peak at 695  $\text{cm}^{-1}$  and 778  $\text{cm}^{-1}$  of tetrahedron of  $\text{SiO}_4$  (Saikia et al., 2008). The performance of waste materials in concrete or blended cement mortar is largely related to the pozzolanic activity which depends on the crystallinity of minerals (Calligaris et al., 2015).

There is limited literature available on the crystalline nature of the minerals, thermal behaviour, organic carbon content and FTIR analysis data of POCP. Besides, POFA is another form of waste in a palm oil mill which has a significant amount of organic carbon and shows pozzolanic activity.

### **2.3 Effect of Thermal Activation**

The effect of heat energy on the chemical composition, mineralogy, morphology and organic carbon content of palm oil mill waste and similar waste materials and their influences on the compressive strength development has been described in this section.

### **2.3.1 Thermal Activation Process**

The thermal activation method is being used by many researchers for increasing the activity of waste materials (Alam et al., 2014; Chandara et al., 2012; Lim et al., 2015). The activation process ultimately leads to excess utilization of waste in cement-based applications. The mechanical and thermal activation methods are used for the development of the quality of the wastes (Alam et al., 2014; Chandara et al., 2012; Lim et al., 2015). The alkali activator is also being used by researchers at the time of mortar preparation, which also improves the activity of waste (Sajedi & Razak, 2010). The activity of POFA is increased by reducing the particle size through grinding. The ground waste gets enough active surface area for showing their reactivity. However, the mechanical activation method cannot remove the organic carbon from wastes which has a negative effect on the compressive strength and fluidity of concrete. The unburned carbon of POFA can be removed through the thermal activation (Chandara et al., 2012; Lim et al., 2015). Moreover, when calcium carbonate is decomposed and the crystal structure of  $\text{SiO}_2$  is disordered through thermal activation. This disordered  $\text{SiO}_2$  is effective to show pozzolanic reactivity. This process will increase the pozzolanic activity of clay (Alam et al., 2014). The thermal activation method is more convenient, easy and low cost method to reduce organic carbon from wastes. A programmable furnace has been used for thermal activation of POFA without particle agglomeration (Chandara et al., 2012).

### **2.3.2 Chemical Composition**

The thermal activation method plays an important role which affects the chemical composition of the waste material. The chemical composition of fly ash varies considerably with the physical and chemical properties of the coal as being burned in power plant and also with the combustion condition. The main ingredients of fly ash are



characterized as silica, alumina, calcium and ferrous oxides (Li et al., 2006). POFA is another form of waste produced as a result of incomplete burning of palm oil shells or fibres at palm oil mills. The chemical composition of POFA is a mixture of silica, aluminum, calcium, ferrous and potassium oxides (Chandara et al., 2010). POFA is composed of  $\text{SiO}_2$ ,  $\text{Al}_2\text{O}_3$ ,  $\text{Fe}_2\text{O}_3$ ,  $\text{K}_2\text{O}$ ,  $\text{CaO}$  and  $\text{MgO}$  at a content of 48.9%, 2.71%, 6.54%, 7.13%, 13.89% and 2.74%, respectively (Noorvand et al., 2013). Researchers found that the percentage of inorganic oxides increased through thermal activation of POFA, clay as well as paper sludge (Ferreiro et al., 2013; Noorvand et al., 2013). The thermal activation process was found to reduce the moisture and organic matters from POFA. This factor is responsible for changing the chemical in POFA and fly ash. The increment in oxide percentage depends on the organic matter content in paper sludge. The thermal activation process also removes the organic materials, moisture and carbonate of paper sludge, significantly. This is the reason for increasing inorganic oxides content in the thermally activated paper sludge compared to raw paper sludge (Ferreiro et al., 2013).

### **2.3.3 Structure of Minerals**

The XRD technique has been used not only for the phase identification of crystalline materials, but also to provide the useful information regarding the crystalline structure of waste material (Snellings et al., 2014). It is possible to predict the crystallinity of the material from the XRD pattern. If a hump occurs in the angular  $2\theta$  range of  $10^\circ$  to  $35^\circ$  indicating that materials possess pozzolanic activity (Chancey et al., 2010; Chandara et al., 2010; Kanadasan & Abdul Razak, 2015). The peak structure in XRD patterns of raw and thermally activated wastes predicts the change of crystalline structure of minerals through the heat energy. Previous studies show that the peak structure and wideness changed through thermal activation, which is an indication of the crystalline state of

minerals in clay (Alam et al., 2015; Zeyad et al., 2013). A significant hump can be found in the XRD pattern of POFA in the  $2\theta$  range of  $10-35^\circ$ , and shows the pozzolonic activity (Kroehong et al., 2011; Noorvand et al., 2013). POFA also reduce the heat of hydration in blended cement (Chandara et al., 2012). For optimum replacement of cement, the activity of waste needs to be increased. The pozzolanic activity of some wastes can be developed through the thermal and mechanical treatment which is mainly due to the reduction in the particle size (Fitos et al., 2015; Souri et al., 2015). The pozzolanic activity will increase due to the disorder state of the molecules. Previous studies show that the thermal activation at the temperatures of  $500^\circ\text{C}$  will not change the structure of minerals of POFA which is shown in **Figure 2.4** (Chandara et al., 2010). The ground and thermally treated POFA are designated as GPOFA and TPOFA, respectively in the **Figure 2.4**. The pozzolanic activity of POFA does not increase through activation condition.

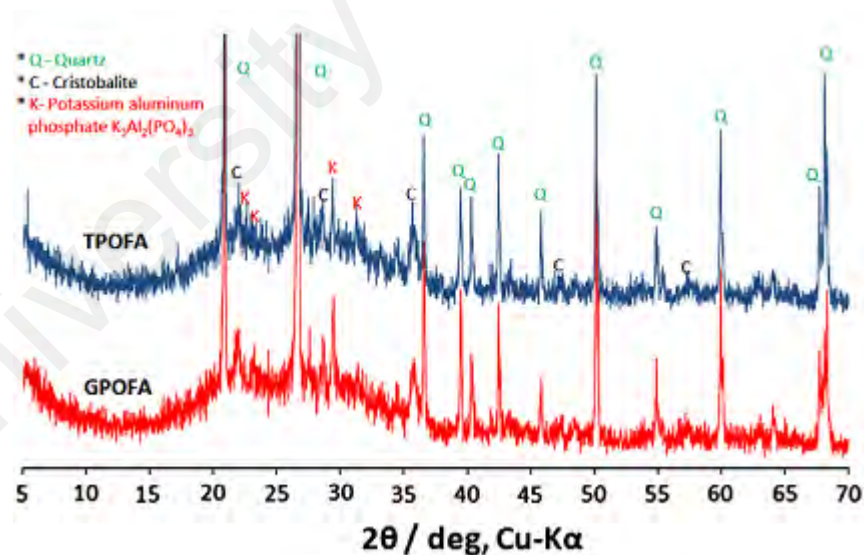


**Figure 2.4:** XRD pattern of GPOFA and TPOFA (Chandara et al., 2010)

### 2.3.4 Microstructure and Morphology

The performance of waste materials in concrete or mortar depends on the microstructure and morphology. These characteristics of the waste materials change through

the thermal activation energy. The thermal activation method is found to reduce the unburned carbon with the morphological change of POFA (Zeyad et al., 2012). The fine particles of POFA accumulate near the aggregate-paste matrix interface and also modify the particle packing density of the matrix which ultimately improve the internal bonding energy (Stroeven & Stroeven, 1999). Microstructure investigation revealed that POFA (which is free from the organic carbon) together with nano silica increased the density of mortar matrix. As a result, compressive strength will increase significantly (Noorvand et al., 2013). Ground POFA (GPOFA) is produced through grinding in a ball mill, whereas treated POFA (TPOFA) is obtained by heating in a programmable furnace at 500°C for 1 hour without agglomeration of particles.

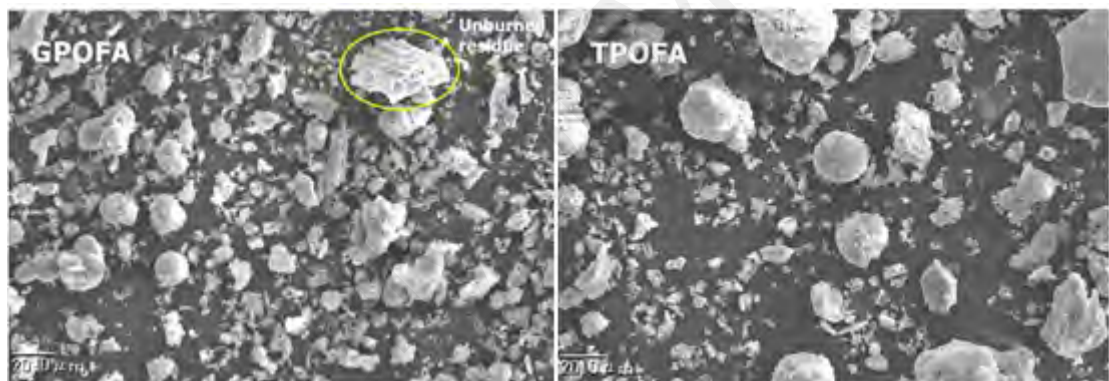


**Figure 2.5:** Micrographs of GPOFA and TPOFA (Chandara et al., 2010)

The SEM micrograph of GPOFA and TPOFA are presented in the **Figure 2.5**. The figure shows that the organic carbon of POFA is removed through thermal activation. The particle size of POFA is also reduced through thermal activation. This is due to the unburned carbon particles, as identified in past literature (Chandara et al., 2010). The organic carbon is removed from the wastes by using heat energy. This also changes the morphology of samples where the porosity is significantly reduced.

### **2.3.5 Organic Carbon**

The organic carbon of waste material has significant influences on the compressive strength of the cement mortar or concrete. There exists a strong possibility to content the organic carbon in the POCP because POC is produced as a result of the incomplete burning of the palm oil fruit bunches, fibre and shell. The palm oil mill waste, i.e. fibre and shell consist of the sugar based polymer like cellulose and hemicelluloses which combines with lignin, protein, starch and inorganic phases (Hesas et al., 2013). The composition of cellulose, hemicelluloses, lignin and extractives are 32.6%, 22.1%, 42.3% and 3.0% of palm oil plants (Lahijani et al., 2012). The factors such as age of plant, climatic condition, soil composition, water quality of the area where the plants are grown have a significant effect on the carbon based-materials in the plants. From the analysis of the oil palm shell (OPS), it was found that TOC was 41.33% (Idris et al., 2010). The literature shows that TOC in POFA was 6.01%. The total organic carbon (TOC) content also depend on the availability of oxygen and incineration time in the boiler. This organic carbon is the result of incompletely burning of shell and fibre in the boiler. The incomplete burning is due to the availability of oxygen and retention time of waste in burning zone of the boiler. Thermal activation was carried out at relatively low temperature of 500°C for 1 hour and the organic carbon was found to decrease from 6.01% to 0.07% of POFA (Tangchirapat et al., 2007).

### **2.3.6 Compressive Strength**

In recent decades, environmental related issues have motivated researchers to focus on finding a new supplementary cementitious materials from wastes and enhance the quality of waste materials, especially intended for using in cement-based applications (Alam & Gul, 2015; Noorvand et al., 2013). Additinally, the addition of waste as a supplementary material in concrete or mortar reduces the compressive strength due to

reduction in the concentration of Portlandite (Ferreiro et al., 2013; Karim et al., 2012; S. Lee et al., 2010).

Several significant studies have focused on the optimization of thermal activation process and effect of heat energy on waste properties, i.e. unburned carbon content, morphology, chemical composition, crystalline state of minerals and their influence on cement-based application. **Table 2.3** presents the thermal activation effect on properties of waste and their influence on cement-based applications. The unburned carbon in POFA (6.01%) will cause problems in the fluidity and the development of compressive strength because the absorption capability of unburned carbon for super plasticizer (SP) is higher compared to other ingredients of cement-based materials. Secondly, this organic carbon has a negative effect on the compressive strength as it increases the porosity of the cement matrix (Chandara et al., 2010; Lee et al., 2003). Thermally activated FA was used to increase the fluidity, sulphate and chloride resistivity of mortar (Ha et al., 2005). The clay and paper sludge contain a significant amount of calcite and kaolin. These wastes when decomposed using the heat energy can be used to produce new oxides which positively influence the strength development (Alam & Gul, 2015; Amin et al., 2016; Vegas et al., 2009). Organic carbon free honeycomb briquette ash is found to increase the compressive strength of geopolymeric bodies up to 65.6 MPa (Lee et al., 2010). Utilization of fly ash having a high loss of ignition will increase the water demand that ultimately decreases the compressive strength (Atiş et al., 2005).

**Table 2.3:** Thermal activation effect on compressive strength

Wastes	Thermal activation	Major change occurred	Main effects	Refs.
POFA	500°C for 1 hour	Reduced unburned carbon content	Fluidity & compressive strength increased	(Chandara et al., 2010)
POFA	500°C for 1.5 hours	Particle size becomes smaller, removed unburned carbon and increased the glassy phases	Long-term compressive strength was significantly increased	(Zeyad et al., 2012)
Clayey waste of Art paper sludge	600–650°C for 2 hours	$\text{Ca(OH)}_2 \rightarrow \text{CaO} + \text{H}_2\text{O}$ $\text{CaCO}_3 \rightarrow \text{CaO} + \text{CO}_2$	Normal consistency for water and compressive strength increase and decreases the setting times	(Ferreiro et al., 2013)
Paper de-ink sludge	700°C for 2 hours	Kaolin converts to meta kaolin and decomposition calcite & talc	Increase compressive strength slightly after 7 days	(Vegas et al., 2009)
Clay	600°C for 3 hours	Kaolinite was converted to metakaolinite	20% replacement show optimum result on strength development, corrosion and chloride resistivity	(Amin et al., 2016)
Kaolin containing mica	700 °C and 750 °C for 3 hours	Partial kaolinite and complete mica phase amorphization	Pozzolanic activity increased	(Ilić et al., 2016)
Natural kaolinitic clay	800°C for two hours	Structural disorder happened and increased pozzolanic activity	Good compressive strength at 25% replacement	(Alam et al. & Gul, 2015)
Honeycomb briquette ash	Froth flotation	Remove unburned carbon	Compressive strength of the geopolymers body increased to 65.6 MPa	(Lee et al., 2010)
Fly ash	900°C for 1 hour	Remove unburned carbon	Suffered severe corrosion, when the carbon level in fly ash was increased	(Ha et al., 2005)

The effect of thermal activation process on the physical properties, chemical composition, morphology, TOC (total organic carbon) content and the crystalline structure of minerals of POCP and their influences on compressive strength development of cement mortar has not been studied yet.

## **2.4 Pozzolanic Activity**

A number of studies have introduced new supplementary cementitious materials produced from wastes for cement-based applications. The reactivity of waste is associated with its' pozzolanic activity. Palm oil clinker (POC) is the most substantial waste material discarded from palm oil mills in Malaysia (Ahmad et al., 2007). According to Malaysia Cement Industry Report 2015, the expansion of the construction activity in Malaysia has increased drastically in the last few years. As the government has been spending a great deal of money on infrastructure development projects, this has created extra pressure to the cement industries. This section will include the chemical composition for pozzolanic reactivity, amorphisity and micro analytical technique for assessing the pozzolanic reactivity of wastes or by-products of industries which had been done in the previous studies.

### **2.4.1 Chemical Composition**

The utilization of the pozzolanic materials in cement production has increased significantly in recent years. The cement industries are looking for new agricultural waste materials instead of natural pozzolan. Several studies have been reported on the various agricultural waste such as rich husk ash (Soares et al., 2015), elephant grass ash (Cordeiro & Sales, 2015), sugarcane bagasse ash (Bahurudeen & Santhanam, 2015), and biomass ash (Demis et al., 2014) that has been used for the partial replacement of OPC in concrete as a pozzolanic material. Additionally, the pozzolanic reactivity of waste will increase through the mechanical (Jaturapitakkul et al., 2011), thermal (Kılıç & Sertabipoğlu, 2015) or combined mechanical and thermal activation methods. Recently, few researches have been conducted on the utilization of POC as an aggregate in different types of concrete for various application purposes. It was found that the mechanical properties of lightweight concrete can be enhanced by using POC (Ahmmad

et al., 2015). The application of POC as an aggregate in concrete has already been proven, but the pozzolanic activity of POCP has rarely been reported. The other form of palm oil mill waste named palm oil fuel ash (POFA) shows the pozzolanic activity and also increases its' reactivity by the reduction of particle size (Kroehong et al., 2011; Lim et al., 2015). The pozzolanic activity of waste depends on the chemical composition, amorphisity, and particle size of the material (Hamidi et al., 2013; Mirzahosseini & Riding, 2014; Sanjuán et al., 2015). A recent work has been conducted for measuring the chemical composition of POCP which were collected from different areas in Malaysia. The variation of the chemical composition in POCP depends on the feeding ratio in a boiler, the burning condition of the boiler, and the geological condition of the respective area where the palm oil tree was grown (Kanadasan et al., 2015). The variation of the pozzolanicity of POCP basis on chemical composition is presented in **Table 2.4**.

**Table 2.4:** Pozzolanicity of POCP based on chemical composition

Name of states	SiO <sub>2</sub>	Fe <sub>2</sub> O <sub>3</sub>	Al <sub>2</sub> O <sub>3</sub>	SiO <sub>2</sub> + Fe <sub>2</sub> O <sub>3</sub> + Al <sub>2</sub> O <sub>3</sub>
Kedah	65.10	6.34	3.28	74.68
Kelantan	73.31	6.13	6.00	85.44
Terengganu	72.64	3.89	5.18	81.71
Penang	69.91	5.15	4.15	79.21
Perak	74.29	2.09	3.11	79.49
Pahang	60.79	15.64	7.27	83.7
Negeri Sembilan	65.64	14.41	7.56	87.4
Selangor	64.84	4.19	3.42	72.45
Melaka	57.41	10.11	4.95	72.47
Johor	69.05	3.71	4.73	77.49
Sabah	62.05	2.20	1.42	65.67
Sarawak	62.52	1.10	0.82	64.44

From the **Table 2.4**, it is apparent that most of the POCP which were collected from different states in Malaysia have pozzolanic activity except that collected from Sabah



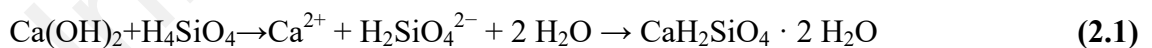
and Sarawak. The lower limit of these oxides show that the pozzolanic activity is 70%. This observation is based on the summation of SiO<sub>2</sub>, Fe<sub>2</sub>O<sub>3</sub> and Al<sub>2</sub>O<sub>3</sub> present in POCP. The reactivity of SiO<sub>2</sub> largely depends on its' crystalline nature.

#### 2.4.2 Amorphisity

The chemical, physical, and morphological characterizations of newly introduced pozzolanic materials are essential for ascertaining its' pozzolanic reactivity (Adrián Alujas et al., 2015; Tantawy et al., 2015). The pozzolanic activity of new waste material largely depends on the amorphisity of the mineral. Only amorphous SiO<sub>2</sub> can participate in a chemical reaction with portlandite (Uchima et al., 2015). Semi quantitative XRD observation revealed that the quartz, cristobalite, quartz low, gehlenite, amorphous present in POCP are approximately 20.0%, 2.9%, 0.5%, 31.7% and 39.9%, respectively (Kanadasan & Abdul Razak, 2015).

#### 2.4.3 Micro Analytical Studies

The pozzolanic reaction is basically an acid-based reaction between the calcium hydroxide, also known as Portlandite (Ca(OH)<sub>2</sub>) and silicic acid (H<sub>4</sub>SiO<sub>4</sub> or Si(OH)<sub>4</sub>). This reaction can be presented as **Equation (2.1)**;



As shown above, the product of chemical reaction is calcium hydroxide hydrate. The stoichiometry of the reaction may differ according to the pozzolanic materials that were involved in this reaction. There are a number of micro-analytical techniques, namely XRD (Calligaris et al., 2015), TGA (Jacoby & Pelisser, 2015), NMR (Fernandez et al., 2011), SEM (Shi et al., 2015), and FTIR (Moraes et al., 2015) which can be used to investigate the pozzolanic reaction stated above. XRD technique was used to assess the

pozzolanic activity by comparing the intensity of mineralogical phase, mainly portlandite present in OPC and pozzolanic materials blended cement paste at different curing times, which also helped to investigate the amorphisity of materials (Adrián Alujas et al., 2015; Adrian Alujas et al., 2015). The dehydrolaxation of  $\text{Ca}(\text{OH})_2$  appeared in the range of 440-500°C in thermogravimetric analysis. However, the relatively lower weight loss of an OPC paste compared to blended cement paste is a logical indication of pozzolanic activity (Khalil et al., 2014) and the intensity of the vibration bands of Si–O, O–H, O–C–O and C–S–H of the cement paste conducted at different curing age showed the state of the pozzolanic reaction (Moraes et al., 2015).

#### **2.4.4 Strength Activity Index**

The performance of the pozzolanic activity can be evaluated by calculating the strength activity index (SAI) (Cordeiro & Sales, 2015). This is a physical way to evaluate pozzolanic activity by comparing compressive strength with OPC at the curing age of 7 and 28 days. A number of researchers had used the strength activity index method for the determination of the pozzolanic properties of different materials (Alam et al., 2015; Lim et al., 2015). The strength activity index of the waste material can be calculated according to ASTM method. The compressive strength of 30% additives blended cement mortar at curing age of 28 days will be more than 75% to fulfil the requirement of the standard ASTM C 311-13 in order to show the pozzolanic activity. The increase in SAI at 28 days may be accredited to the reaction of the active phase with Portlandite produced as a result of cement hydration. Also, the addition of waste will cause a decrease in the compressive strength at the curing age of 7 days due to the dilution effect and delay of pozzolanic reaction. The strength activity index of ground POFA (GPOFA) (Lim et al., 2015), ultra fine POFA (UPOFA) (Lim et al., 2015), fly

ash (Jaturapitakkul et al., 1999) and thermally activated clay (Alam et al., 2015) were 84, 105, 117 and 99, respectively.

The analysis of the chemical composition and mineralogical data available in the literature predict that POCP may be a pozzolanic material. Thus, further investigation is necessary for the conformation of the pozzolanic reactivity of POCP.

## **2.5 Fresh and Hardened Properties**

The effect of the waste material characteristics on setting and hardening properties of cement is an important consideration for needed to be studied supplementary cementitious material. However, the incorporation of waste as supplementary material in cement-based applications may affect the setting time, expansion and hardening properties of the concrete or mortar. This section will discuss the effect of the characteristics of waste on setting and hardening properties of the cement and sustainability parameters.

### **2.5.1 Water Consistency and Setting Time**

The effect of supplementary materials on setting and hardening performance of concrete, cement paste as well as mortar largely depends on the characteristics of admixture. Palm oil clinker is a waste material which is significantly discarded from palm oil mills (Garcia-Nunez et al., 2016; Siew et al., 2008). The feasibility of palm oil clinker powder (POCP) waste in cement-based significantly depends on the influence of its characteristics on the setting and hardening properties of the cement.

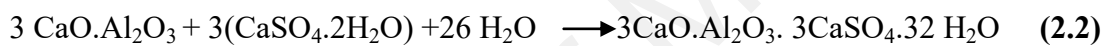
Previous studies show that the palm oil clinker (POC) consists of a number of inorganic oxides. The content of inorganic oxides in POC is increased through the burning process of the boiler section in a palm oil mill. The burning system enriches

the suitability for using POC in cement-based applications rather than municipal solid waste (Li et al., 2012). Waste material such as ladle slag (Serjun et al., 2015), basic oxygen furnace steel slag (Zhang et al., 2011), palm oil fuel ash, rice husk ash (Rukzon & Chindapasirt, 2009), sewage sludge ash (Pavlik et al., 2016), coal bottom and fly ashes are also produced by the burning system. Although, all these wastes were obtained through burning route, there exist a lot of characteristic differences. This is mainly due to the type of raw materials used as well as the burning condition. Previous studies found that the setting and hardening behaviour of the blended cement is influenced by the characteristics of baggage ash, MSWI bottom ash, POFA, zeolitic tuff, perlite, steelmaking slag, pumic ash, volcanic ash, corn cob ash and coal mining waste (Adesanya & Raheem, 2009; Erdem et al., 2007; Frías et al., 2012; Ganesan et al., 2007; Hossain, 2003; Kourounis et al., 2007; Li et al., 2012; Singh et al., 2000; B. Yilmaz & Ediz, 2008).

The water demand for normal consistency depends on the chemical structure, specific surface area and porosity of the cement admixtures (Lea et al., 1970). The analysis of the results for other wastes which are available in the literature found that the water demand varies based on several characteristics of adding materials. The water consistency increased in the blended cement due to the large particle size (Erdem et al., 2007; Ganesan et al., 2007; Singh et al., 2000; Turanli et al., 2004; Yilmaz & Ediz, 2008), hygroscopic nature (Ganesan et al., 2007; Singh et al., 2000) and microspores (Ghofrani et al., 2015; Tangchirapat et al., 2007; Yilmaz et al., 2007), amorphisity (Öner et al., 2003; Turanli et al., 2004), chemical composition (Öner et al., 2003; Rai et al., 2002) and  $\text{Ca}^{+2}$ ,  $\text{Pb}^{+2}$ ,  $\text{Cd}^{+2}$  and  $\text{Cu}^{+2}$  ions containing minerals (Li et al., 2012) in the supplementary materials. However, the water demand will decrease in the blended cement due to the dilution factor (Adesanya & Raheem, 2009; Hossain et al., 2003), mineralogical and chemical composition (Kourounis et al., 2007) of the adding

materials. The water demand of the activated coal mining waste blended cement will increase up to 10% replacement level because of the high absorption of water molecules by the active fine particles and reduced by increasing of the replacement level due to the effect of the heavy metals content in activated mining coal waste (Frías et al., 2012).

The setting behaviour of concrete or mortar or cement paste is controlled by adding the gypsum ( $\text{CaSO}_4 \cdot 2\text{H}_2\text{O}$ ) as well as the tricalcium aluminate ( $\text{C}_3\text{A}$ ) content in the cement. The function of gypsum is to delay the hydration reaction by forming the ettringite with the active phases of OPC clinker as shown in the reaction presented in **(Equation (2.2))**.



The early reaction rate of cement depends on the ionic species ( $\text{Ca}^{+2}$ ,  $\text{SO}_4^{-2}$ ,  $\text{OH}^{-1}$  and  $\text{CO}_3^{-2}$ ) that are available in the system to make barrier over the grains of the aluminates and ferrite phases. The availability and activity of these ions are governed by few factors such as allocation of  $\text{Al}_2\text{O}_3$  in the clinker phases, the particle size, the quality and quantity of the gypsum. Additionally, the setting time of the blended cement is influenced by the particle size, specific surface area and mineralogical structure of the supplementary materials (Lea et al., 1970). Literature survey shows that the setting time in blended cement will increase due to the bigger particle size (Tangchirapat et al., 2007), high porosity (Tangchirapat et al., 2007), hygroscopic nature (Ganesan et al., 2007; Singh et al., 2000), low lime content (Adesanya & Raheem, 2009), mineralogical composition (Yılmaz & Ediz, 2008), amorphous mineral content (Öner et al., 2003; Turanli et al., 2004), high content of the  $\text{Ca}^{+2}$ ,  $\text{Pb}^{+2}$ ,  $\text{Cd}^{+2}$  and  $\text{Cu}^{+2}$  ions (Li et al., 2012) in supplementary materials. Furthermore, the dilution effect also plays an important role in the rate of hydration reaction (Asavapisit & Ruengrit, 2005; Erdem et al., 2007;

Ganesan et al., 2007; Kourounis et al., 2007; Singh et al., 2000). A few properties including active lime content (Aruntaş et al., 2010; García et al., 2008), ultra fine particle size (Asavapisit & Ruengrit, 2005), pseudomorphic layer (Rai et al., 2002) of the supplementary materials accelerate the rate of hydration reaction. Previous studies show that the setting time of the zeolitic tuff blended cement will increase up to 10%, then decrease at higher replacement level due to the diffusion-controlled effect (B. Yılmaz et al., 2007). The setting time is high up to 10% replacement level of OPC by coal mining waste which is a reflection of the greater fineness of the supplementary material. Raising the percentage of activated coal waste from 10% to 20% in the blended cements will delay the initial setting time slightly which is due to low concentrations of heavy metals such as cadmium and nickel in coal ash (Frías et al., 2012).

### **2.5.2 Volume Stability**

The effect of the supplementary materials on the volume change of concrete or mortar is an important consideration for developing new blended cement. The sound cement will not expand at the time of drying and has no chance to develop a crack in the concrete. The expansion is caused by the excessive amount of the active free lime (CaO) or magnesia (MgO) or SO<sub>3</sub> (B. Yılmaz & Ediz, 2008). Previous studies found that the soundness of the granulated blast furnace slag (GBFS) blended cement increased with the increasing replacement levels for its' mineralogical composition (Öner et al., 2003). Whereas, the activated coal mining wastes did not interfere in the volume stability of the blended cement ( Frías et al., 2012).

### 2.5.3 Rheological Properties

The rheological behaviour will directly influence the microstructure of mortar or concrete. The rheology of OPC and 30% limestone blended cement pastes are observed to be almost similar (Montes et al., 2013). The organic carbon of POFA will reduce the fluidity of blended cement paste. This is due to the excess absorption capacity of the unburned carbon to super plasticizer (SP) (Chandara et al., 2010). The early aged compressive strength will decrease with the raising of the replacement levels due to the dilution effect as well as chemical and mineralogical composition of the waste materials. The GBFS contain the  $C_2S$ ,  $C_3S$  and  $C_3A$  phases, but it is in low quantity compared with OPC clinker which takes part in hydration reaction and influences the fluidity of paste and concrete (Wang et al., 2011).

### 2.5.4 Mechanical Properties

The mineralogical features of the OPC clinker, pozzolanic reactions, particle size, reactive  $SiO_2$  ratio and water demand of the composite or blended cement are responsible for the compressive strength of the cement which is a function of hardened properties (Lea, 1970). The porous nature of the siliceous waste materials causes of the increasing water demand, which ultimately leads to decrease in the compressive strength (Kocak & Nas, 2014). The compressive strength will decrease with rising replacement levels, which is due to the dilution effect (Erdem et al., 2007) as well as chemical and mineralogical composition (García et al., 2008; Rai et al., 2002) of the supplementary materials. Slag contains dicalciumsilicate ( $C_2S$ ), tricalciumsilicate ( $C_3S$ ) and tricalcium aluminate ( $C_3A$ ) phases, but the content is less compared with OPC clinker which takes part in the hydration reaction (Siddique & Bennacer, 2012; Wang et al., 2011) and develop the compressive strength. The reactive  $SiO_2$  of wastes reacts with liberated  $Ca^{+2}$  ions in cement-based system to form C-S-H gel (Kocak & Nas, 2014)

which in turn will develop compressive strength significantly in later age (Turanli et al., 2004). Palm oil, fuel ash (POFA) is another form of waste of palm oil mill which shows pozzolonic activity (Chandara et al., 2012; Noorvand et al., 2013). The porosity of the supplementary materials increases the air content or porosity of the concrete or mortar matrix that causes the reduction of the compressive strength (Tangchirapat et al., 2007). The 28 days compressive strength is higher at 10% replacement level, whereas, 90 days compressive strength is almost similar with OPC resulting from the effect of the weak pozzolanic activity of activated coal mining waste (Frias et al., 2012). Previous study also found that the low compressive strength in early aged of siliceous wastes blended cement is due to the lack of sufficient portlandite (CH) to react with available reactive SiO<sub>2</sub> in the reaction medium (Yilmaz et al., 2007). Finally, it is clear that the fine, active, nonporous particles of the supplementary materials can develop the density of the interfacial transition zone among the aggregate and paste which ultimately leads to strength development.

### **2.5.5 Sustainability and Resource Conservation**

Increase in cement production without increasing the environmental problems is a big challenge to the modern Portland cement industries. The Portland cement producers are responsible for the emission of about 5-8% of the total global CO<sub>2</sub> emission which is a very concerning issue due to environmental facts (Coskun, 2011; Snels et al., 2014), and cement production will increase from 2,540 million tonnes (Mt) in 2006 to between 3,680 Mt and 4,380 Mt in 2050 (Hasanbeigi et al., 2013). As a result, the natural resources of OPC clinker will decrease due to the fulfillment of the uprising demand of OPC. The sustainable waste management in any country largely depends on the strong commandments of the managing authority of the country as a result the huge expense associated with the waste separation and reduction (Permana et al., 2015). It is



very difficult in a low income city to spend huge money to import the modern technology for the purpose of waste separation and recycle. The public awareness is also a factor to achieve the goal of sustainable waste management. The solid waste management in developing countries is becoming a demanding assignment (Omran et al., 2009; Saeed et al., 2009) as a result of their rapid urbanization (Murad & Siwar, 2007). In addition, the quantity of solid waste increases significantly with the development of a country (Moh & Manaf, 2014). A target was set in Malaysia to achieve a goal within 2020 for sustainable waste management. Generally, the landfill is a common and cheaper method for solid waste disposal rather than incineration. The current landfill sites for solid waste disposal in Malaysia have become saturated or exceed the highest capacity. Introducing new landfill sites are not easy due to the deficiency of land and the enhancement of the price of land. The recycling of wastes is not effectively executed in Malaysia for waste disposal compared to Singapore due to their public awareness. With the current progress, it is not possible to achieve the recycling target of 22% by 2020 (Periathamby et al., 2009). The incorporation of waste materials of other industries as raw materials in cement factory can be a way to achieve their goal of sustainability. Previous studies show that the incorporation of waste in cement production reduced the manufacturing cost and environmental contamination. The utilization of incinerated sewage sludge in blended cement production decreased energy consumption by approximately 10% of the replacement level of 10%. The greenhouse gas emission was reduced twenty times compared with the Portland cement production and also had a significant economic advantages (Pavlik et al., 2016). The emission of greenhouse gases (GHG) is directly related to the proportion of clinker used in cement production at industrial practices. The percentage of addition of fly ash and slag with ordinary Portland cement clinker for cement production also ensures the extent of cost reduction (Etetim et al., 2013). The utilization of oxygen furnace steel

slag in blended cement is supportive to save natural resources as well as energy, reduction of the CO<sub>2</sub> emissions and expenditure (Zhang et al., 2011). A trial basis investigation in industrial scale for the addition of polymer which obtained from palm oil waste in cement production showed that the production increased by 8.3-27.5% efficiency in saving and the grinding energy was in the range from 7.7 to 21.5% of ordinary Portland cement. In addition, the strength increased within the range from 7.31 to 34.8% at 2 days, and from 3.85 to 57.58% at 28 days cured. Research also observed that the incorporation of fly ash in cement reduced the CHG and toxic gasses at range between 21.90 to 90.0% (Chuan et al., 2015).

The characteristics of the supplementary materials play a vital role in the setting and hardened behaviour of the blended cement. The feasibility of POCP as a supplementary cementitious material largely depends on these properties of the blended cement. The effect of the characteristics of POCP on the setting and hardened properties of the cement will be explored in this study. These are the requirements of the different standard of cement in the world. However, a conclusion can be drawn that the addition of waste or by-product from industry as supplementary cementitious materials in cement production is an effective way to achieve the target of sustainability of the cement industry.

## **2.6 Potential Radiological Hazards**

Relevant technical benefits supporting the potential use of POC as an aggregate in concrete have been documented in recent researches. However, the health hazards resulting from the presence of naturally occurring radioactive materials in POC have not been studied so far. Thus, it is important to assess the concentrations of <sup>226</sup>Ra, <sup>232</sup>Th and <sup>40</sup>K radionuclides and the potential radiological risk for the incorporation of POC as ingredients of building materials. This section will discuss the radiological

nuclides level in Malaysia earth materials, health hazards and the investigating process of other waste which have been used as an ingredient of building materials.

### **2.6.1 Radioactivity in Earth Materials**

A summary of earlier studies on the radioactivity in Malaysian earth materials and water is presented in **Table 2.5**. The presence of naturally occurring radioactive materials (NORMs) in soil, in water and/or in all earth-born materials is shown at heterogeneous distribution. Thus, the levels of natural radioactivity in soil, water, building materials as well as plants in different regions of Malaysia showed a large deviation following the variation of geographical and geological origin (Ahmad et al., 2015). Radionuclide available in soil (Ahmad et al., 2015; Asaduzzaman et al., 2015; Saleh et al., 2013), natural coal (Amin et al., 2013; Đurašević et al., 2014) and water (Ramli et al., 2005) are taken up by plant tissue in the similar way to the uptake of minerals by the plant-root system. The presence of natural radionuclides of uranium, thorium and potassium in oil palm fruits, shell, nut fibre is naturally in low level as like other waste materials which do not create a significant threat to the end users (Ramli et al., 2005). Furthermore, the majority of  $^{238}\text{U}$  and  $^{232}\text{Th}$  and their progenies are not liberated via the burning process, rather they are become enrich in the residual waste materials, i.e. POC and POFA as like as the inorganic oxides (Peppas et al., 2010). A number of chemical and physical change such as the removal of organic ingredients and moisture, which are present in nuts, fibre, shell of palm oil (Aswood et al., 2013) are occurring at the time of the combustion process in the boiler, which either enrich or redistribute the inorganic oxides (Chandara et al., 2012) and radionuclides in POC and POFA.

**Table 2.5:** Radioactivity in soil and water of malaysia

Study Area	Activity concentration (Bq kg <sup>-1</sup> )				Sample	Refs.
	<sup>238</sup> U	<sup>226</sup> Ra	<sup>232</sup> Th	<sup>40</sup> K		
Kinta district, Perak	196 ± 43	----	628 ± 169	475 ± 89	Soil	(Ahmad et al., 2009)
Northern peninsular	--	51±4.3	22±1.9	189±16.5	Soil	(Muhammad et al., 2012)
Cameron highlands, penang	203.8±2.0	---	186.2±3.4	---	Soil	(Aswood et al., 2013)
Pontian district, Johor	--	37 ± 3	53 ± 4	293 ± 14	Soil	(Saleh et al., 2013)
Sungai Petani, Kedah	---	51.1±5.8	78.44±6.4	125.7±7.3	Virgin Soil	(Ahmad et al., 2015)
Sungai Petani, Kedah	---	80±5.8	116.9±7.9	200.7±18.2	Agricultural Soil	(Ahmad et al., 2015)
Northern Malaysia Peninsula	---	57±2	68±4	427±17	Soil	(Almayahi et al., 2012b)
Northern Malaysia Peninsula	---	2.86±0.8	3.78±1.8	152±12	Water	(Almayahi et al., 2012b)
Ontian district, Johor	---	37 ± 3	53 ± 4	293 ± 14	Soil	(Saleh et al., 2013)
Perak State	127 ± 97	---	304 ± 28	302 ± 29	Soil	(Apriantoro et al., 2013)
Standard limit		50	50	500		

## 2.6.2 Health Hazards

The radioactive progenies of <sup>226</sup>Ra (<sup>238</sup>U) and <sup>232</sup>Th can release alpha and/or beta particles followed by gamma-rays until their stable end product of <sup>206</sup>Pb and <sup>208</sup>Pb, respectively. Although, most of the  $\alpha$  and  $\beta$  particles do not have enough penetrating power to come out into the indoor building environment from their concrete medium, majority of the  $\gamma$ -rays go through the concrete matrix without any trouble and comes into the indoor atmosphere of the building (Asaduzzaman et al., 2015). On the other hand, the <sup>238</sup>U and <sup>232</sup>Th sub-series headed by <sup>226</sup>Ra and <sup>228</sup>Ra are responsible to transmute as radon (<sup>222</sup>Rn) and thoron (<sup>220</sup>Rn) via emissions of alpha particles. Since, the <sup>222</sup>Rn and <sup>220</sup>Rn are radioactive inert gases, they can easily come out into the indoor environment from the concrete. Once these gases are in the indoor environment, they

can easily stack-up with the dust particles, and may enter the human body via respiratory systems. Long-termed exposures to elevated levels of low dose radiation from  $^{222}\text{Rn}$  and its' alpha emitting decay progenies can cause lung cancer (Almayahi et al., 2012a). A number health problem arise from the radiation originated from building material. Aside from the general view point that our society pay attention to this issue, a notable number of researchers and many national and global organizations are interested in addressing this issue (Kovler et al, 2012; Omar et al., 2002; Trevisi et al., 2012; Trevisi et al., 2013).

### **2.6.3 Radiological Hazards Investigation**

In order to assess the adverse effect of radiological hazards on human health, several hazard indices have been suggested by a number of investigators. These measures include the absorbed gamma dose rate in the indoor environment and the corresponding annual effective dose, the radium equivalent activity, the external and internal hazard indices, the alpha index (internal index) and the gamma activity concentration (gamma index) (Gupta et al., 2013; Rahman et al., 2013). All the aforementioned hazard indices were calculated for individuals living in domestic dwellings and for individuals at the workplace to evaluate the potential radiation risks arising from the utilization of the waste materials in concrete. The  $\gamma$ -ray spectrometer with HPGe detector is a very effective apparatus which is used by researchers for the assessment of the levels of  $^{226}\text{Ra}$ ,  $^{232}\text{Th}$  and  $^{40}\text{K}$  in the building materials. The relevant data are obtained using 16k MCA and was analyzed by the Gamma-vision 5.0 software in researches (Asaduzzaman et al., 2015).

The radio nuclides level and the possible radiological risks to human health due to the utilization of such materials in building construction are not identified so far. The data will be obtained in this study will help understanding the suitability of POC to be

used as ingredients of construction materials. Also, it will serve as references for future radiological loading of Malaysian environments.

## **2.7 Heavy Metal Levels and Leaching Toxicity**

Palm oil mills produce approximately 5% by weight of the total oil palm waste at bottom of the burning process (800°C-1000°C) as palm oil clinker (Safuiddin et al., 2011). The suitability of POC application in concrete production has been proven by recent studies. Although, this waste is commonly dumped in open land and a portion is disposed by land filling in current disposal practices. However, due to rapid urbanization in recent years, the land filling space has become ever scarce in Malaysia which, in turn has increased the cost of disposal. This type of waste changes the soil composition badly and also contribute to the contamination of ground water (Kanadasan & Razak, 2014) and surface water. In Malaysia, 99% of domestic useable water comes from surface water (Azrina et al., 2011). This section is arranged according to the possibility of heavy metals in POCP, process of characterization, mobility and bioavailability of such waste materials.

### **2.7.1 Possibility of Heavy Metals in POC**

Heavy metals can be transferred into the soil - plant system via a number of ways, i.e. excessive soil erosion, high rainfall, overflowing flood and excessive use of fertilizer for cultivation. Studies have found that magnesium (Mg), nickel (Ni), chromium (Cr), cobalt (Co), and manganese (Mn) can enter from rock such as serpentinitic to soil via soil erosion, high rainfall and overflowing flood methods (Aziz et al., 2015). The long term utilization of phosphate rock fertilizer for the oil palm plantations is an effective way to increase the Zn and Cd content in the soil. The palm oil tree can uptake the Cd and Zn from soil using their root like other minerals and

water (Azura et al., 2012). Since, the burning of palm oil wastes in boiler leads to increase in the trace elements as well as major oxides, i.e.  $\text{SiO}_2$ ,  $\text{K}_2\text{O}$ ,  $\text{MgO}$  and  $\text{Fe}_2\text{O}_3$  due to the reduction of the organic carbon (Kanadasan et al., 2015). There is a possibility of presence of the heavy metals in POC which may leach into the environment.

### **2.7.2 Heavy Metals Characterization**

The heavy metals of the various ashes were determined using inductively coupled plasma mass spectrometry (ICP-MS), atomic absorption spectrometry, instrumental neutron activation analysis and energy dispersive X-ray fluorescence (EDXRF) in previous studies. The comparative analysis found that ICP-MS and EDXRF are more accurate and precise methods than others methods (Mohammed et al., 2016). The FESEM is an apparatus which is mainly used for micro structure investigation of leaching residue (Jang et al., 2015). The FESEM-EDX is used to find out the major element content in particular points or area of the micrograph (Shi et al., 2011). Additionally, the XRD is used to determine crystalline minerals present in the materials (Haiying et al., 2010; PÖYKIÖ et al., 2016). The chemical composition, organic carbon content and mineralogy determination are important to select the experimental condition, extraction reagent; apparatus which can be used for characterization of elements. The ICP-MS is a widely used apparatus for the determination of the heavy metals (Tiwari et al., 2015). Heavy metal mobility and bioavailability depend strongly on their chemical and mineralogical forms in which they occur (Li et al.). Several speciation studies have been conducted to determine the different forms of heavy metals and their total metal content. Studies also indicate that heavy metals favorably concentrate on the particle surfaces (Xie & Zhu, 2013), making them more easily to be extracted from fly ash by the contact with an aqueous solution.

### 2.7.3 Pervious Concrete and Leaching Possibility

Recently, few works have been done on the utilization of POC in pervious concrete (PC). Replacing granite with 25% POC was identified to have a superior performance compared to other replacement levels. The 28 days compressive strength obtained in the range from 3.43 MPa to 9.51 MPa which is acceptable for non structural application such as pedestrian and walkways. **Figure 2.6.** presents a cross section of pervious concrete made with POC coarse aggregate (Ibrahim & Razak, 2016). Heavy metals can easily be transferred into ecosystem and food chain which can cause of human health problem(Shaheen & Rinklebe, 2015). The heavy metal characterizations and leaching toxicity assessment of POC are being very much motivated for environmental contamination, disposal practices and the utilization in pervious concrete.



**Figure 2.6:** Cross section of pervious concrete (Ibrahim & Razak, 2016)



#### **2.7.4 Mobility and Bioavailability**

Heavy metal mobility and bioavailability depend strongly on their chemical and mineralogical forms (Li et al.). The major mineral content in POC is quartz and cristobalite (Kanadasan & Abdul Razak, 2015). In literature, it was found that there is variation in chemical composition and minerals of POC which were collected from different area of Malaysia (Kanadasan et al., 2015). This variation is due to burning condition, raw feeding in boiler and geological condition from where palm oil shells were grown. The leach ability of heavy metals from POC depends on the bonding force of trace element in its matrix. The weak bonded metals fraction can easily leach out with water resulting in change of the pH of soil and significantly contaminate nature (Singh & Kalamdhad, 2013). The toxicity of heavy metals can be calculated as a ratio of water-soluble fraction and total fraction (Pan et al., 2013; Singh & Kalamdhad, 2013). Therefore, by means of the shorter contact time, preliminary information can be obtained about the long lasting leaching process through the Toxicity Characteristic Leaching Procedure (USEPA TCLP 1311, 1992). The test can be carried out for the determination of the heavy metal leaching behaviour in the weakly acidic medium. The characterization of heavy metal of POCP and possible risk has rarely been measured.

#### **2.8 Research Gaps**

From the detailed literature review, several research works have been done to mitigate palm oil mill wastes, i.e. palm oil clinker and palm oil fuel ash are being used as an ingredient of the building materials. The feasibility assessment of palm oil clinker powder as supplementary cementitious materials in cement-based application has rarely been investigated. Research gaps as found from the literature review has been pointed out as follows:

1. Characterization of POCP for utilization in cement-based applications;
2. Thermal activation effect on POCP properties and their influences on strength development of cement mortar;
3. Assessment of pozzolanic activity of POCP;
4. Effect of POCP characteristics on the setting and hardening properties of cement and the incorporation of POCP in cement impact on the cost, greenhouse reduction and saving of the natural resources;
5. Potential radiological hazard of POCP when used as ingredient of building materials;
6. Heavy metal levels and leaching toxicity of POC.

University of Malaya

## CHAPTER 3: MATERIALS AND METHODS

### 3.1 Introduction

This chapter details the sampling procedures and experimental methods for assessing the feasibility of POCP as supplementary cementitious materials in cement-based applications. Micro analytical techniques of POCP characterization, heat energy effect on POCP properties and their influences on strength development and the pozzolanic activity measuring procedures extensively discussed. Moreover, the characterization procedure of radio nuclides and heavy metal levels, and the potential risk of its the incorporation in building materials are also explained in this chapter.

### 3.2 Characterization Procedures

The sample collection area, procedure and physical appearances of palm oil clinker (POC) used in this study are explained in this section. POC was converted to palm oil clinker powder (POCP) through grinding. The characterization of POCP has been done using XRF, FESEM-EDX, XRD, TGA, TOC, SEM and FTIR techniques. The model of the apparatus, photographs and operation condition are also discussed in this section. The physical properties, i.e. particle size, specific surface area and specific gravity analysis methods are also explained.

#### 3.2.1 Material

The POC used in this study was collected from a palm oil mill situated at Dengkil, Malaysia. The location of sample collected is presented in **Figure 3.1**. Samples were collected every alternative hour from the waste outlet of the mill for a month and stored in reserve drum. The collected POC was converted into small size using a jaw crusher then homogenized in rotary pan mixture. This crushed POC is then converted into palm

oil clinker powder through grinding in a ball mill for 6 hours with 150 RPM. The POCP was oven dried in programmable furnaces at 100°C for 3 hours for removal of moisture from the samples. The resultant homogenous powder material thus obtained has been used in this study. The picture of bulk quantity, big chunk of POC and POCP are depicted in the **Figure 3.2**.

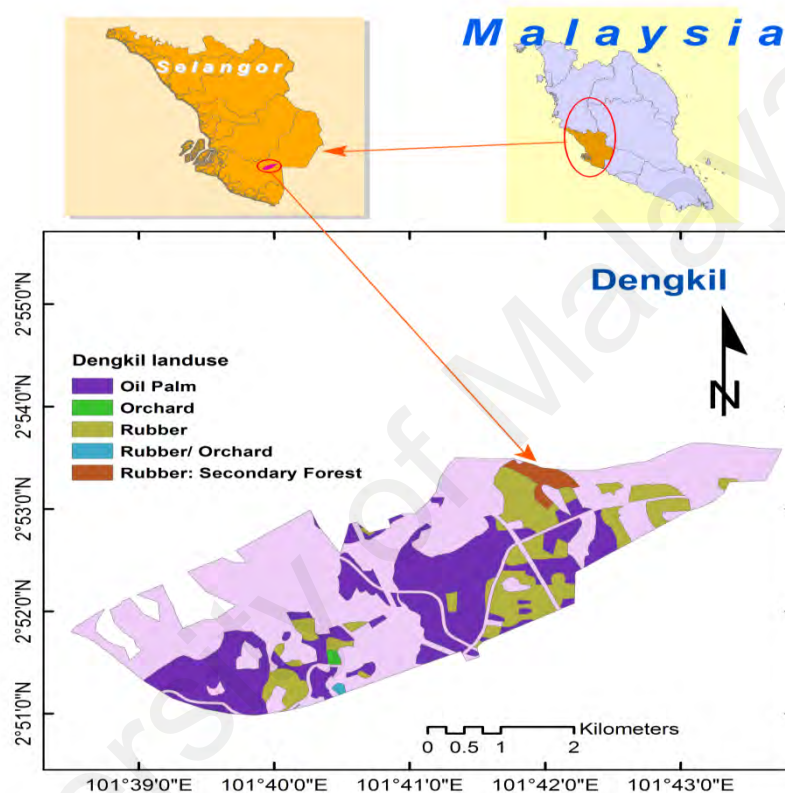


**Figure 3.1:** Selection and sampling area of POC (Dengkil, Malaysia)

The land used map of Selangor, Malaysia is collected from the Department of Agriculture, Malaysia (DOA, 2010). Dengkil is an oil palm plantation estate of Malaysia, where most of the local people engaged in the cultivation of land for palm oil due to its suitable characteristics. It is situated 25 meters above from the sea level, and the climate is humid. The landscape of this area is mainly covered with rain-fed croplands. The characteristic of the soil is high in organic matter and gray in color.



**Figure 3.2:** Photographs of (A) POC, (B) big chunk and (C) POCP

### 3.2.2 Physical Properties

The physical properties measuring methods and apparatus will be described in this section. The specific surface area was determined using the Blaine apparatus and particle size by the Malvern particle size analyzer.

### 3.2.3 Chemical Composition

A fully integrated X-ray fluorescence (XRF) spectrometer, the PANalytical (AXios<sup>max</sup>) with advanced elemental excitation capabilities with sophisticated instrument control and analytical software was used for the chemical composition analysis. The elemental composition of POCP was determined using model of SU8220 of Hitachi Corporation. The model of coating apparatus was Q 150A S of Quorum.

### 3.2.4 Minerals

A multipurpose XRD named “Empyrean” of Penalytical corporation was used for mineralogical investigation. XRD has a cutting-edge technology. Moreover, the Empyrean has a perfect XRD platform to the characterization of materials. The XRD was recorded at room temperature. XRD was operated with a Cu K $\alpha$  X-ray source set to cover a  $2\theta$  range of 10–80° and to record data at 0.04° steps and a speed of 0.004°/minute in this experiment.

### 3.2.5 Crystallinity

The ground samples were dried in a hot air oven at 110°C to remove the moisture content which was absorbed from atmospheres. Using the KBr pellet technique, the sample was mixed with KBr with a ratio of 1:30. The mixture was then pressed into a transparent disc in the dye at sufficiently high pressure. Using the Perkin Elmer Frontier FTIR spectrometer, the infrared spectra of POCP sample was recorded in the region 4000–400cm<sup>-1</sup>. The resolution and accuracy of the instrument was 0.001 cm<sup>-1</sup> and 74cm<sup>-1</sup>, respectively.

### 3.2.6 Thermal Stability

TGA was used to determine the thermal stability of POCP and its’ volatile component of monitoring the weight loss with time when the specimen was heated using TGA/SDTA851. This measurement was carried out of 27.5 mg samples at inert atmosphere by using N<sub>2</sub> gas with flow 100ml/minutes. The heating rate was 10°C/minute from 47°C to 970°C. This technique has been used by many researchers for the investigation of thermal behaviour of waste materials, synthesis product, nano composite, alloy, etc. (Bai et al., 2014; Lim et al., 2015; Mohammadi & Barikani, 2014).

### **3.2.7 Organic Carbon**

The TOC-L series apparatus was used for the determination of the organic and inorganic carbon content in POCP. This apparatus adopts the 680°C combustion catalytic oxidation method, which was developed by Shimadzu and is now used worldwide. This is the highest level of detection sensitivity available with the combustion catalytic oxidation method. The blank check function evaluates system blanks by measuring ultra pure water processed automatically within the instrument.

### **3.2.8 Morphology**

The Phenom tabletop SEM's (Scanning Electron Microscope) were used for morphological analysis of POCP. Next to this, the Phenom series tabletop SEM can be equipped with Pro Suite, which makes measurements of the images easy and reproducible. Acceleration voltage was used at 10kV. The ultimate high-resolution sample holder was used.

## **3.3 Effect of Thermal Activation and Compressive Strength Measurement**

This section explains the designed of experiment to assess the effect of heat energy on POCP characteristics, i.e. microstructure, organic carbon content and morphology and their influences on the development of the compressive strength of mortar.

### **3.3.1 Materials and Methods**

The POC was collected from palm oil mill, located in Dengkil in Kuala Lumpur, Malaysia. The sample preparation process has already been described in the characterization section. The POCP was sieved through 150  $\mu\text{m}$  and the material passing of 150  $\mu\text{m}$  was used for thermal activation. The OPC (CEM I 42.5N) was obtained from a local cement factory. Blaine specific surface area (SSA), specific

gravity and loss on ignition (LOI) were measured according to the ASTM standard. SSA, LOI, specific gravity of cement used were 365 m<sup>2</sup>/kg, 1.21% and 3.15 g/cc, respectively.

### 3.3.2 Thermogravimetric Analysis

TGA is used to determine the thermal stability of POCP. This TGA result is guided to select the thermal activation temperature. The volatile component monitors the weight loss with respect to the time when the specimen is heated. This measurement is carried out using 16.35 mg samples at inert atmosphere using N<sub>2</sub> gas with flow 100ml/minutes. The heating rate was 10°C/minute from 100°C to 950°C. The TGA curve of POCP is shown in **Figure 3.3**. Initially, the process removes water and high volatile (like, 'light' and 'oily') biopolymer from POCP during the heating up to 170°C. The first major mass loss was observed in the temperature range from 340°C to 580°C due to degradation of lignin and cellulose and minimal contribution through the decomposition of CaCO<sub>3</sub>.

The lignin and cellulose of POCP did not burn completely in the boiler of the palm oil mill from where POC was collected. Another minor weight loss was observed within the range of 580°C to 650°C due to the degradation of lignin. It is highly improbable for lignin and cellulose of POCP to be completely burned in the firing zone of a boiler (Nabinejad et al., 2015; Ninduangdee & Kuprianov, 2013; Sen et al., 2015b).



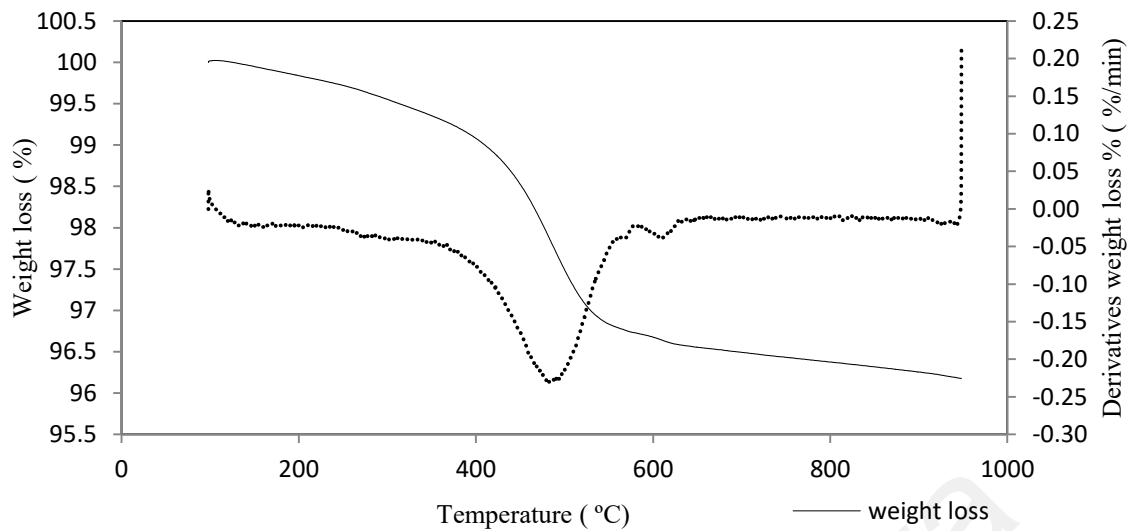


**Figure 3.3:** Thermal analysis of POCP under nitrogen atmosphere

### 3.3.3 Thermal Activation Process

The thermal activation temperature was selected as 300°C, 580°C and 650°C based on TGA analysis report of the POCP in the study. **Table 3.1** presents the thermal activation applied to POCP.

**Table 3.1:** Thermal activation applied to POCP

Designation of activated POCP	Burning temperature (°C)	Retention time (hours)
TPOCP <sub>300</sub>	300	3
TPOCP <sub>580</sub>	580	3
TPOCP <sub>650</sub>	650	3

Thermal activation of POCP samples weighing 500g in silica crucible was carried out in a programmable furnace using a heating rate of 10°C/min. This produces a material without unburned carbon and prevents particle agglomeration as also reported by Chandara et al. (Chandara et al., 2012). POCP was subjected to different heating patterns from room temperature to 300°C, 580°C and 650°C, respectively at the rate of 10°C per minute and kept constant for 3 hours. It was allowed to cool at the same rate

of room temperature in the furnace, as shown in the heating patterns in **Figure 3.4**. The TPOCP<sub>300</sub> was produced through thermal activation according to the pattern 'A'. The TPOCP<sub>580</sub> and TPOCP<sub>650</sub> were also produced according to Patterns 'B' and 'C', respectively.

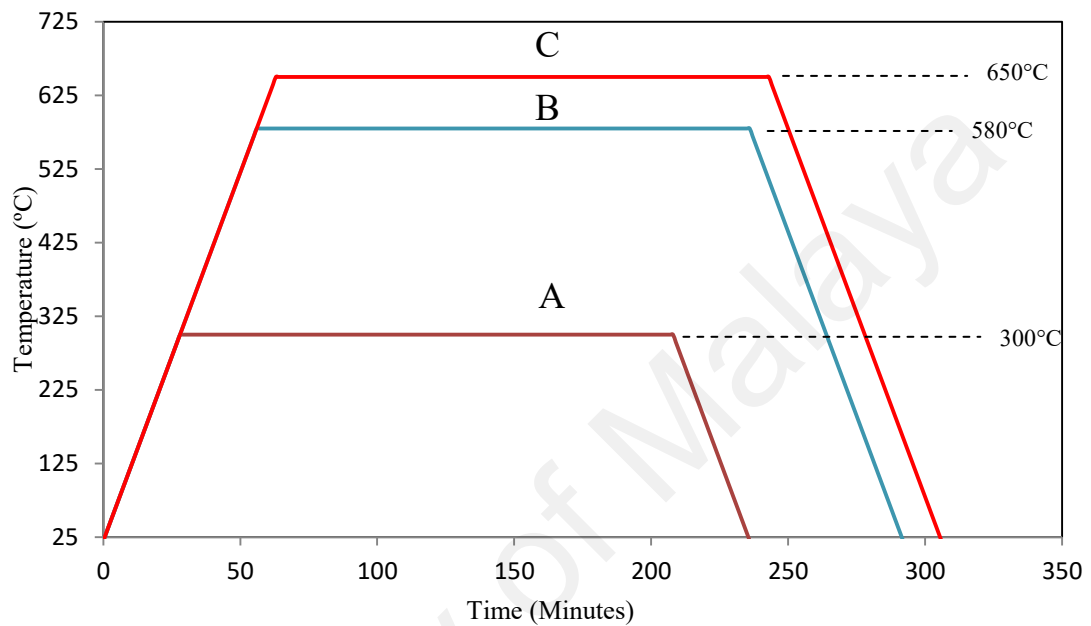


**Figure 3.4:** Heating patterns

### 3.3.4 Micro Analytical Techniques

The change of chemical composition, mineralogy, TOC and morphology of POCP through thermal activation were measured using the XRF spectrometer (Epsilon-5), XRD (Empyrean), TOC-L and SEM (Phenom Pro-Series tabletop), respectively. The operating condition and photographs of the apparatus are already present in the characterization section.

### 3.3.5 Mix Proportion and Curing

The blended cements were prepared under control mixing in a ball mill, to ensure homogeneity by adding 30% POCP or 30% TPOCP and 70% OPC. Particles passing 90

$\mu\text{m}$  were used in the blending process with OPC. The water/binder (W/B) and binder/sand (B/S) ratios used were 0.40, 0.50, respectively, in the investigation of compressive strength of OPC, POCP and thermally activated POCP (TPOCP) blended cement. The sand used in the study is specially graded processed silica sand. Four groups of sand, i.e. 16/30, 8/16, 30/60 and 50/100 were used in the ratio of 0.35, 0.25, 0.2 and 0.2, respectively. The water absorption of mixed sand was 0.35%. The 30 mortars were produced in each batch. Initially, the mixed silica sand was mixed for one minute. Subsequently, cement was put into the mix, followed by 1 minute of mixing. Mixing water was then added to the mix, and the mixing continued for 2 minutes. The required amount of SP was added and mixed for 2 minutes to achieve a flow of  $140 \pm 10$  mm. The molds were filled with fresh mortar at two layers. The measurement of flow was done using a flow table. The specimens were demoulded after 24 hours and then cured in water at room temperature of  $27 \pm 3^\circ\text{C}$  and  $65 \pm 10\%$  humidity. The air content of fresh mortars was measured according to the standard (ASTM C 231M-14, 2014).

### **3.3.6 Test of Hardened Mortar**

The compressive strength results of three 50 mm cube specimens were used to calculate the average value for each batch of specimens. Compressive strength measurements were carried out using an ELE testing machine capacity of 3000 kN, and a loading rate of 0.5 kN/sec.

### **3.4 Pozzolanic Reactivity Measurement**

The incorporation of POCP as supplementary materials in cement-based applications largely depends on its' pozzolanic activity. The experiment is designed in this section for the assessment of the pozzolanic activity. The apparatus and procedure used to

determine the properties of POCP and POCP blended cement paste will also be explained in this section. The strength activity index measuring procedure would also be discussed.

### **3.4.1 Properties Investigation**

The chemical composition (major oxides) of the POCP was observed using panalytical (AXios<sup>maX</sup>) spectrophotometer and the phase composition was determined by XRD (PANalytical- Empyream). The Malvern particle size analyzer was used for the particle size investigation in aqueous solution mode. The morphology of POCP was performed using the Phenom table top of SEM while the specific surface area was explored using Blaine apparatus.

### **3.4.2 Paste Preparation**

The OPC (70%) and POCP (30%) were put into the tube mills which are cylindrical rotating drums; containing steel balls at RPM 150 for 30 minutes to ensure homogeneity. This palm oil clinker powder blended cement (POCPC) was placed into the pan of the mixer machine. After two minutes of mixing, water was added and mixed up for 2 minutes. The required amount of water was added to maintain the flow  $110 \pm 5$  mm of the paste by adding excess de-ionized water. The flow of paste was performed using standard flow table test apparatus. Finally, the mixing continued for a further 2 minutes and the paste was molded into  $50 \times 50 \times 50$  mm<sup>3</sup> steel molds. After 24 hours, the mold was opened and the molded paste was poured into water for curing. The powder of OPC and POCPC paste-mortar of curing age (3, 28 and 90 days) was used for micro analytical studies. The temperature and humidity of the curing room were at  $65 \pm 10\%$  and  $25 \pm 4^\circ\text{C}$ , respectively. The hydration reaction of the powder of OPC and POCPC paste for further micro analytical investigation was stopped at 1:1::ethanol: acetone.

### **3.4.3 Micro Analytical Characterization of Paste**

The micro analytical characterization of the paste was conducted using different instrumental techniques. The phase composition was determined by XRD using (PANalytical-Empyream). The thermal behaviour of hydrated cement paste was investigated using TGA (TGA/SDTA851<sup>e</sup>) at 10°C/minutes from 25°C to 987°C in N<sub>2</sub> atmosphere. The functional groups of hydrated cement paste were observed using FTIR (PerkinElmer, Frontier) spectrophotometer. The microstructure of mortar fracture was observed using model of SU8220 of Hitachi Corporation.

### **3.4.4 Strength Activity Index Measurement**

The mortar for a strength activity index was measured according to ASTM C331-13. The curing and mixing water used in this experiment was double distilled water to overcome the effect of water composition.

## **3.5 Fresh and Hardened Properties Determination**

The setting time, expansion, viscosity and compressive strength determination procedure will be described in this section. The experiment has been designed here so as to assess the POCP characteristic effect on setting and hardening properties of cement.

### **3.5.1 Properties of POCP**

The chemical composition of the POCP has been observed using panalytical (AXios<sup>maX</sup>) spectrophotometer. The Malvern particle size analyzer was used for the particle size investigation. The morphology of POCP was performed using the Phenom table top of SEM while the specific surface area was explored using Blaine apparatus.

Loss of ignition was tested using furnaces. The specific gravity was determined using a specific gravity bottle.

### 3.5.2 Blended Cement Composition

The blended cements were prepared in a control mixing ball mill to guarantee homogeneity by running 30 minutes at 150 RPM. The mixing ratio of blended cements is shown in **Table 3.2**.

**Table 3.2:** Mixing ratio of blended cement

Name of samples	OPC (%)	POCP (%)
OPC	100	--
POCP10	90	10
POCP20	80	20
POCP30	70	30
POCP40	60	40
POCP50	50	50
POCP60	40	60

### 3.5.3 Physical Properties of Blended Cement

The specific gravity of OPC and POCP were measured according to the ASTM C 188 method (ASTM Standard, 2009) and the insoluble residue (IR) and loss of ignition (LOI) were obtained using ASTM C 114 methods (ASTM Standard, 2013). Fineness of raw materials along with blended cements was determined by Blaine apparatus according to standard ASTM C209 and the residue by ASTM C 430, respectively (ASTM Standard, 2011a, 2011b). The setting behaviour and water consistency of the pastes were resolved according to ASTM C187 (ASTM Standard, 2004) and ASTM C191 (ASTM Standard, 2008), respectively by using a Vacat apparatus. The flow of mortar was determined using a flow table. The Lechatelier mould was used for

soundness determination according to the standard method of ASTM C1437 (ASTM Standard, 2000).

#### **3.5.4 Viscosity Measurement**

The method of paste preparation is significant for determining the rheological behaviour. The mixing time, type of mixing bowl and water/cement ratio are associated with this measurement. The cement was mixed in a bowl for 30 seconds in mixer with slow speed. Then water was poured into the bowl within 30 seconds and mixed 60 seconds at slow speed. The paste was put into the cylindrical Viscometer cone. The fluidity of the paste was determined using a Brookfield viscometer. The measuring time was about 60 seconds with stress cycle from 0 to 200 Pa.S.

#### **3.5.5 Preparation and Test of Cement Mortar**

In this experiment, water to cement ratio (W/C) was kept at 0.40 and cement to sand ratio (C/S) was kept at 0.50 in all the mixtures. The sand used in the study was graded silica sand. The mixed portion of the sand as 16/30-35%, 8/16-25%, 30/60-20%, 50/100-20% was used throughout the whole experiment. At first, four groups of silica sands were mixed. After one minute, OPC or POCP blended cement was put into the mixture, followed by 1 min of mixing. Mixing water was then added to the mix, and the mixing process was continued for 2 minutes, after which the required amount of SP was added. The mixing was then continued for 2 minutes and finally the mould was filled with fresh mixture at two layers. Flow of mortar mixture was maintained at  $170 \pm 10$  mm. After 24 hours of casting, the specimens were demoulded and then cured in water at room temperature ( $27 \pm 3^\circ\text{C}$ ) with  $65 \pm 18\%$  humidity. Flexural strength measurement was performed using a mortar beam of size 40 mm, 40 mm and 160 mm. The average of the three samples' strength has been taken as the result for accuracy.

### 3.6 Radiological Hazards Determination

The experiment has been designed here to investigate the radiological hazards when palm oil mill waste is used as ingredient of building material. This section will also explain the characterization methods of the radionuclides and then calculate the hazard indicators.

#### 3.6.1 Sample Preparation

POC and POFA were collected from a palm oil mill in Dengkil, Malaysia. The schematic diagram of a typical power generation with POC & POFA by-product in palm oil mill is shown in the **Figure 3.5**. Samples were collected every alternative hour from the waste outlet of the mill for a month and stored in reserve drum. The bulk quantity of POFA samples was homogenized in laboratory using rotary pan mixture. The collected POC is converted into small stones using a jaw crusher then homogenized in rotary pan mixture. This crushed POC is then converted into palm oil clinker powder through the grinding in a ball mill for 6 hours rotation with 150 RPM. The resulting homogenous materials were used in this study. Six samples of a homogeneous mixture of palm oil clinker were tested that are designated as POC1, POC2, POC3, POC4, POC5 and POC6. POFA was labelled in similar fashion.



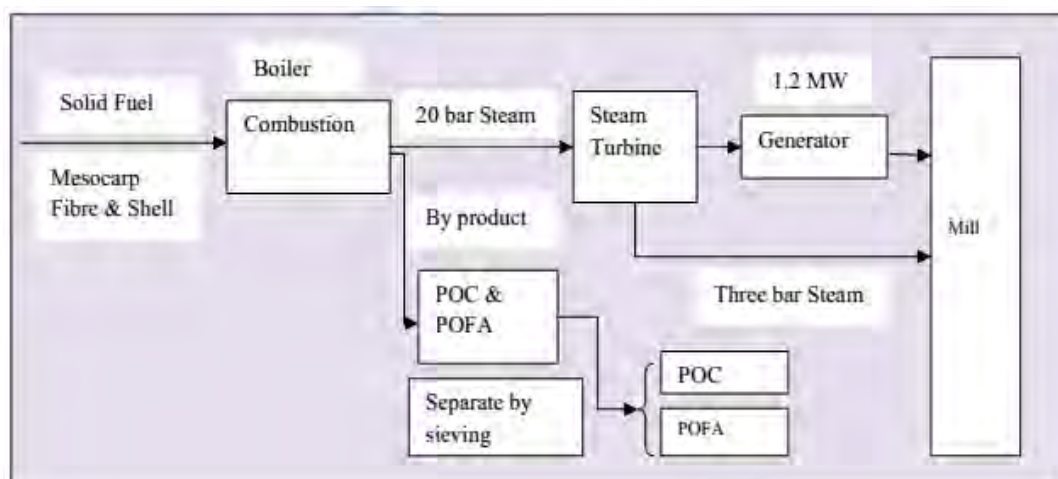


**Figure 3.5:** Schematic diagram of POC & POFA production (Yusoff, 2006)

POC and POFA were dried out in programmable furnaces at 110°C for 3 hours for removal of moisture. Samples are sieved using 150 µm sieves to make them homogeneous. Approximately 350-450 g of POC or POFA samples were placed into a Marinelli beaker; sealed and they were kept there for about 4-5 weeks to reach secular equilibrium of the  $^{226}\text{Ra}$  and  $^{228}\text{Ra}$  and their progenies prior to gamma spectroscopy.

### 3.6.2 Characteristics of POC and POFA

The major oxides of the POC and POFA were determined using Panalytical (AXios<sup>maX</sup>) X-ray Fluorescence spectrophotometer. The specific surface area and loss of ignition was measured according to ASTM standards. The chemical composition and physical properties such as specific surface area and loss of ignition of POC and POFA are shown in **Table 3.3**. The major oxides, i.e.  $\text{SiO}_2$ ,  $\text{Al}_2\text{O}_3$ ,  $\text{Fe}_2\text{O}_3$  and  $\text{K}_2\text{O}$  are significantly present in POC and POFA (Kanadasan & Razak, 2015; Ranjbar et al., 2016).

**Table 3.3:** Properties of POC and POFA

Parameters	POC	POFA
SiO <sub>2</sub> (%)	61.29	60.15
Al <sub>2</sub> O <sub>3</sub> (%)	5.89	4.34
Fe <sub>2</sub> O <sub>3</sub> (%)	4.31	3.87
CaO (%)	3.20	2.90
MgO (%)	3.16	3.68
SO <sub>3</sub> (%)	0.10	0.08
K <sub>2</sub> O (%)	10.79	12.23
P <sub>2</sub> O <sub>5</sub> (%)	3.12	2.12
TiO <sub>2</sub> (%)	0.12	0.10
Specific surface area (m <sup>2</sup> /kg)	418	423
Loss of ignition (%)	3.49	6.12

### 3.6.3 Measurement of Radioactivity

The levels of <sup>226</sup>Ra, <sup>232</sup>Th and <sup>40</sup>K in the POC and POFA were determined using  $\gamma$ -ray spectrometer with HPGe detector from ORTEC. The relative efficiency of the p-type coaxial HPGe  $\gamma$ -ray spectrophotometer was 28.2% and an energy resolution of the 1.67 keV-FWHM at 1332.5 keV peak of <sup>60</sup>Co. The detector is shielded by thick cylindrical lead to minimize gamma-ray background in laboratory site. The 16k MCA was used for acquisition of data from the detector. The Gamma-vision 5.0 software was used for the analysis of the spectrum.

The energy calibration and photo peak efficiency evaluation of the detector were performed by a multi-nuclide gamma source (500 ml Marinelli beaker geometry which has the same geometry of the sample containing Marinelli beaker) containing <sup>241</sup>Am (59.54 keV), <sup>109</sup>Cd (88.04) keV, <sup>57</sup>Co (122.06 keV), <sup>85</sup>Sr (214.01 keV), <sup>137</sup>Cs (661.66 keV), <sup>60</sup>Co (1173.23; 1332.49 keV) and <sup>88</sup>Y (1836.06 keV). Each sample was counted for 24 hours and the background count of the gamma-ray spectrometry of room for the

same counting time was subtracted from the sample count to get the net count. **Equation (3.1)** was used to calculate the activity concentrations of  $^{226}\text{Ra}$ ,  $^{232}\text{Th}$  and  $^{40}\text{K}$ , which has also been reported elsewhere (Monika Gupta & Chauhan, 2012; Khandaker et al., 2012).

$$C = \frac{N \times 1000}{\varepsilon_{\gamma} \times \rho_{\gamma} \times T_s \times M_s} \quad (3.1)$$

where, C, N,  $\varepsilon_{\gamma}$ ,  $\rho_{\gamma}$ ,  $T_s$ , and  $M_s$  represents the radioactivity of the sample (Bq/kg), net counts of the respective photo-peaks, HPGe detector efficiency of the relevant  $\gamma$ -ray energy,  $\gamma$ -ray emission probability of the respective energy, counting period of the sample (seconds) and sample mass (grams), respectively.

The activity concentration of  $^{226}\text{Ra}$  was calculated using the  $\gamma$ -ray lines from  $^{214}\text{Pb}$  at the 351.93 keV (35.6%), from  $^{214}\text{Bi}$  at the 609.31 KieV (35.6%), from  $^{214}\text{Bi}$  at the 1120.291 KieV (14.92%) and from  $^{214}\text{Bi}$  at the 1764.49 KieV (15.3%). The activity concentration of  $^{232}\text{Th}$  was estimated via the  $\gamma$ -ray lines from  $^{212}\text{Pb}$  at the 238.63 KieV (46.6%), from  $^{208}\text{Tl}$  at the 510.77 KieV (22.6%), from  $^{208}\text{Tl}$  at the 583.19 KieV (85%) and from  $^{228}\text{Ac}$  at 911.22 (25.8%). While the activity level of  $^{40}\text{K}$  was obtained from its single  $\gamma$ -ray line at the 1460.82 keV (10.66%). The characteristics  $\gamma$ -ray spectrum of POC and POFA counted for 86,400 seconds is shown in **Figure 3.6** and **Figure 3.7**, respectively.

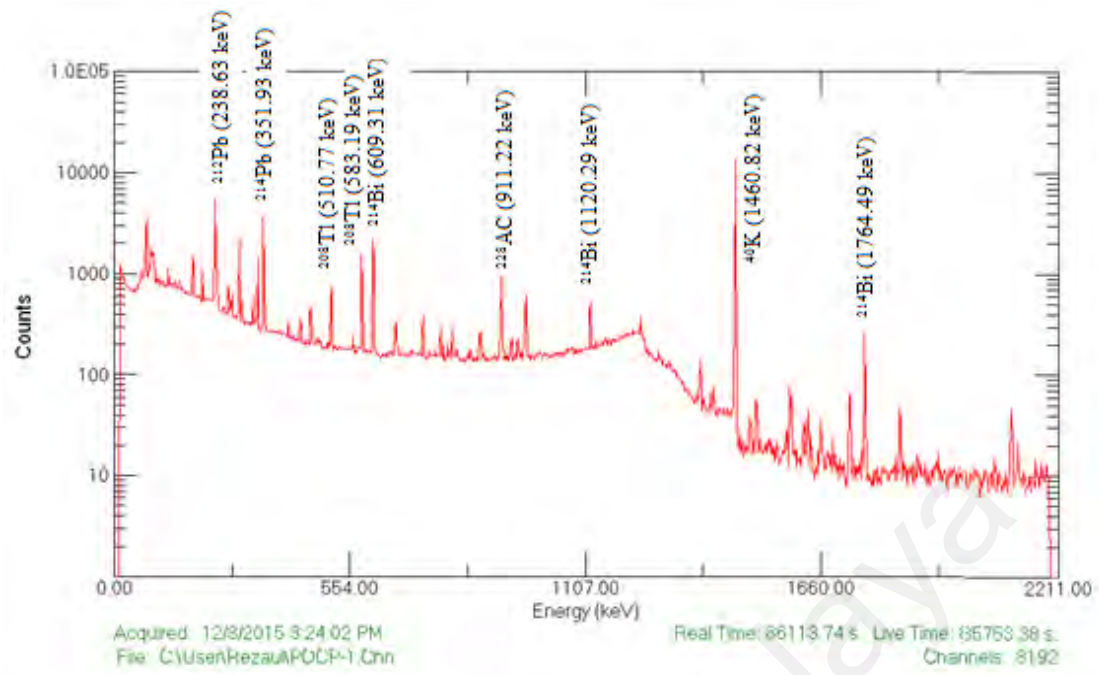


Figure 3.6: Characteristic  $\gamma$ -ray spectrum of POC

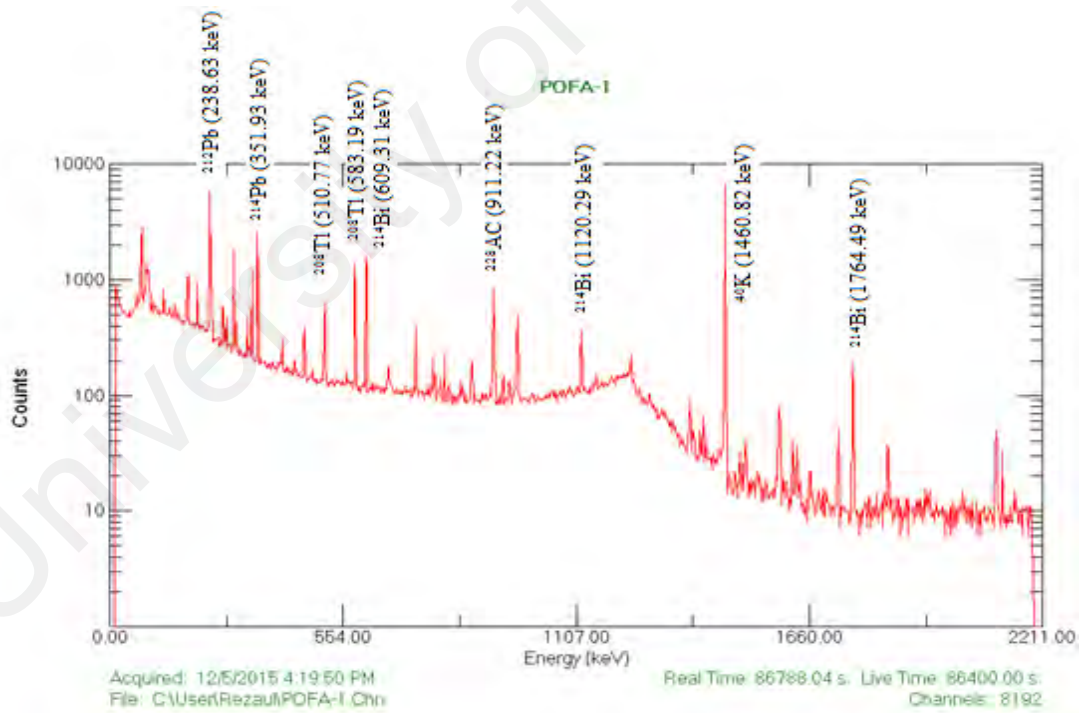


Figure 3.7: Characteristic  $\gamma$ -ray spectrum of POFA

### 3.6.4 Radiological Hazard Indices Calculations

Gamma-rays emitted from  $^{226}\text{Ra}$  and  $^{232}\text{Th}$  decay series can infiltrate the concrete media and attain indoor atmosphere which causes adverse health effects such as cancer to the dwellers. For the assessment of unnecessary  $\gamma$ -radiation and their deleterious health effect which originate from construction materials, several health hazard indicators such as radium equivalent activity, indoor absorbed gamma dose rate, annual effective dose, the alpha and gamma index, external and internal indices have been recommended by many researchers (Gupta et al., 2013; Rahman et al., 2013). The aforesaid hazard indices were calculated for dwellers residing in the house and/or the workplace to assess the risks of radiation caused by the incorporation of palm oil mill waste in concrete.

#### 3.6.4.1 Radium equivalent activity ( $\text{Ra}_{\text{eq}}$ )

Generally, the activity levels of  $^{226}\text{Ra}$ ,  $^{232}\text{Th}$  and  $^{40}\text{K}$  in any environmental matrix are not homogeneous. Consequently, the distribution of these radionuclides in the palm oil mill was found to be non uniform. To make them uniform, a common index called radium equivalent activity ( $\text{Ra}_{\text{eq}}$ ) has been introduced in the literatures which quantify the total activity and radiation risk originated from construction media. The  $\text{Ra}_{\text{eq}}$  was calculated using **Equation (3.2)** in which 370 of  $^{226}\text{Ra}$ , 259 of  $^{232}\text{Th}$  and 4810 of  $^{40}\text{K}$  generate the same gamma dose (Amin et al., 2013; Gupta et al., 2013; Kobeissi et al., 2013; Rahman et al., 2013).

$$\text{Ra}_{\text{eq}} = 370 \left( \frac{C_{\text{Ra}}}{370} + \frac{C_{\text{Th}}}{259} + \frac{C_{\text{K}}}{4810} \right) \quad (3.2)$$

where,  $C_{\text{Ra}}$ ,  $C_{\text{Th}}$  and  $C_{\text{K}}$  represent the activity levels ( $\text{Bq kg}^{-1}$ ) of  $^{226}\text{Ra}$ ,  $^{232}\text{Th}$  and  $^{40}\text{K}$ , respectively.

### 3.6.4.2 Absorbed $\gamma$ -dose rate

The external absorbed dose rate in the outdoor air experienced by the individuals due to the studied radionuclides was estimated using **Equation (3.3)** (Alharbi et al., 2011; Asaduzzaman et al., 2015; Khandaker et al., 2012; Rahman et al., 2013).

$$D_{\text{out}}(\text{nGyh}^{-1}) = 0.427C_{\text{Ra}} + 0.662C_{\text{Th}} + 0.432C_{\text{K}} \quad (3.3)$$

where, 0.427, 0.662 and 0.432 Gy h<sup>-1</sup> are the dose coefficient for <sup>226</sup>Ra, <sup>232</sup>Th and <sup>40</sup>K to convert the activity concentration into doses (Khandoker Asaduzzaman et al., 2015). C<sub>Ra</sub>, C<sub>Th</sub> and C<sub>K</sub> represent the activity levels (Bq kg<sup>-1</sup>) of <sup>226</sup>Ra, <sup>232</sup>Th and <sup>40</sup>K, respectively. Due the use of earth-originating materials in the construction of buildings, the exposure to  $\gamma$ -rays in indoor air are generally higher than the exposure in an outdoor environment. Recently, fly ash and palm oil mill wastes (POC and POFA) are used as ingredient in building materials such as concrete to increase its performance. Therefore, the evaluation of their radiological effects on indoor air is important. By considering that the indoor contribution of dose is 1.4 times greater than outdoor, the indoor absorbed dose rate was estimated by **Equation (3.4)** (Asaduzzaman et al., 2015; El Arabi et al., 2008; Monika Gupta & Chauhan, 2012; United Nations Scientific Committee on the Effects of Atomic Radiation, 2000).

$$D_{\text{in}}(\text{nGyh}^{-1}) = 1.4 \times D_{\text{out}}(\text{nGyh}^{-1}) \quad (3.4)$$

### 3.6.4.3 Annual effective dose

The annual effective dose in indoor experienced by individuals residing in a building caused by using radioactivity in the ingredients of building materials was calculated by the **Equation (3.5)** (Asaduzzaman et al., 2015).

$$E_{\text{in}}(\text{mSvy}^{-1}) = D_{\text{in}}(\text{nGyh}^{-1}) \times 8760\text{h} \times 0.7 \text{Svy}^{-1} \times 0.8 \times 10^{-6} \quad (3.5)$$

where, 8760 is the hours in a year,  $0.7 \text{ SvGy}^{-1}$  is the conversion coefficient from the absorbed dose rate in air to effective dose experienced by adult population and 0.8 is the indoor occupancy factor, considering that people spend 80% (on an average) of their time in indoor environment at home and/or office/work places (Asaduzzaman et al., 2014; Asaduzzaman et al., 2015; Monika Gupta & Chauhan, 2012; Rahman et al., 2013; Solak et al., 2012).

#### 3.6.4.4 Gamma index

The gamma index ( $I_\gamma$ ) is widely used as screening tool for the characterization of materials that are used in building construction to avoid or limit unnecessary  $\gamma$ -radiation generated from the component of construction materials (Solak et al., 2012). The European Union suggested the following formula (**Equation (3.6)**) to assess the gamma index for a specific construction material.

$$I_\gamma = \frac{C_{\text{Ra}}}{300 \text{ Bq/kg}} + \frac{C_{\text{Th}}}{200 \text{ Bq/kg}} + \frac{C_{\text{K}}}{3000 \text{ Bq/kg}} \quad (3.6)$$

where,  $C_{\text{Ra}}$ ,  $C_{\text{Th}}$  and  $C_{\text{K}}$  represent the activity levels ( $\text{Bq kg}^{-1}$ ) of  $^{226}\text{Ra}$ ,  $^{232}\text{Th}$  and  $^{40}\text{K}$ , respectively. For building material, exemption dose limit of  $0.3 \text{ mSv y}^{-1}$  satisfy the  $\gamma$ -index of  $I_\gamma \leq 0.5$ . Conversely, the maximum dose limit of  $1 \text{ mSv y}^{-1}$  corresponds to  $\gamma$ -index of  $I_\gamma \leq 1$  (Asaduzzaman et al., 2015).

#### 3.6.4.5 Alpha index

Alpha radiation owing to the breathing of radon released from construction media is generally assessed by alpha index ( $I_\alpha$ ) with the following **Equation (3.7)** (Asaduzzaman et al., 2015; Monika Gupta & Chauhan, 2012; Khandaker et al., 2012; Righi & Bruzzi, 2006; Solak et al., 2012).

$$I_{\alpha} = \frac{C_{Ra}}{200 \text{ Bq/kg}} \quad (3.7)$$

where,  $C_{Ra}$  represents the activity level ( $\text{Bq kg}^{-1}$ ) of  $^{226}\text{Ra}$ . The release of radon from a specific building environment can enhance the radon levels in indoor atmospheres and may go beyond until the tolerable limit of  $200 \text{ Bq m}^{-3}$  when the activity level of  $^{226}\text{Ra}$  surpass a value of  $200 \text{ Bq kg}^{-1}$  therefore, the safe limit for an alpha index is  $\leq 1$  (Monika Gupta & Chauhan, 2012; Porstendörfer et al., 1996; Righi & Bruzzi, 2006; Solak et al., 2012).

#### 3.6.4.6 Health hazard indices

To keep the external and internal radiation dose within tolerable limits, external health hazard index ( $H_{ex}$ ) and internal hazard index ( $H_{in}$ ) are sometimes used for the characterization of construction materials. The  $H_{ex}$  was estimated using the following formula as presented in **Equation (3.8)** (Asaduzzaman et al., 2015; Beretka & Mathew, 1985)

$$H_{ex} = \frac{C_{Ra}}{370} + \frac{C_{Th}}{259} + \frac{C_K}{4810} \quad (3.8)$$

$H_{ex}$  must be below the unity in order to keep the external dose from a building material to  $1.5 \text{ mSv y}^{-1}$  (Alharbi et al., 2011; Ghose et al., 2012; Khandaker et al., 2012; Kobeissi et al., 2013). Internal health hazard index ( $H_{in}$ ) can be estimated by the **Equation (3.9)** (Alharbi et al., 2011; Beretka & Mathew, 1985; Khandaker et al., 2012).

$$H_{in} = \frac{C_{Ra}}{185} + \frac{C_{Th}}{259} + \frac{C_K}{4810} \quad (3.9)$$



Radon and its progenies that originated from building material can cause a risk of respiratory tracts once inhaled.  $H_{in}$  must be less than unity for the safe utilization of a construction material (Ghose et al., 2012; Kobeissi et al., 2013).

### 3.7 Heavy Metal Leaching Risk Assessment

The feasibility assessment of palm oil clinker (POC) in concrete has been proven in recent years. In addition, it is disposed in open land or used for covering potholes on the road. These materials may contain heavy metals that tend to leach out and contaminate the soil and water. However, detection of heavy metal in palm oil clinker has not yet been performed. In the present research, experimental study has been carried out to detect heavy metal levels and corresponding assessment of its risk. The apparatus used and the procedure adopted for this purpose will be explained in this section.

#### 3.7.1 Sample Preparation

The Palm oil clinker (POC) was collected from a palm oil mill, Dengkil, Malaysia. The sample preparation technique was explained in the **Section 3.6.2**. The properties of POC are depicted in **Table 3.3**.  $SiO_2$  is the major chemical oxide present in POC with some other inorganic oxides. The Si, Al, Fe, Ca, K, S, P, Mg and Ti elements are more than 90% (Kanadasan & Abdul Razak, 2015). The chemical composition of POC depends on the operating condition of the boiler as well as the chemical composition of the parent palm oil shell or bunches (Kanadasan et al., 2015). The TOC-L series was used for the determination of the organic carbon present in POC. This measurement showed that organic carbon (3.35%) was present in POC. The model-SU8220 of Hitachi Corporation (FESEM-EDX) was used to analyze the heavy metal of POC sample. The beam current and accelerating voltage were 10 mA and 15 KV, respectively. The

mineralogical composition of the POC was determined using X-ray diffraction technique (model; Empyrean, Penalytical).

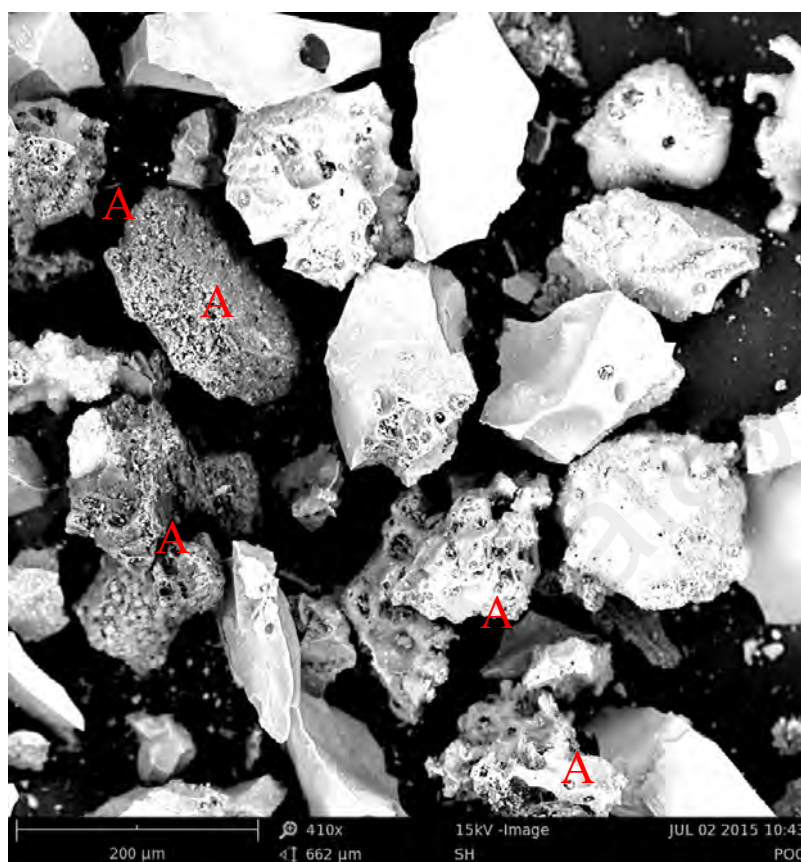


**Figure 3.8:** Micrograph of POC sample

The SEM of Phenom tabletop along with Pro Suite software was used for morphological analysis of POC sample. Acceleration voltage of 10 kV was used. Micro pore is noted using 'A' in the **Figure 3.8**. The POC is blackish in colour, porous and irregular in shape. The colour and porosity is due to the organic carbon in POC. The experimental results of POC properties will help to select the chemical reagent as well as the digestion procedure for heavy metals measurement.

### 3.7.2 Chemical Reagents

The chemical reagents that were used are  $\text{HNO}_3$ ,  $\text{HF}$ ,  $\text{HClO}_4$  and  $\text{HCl}$  for digestion, while Glacial acetic acid,  $\text{H}_2\text{O}_2$  (30%),  $\text{HONH}_2 \cdot \text{HCl}$  and  $\text{C}_2\text{H}_3\text{O}_2\text{NH}_4$  for sequential

digestion of POC in this experiment. Also, the chemical reagents used in this research were in analytical grade, which was supplied by the Merck, Malaysia.

### 3.7.3 Digestion of POC

The total concentrations of the targeted heavy metals were determined with the assistances of ICP-MS (Penalytical, 7500 series). The complete decomposition of POC is essential for accurate measurement of the heavy metals. One gram of air dry POC sample was used for digestion. The particle size distribution of POC sample which was used for digestion is presented **Figure 3.9**.

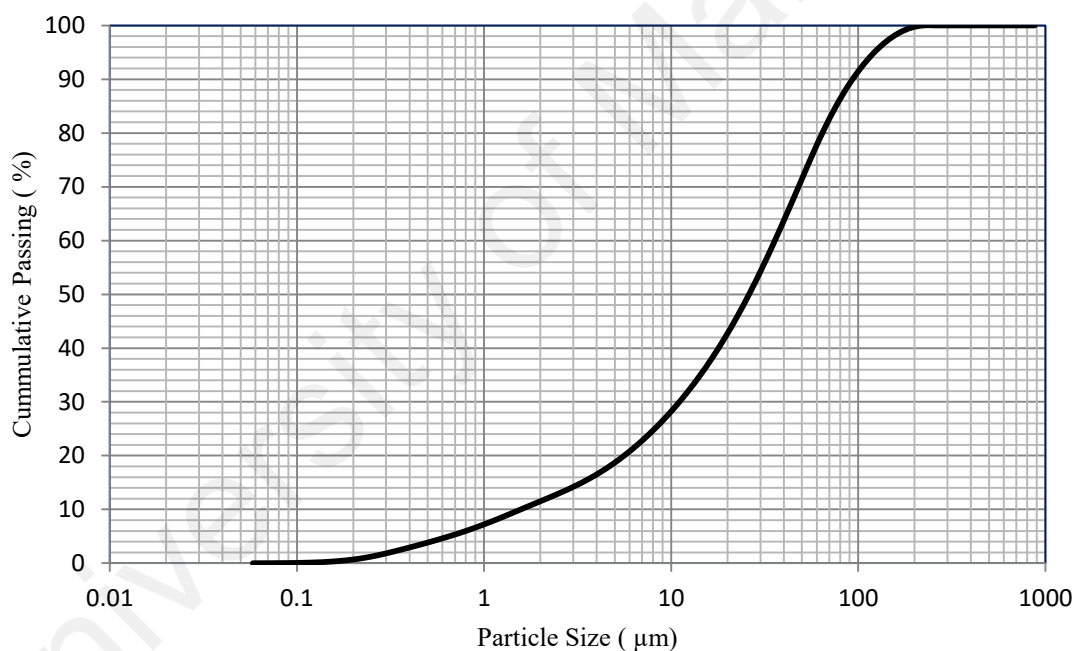


**Figure 3.9:** Particle size of POC

EPA methods 3052 was applied to the total heavy metal analysis of varieties of matrices such as soil, fly ash and bottom ash. This method is proven and most versatile. The POC contain 3.35% of organic carbon. The XRF analysis showed that the main ingredients of POC are  $\text{SiO}_2$ ,  $\text{MgO}$ ,  $\text{CaO}$ , and  $\text{Al}_2\text{O}_3$ . This chemical composition assists in the selection of the reagent for digestion. It allows for variation in reagent. The

selection of the digestion reagent depends on the sample matrix. The apparatuses were washed carefully with acid and reagent water for accurate results. The weight of POC was measured using the analytical balance with accuracy nearest 0.0001 g into an appropriate vessel. The POC sample was put into a vessel which had a mixture of 9 ml concentrated nitric acid and 5 ml concentrated hydrofluoric acid in a fume hood environment. Then, 5 ml of HClO<sub>4</sub> was added for decomposition of organic components. After adding the HClO<sub>4</sub> acid the color of digestion became cream yellow. The sample was run at microwave condition (Multi wave PRO, rotor 16 MF100, p-rate 0.80, 180°C and ramp -100) for digestion. The hydrochloric acid (2ml) and nitric (2ml) was used in it for stabilization of Ag and Ba. The solid phase of POC sample almost disappeared in the solution. The digestive solution was then transferred to 100 ml volumetric flask and diluted to the volume with deionized water containing 3% of nitric acid. This solution was used for ICP-MS analysis.

### 3.7.4 Speciation Analysis

Speciation of heavy metals was determined using the sequential chemical extraction methods. Four steps of sequential chemical extractions were used for phase information (Wang et al., 2015), which is shown in **Table 3.4**.

**Table 3.4:** Sequential extraction

Step	Fraction	Extraction Reagent	Extraction Condition
R1	Acid extractable	40ml 0.11mol/L, CH <sub>3</sub> COOH	Agitation (30±2 RPM), 16 h, 22±5°C
R2	Reducible	40ml 0.5 mol/L NH <sub>2</sub> OH.HCL (pH=2.0)	Agitation (30±2 RPM), 16 h, 22±5°C
R3	Oxidizable	10ml H <sub>2</sub> O <sub>2</sub> (8.8 mol/L) (pH=2.0), then 50ml 1mol/L NH <sub>4</sub> OAC (pH=2.0)	Agitation, 1 h 22±2°C, Water bath, 1 h then cools
R4	Residual	HNO <sub>3</sub> /HCl	Digestion

First, 1 g of sample was added into the Teflon beaker. This is a sequential method in which first step residue was used in the next step. However, the residue was washed with deionised water before used in the next step. The pH at second step was adjusted by 1N HNO<sub>3</sub>. The R1, R2, R3 and R4 are denoted as soluble and exchangeable metals fraction, carbonates, oxides and reducible metals fraction, bound to organic matter, oxidizable and sulphidic metals fraction and residual metals fraction, respectively. The residual sample containing beaker was heated up to dryness for about 6 hours on a heating plate followed by the addition 5ml of nitric acid and 5ml of water and the solution was filtered in a filter paper of medium porosity into a 50ml volumetric flask. The volume was completed with water (Pontes et al., 2010). An average of three samples was reported as the results of this experiment.

### 3.7.5 Leaching Toxicity Measurement

A number of methods have been developed by several institutes and agencies to analyze the leaching behaviour of materials. The leaching behaviour of POC was investigated by applying TCLP of USEPA1311, 1992. A number of researchers have investigated elements of the sample in an acidic environment by applying the TCLP methods (Lincoln et al., 2007; Sun et al., 2006). The particle size of POC which was used for leaching test is given in **Figure 3.10**. Five grams of POC with particle size less than 9.5 mm (solid sample: solution ratio = 1:20) was added to acetic acid (100ml) at pH  $4.93 \pm 0.05$  in a covered conical flask. This flask was agitated at 25°C for 18 hours in a control shaker by sitting at  $30 \pm 2$  RPM. The extract was filtered into a 100 ml flask with a 0.45- $\mu$ m pore size syringe filter, and then it was acidified by nitric acid to pH < 2. This procedure is tabulated in the **Table 3.5**. The pH was determined on unfiltered

aliquots of leachate using a handheld Orion pH meter, which was stored in a polycarbonate tube for the analysis of heavy metal.

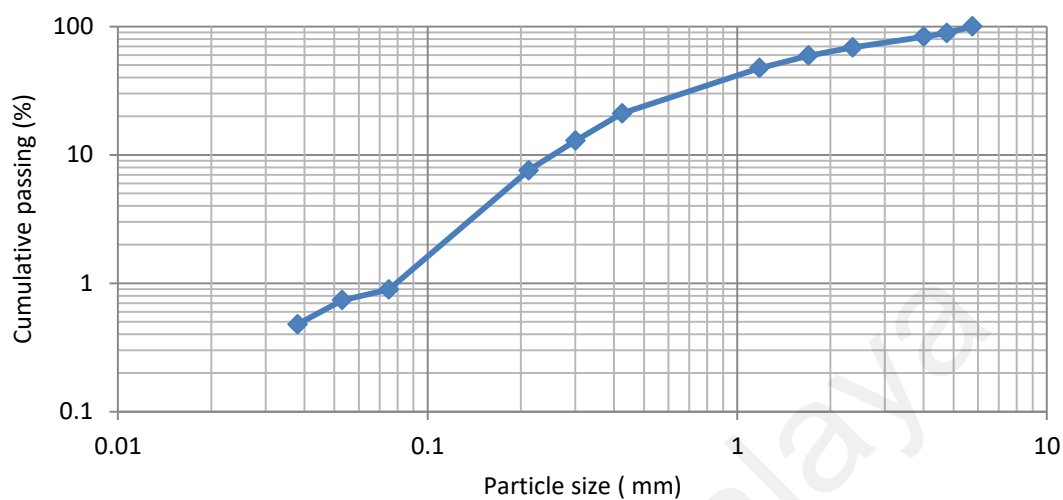


**Figure 3.10:** Particle size of materials used in leaching test

**Table 3.5:** Leaching test parameters

Characteristics	USEPA 1311 TCLP, 1992
Test type	Batch
Solid to leachate ratio	1:20
Leachate pH	4.93
Particle size	Shows in <b>Figure 3.10</b>
Sample mass/ leachate volume	5gm/100ml
Duration of agitation	18 h
Agitation system	Controlled shaker
Filtration	Syringe
Filter type	Nitrocellulose
Filter pore size	0.45 $\mu\text{m}$

The trace elements of POC were obtained by inductively coupled plasma-mass spectrometry (ICP-MS). TCLP analyses were performed on sample triplicates and average values were used as a result.

## CHAPTER 4: RESULTS AND DISCUSSIONS

### 4.1 Introduction

The technical, environmental and economical feasibility of palm oil clinker powder as supplementary cementitious material has been investigated in the present research. The results of characteristic properties of POCP, TPOCP and blended cement pastes are presented graphically in order to reveal a clear trend. The outcomes of the results are discussed elaborately from technical viewpoint and references have been added in support of the arguments. The radiological hazard indicators for POCP are compared with those POFA and fly ash. The heavy metal levels in POCP and their leaching behaviour will also be explained.

### 4.2 Characterization of Palm Oil Clinker Powder

The physical properties, i.e. particle size, specific surface area, loss of ignition, chemical composition, elemental composition, mineralogy, organic carbon, thermal stability and morphology of POCP has been presented and discussed in this section. The morphological differences between POCP and FA have also been discussed. A comparison in the chemical composition and mineralogy among the POCP and commonly used waste materials in cement was studied. The crystallinity of POCP is also explained at the bottom of this section.

#### 4.2.1 Physical Properties

The physical characterization includes Blaine SSA, LOI, specific gravity, particle size and morphology. These parameters were selected as they have important impact on the reactivity of POCP. POC is solid waste materials like a big chunk. Previous study also stated that POC is a solid stone like materials (Ahmmad et al. , 2015). The particle

size and shape of POC depends on the burning condition of the boiler. The POC is a by-product of incomplete burning of palm oil waste which consists of organic carbon at temperature range between 500- 800°C in the boiler. POC is blackish in color, porous and irregular in shape which is shown in **Figure 4.1**. POCP is obtained through the grinding process of POC. The specific gravity of POCP is 2.55 g/cc, compared to Portland cement which is 3.15 g/cc, which makes it lighter. Specific gravity is a physical property which depends on chemical composition, internal micro porosity, particle size and specific surface area. Researchers have reported that POC is light and suitable to use in the production of lightweight concrete (Ahmmad et al., 2015). The specific surface area of POCP is 383 m<sup>2</sup>/kg. **Figure 4.2** presents particle size distribution of POCP used in this study.

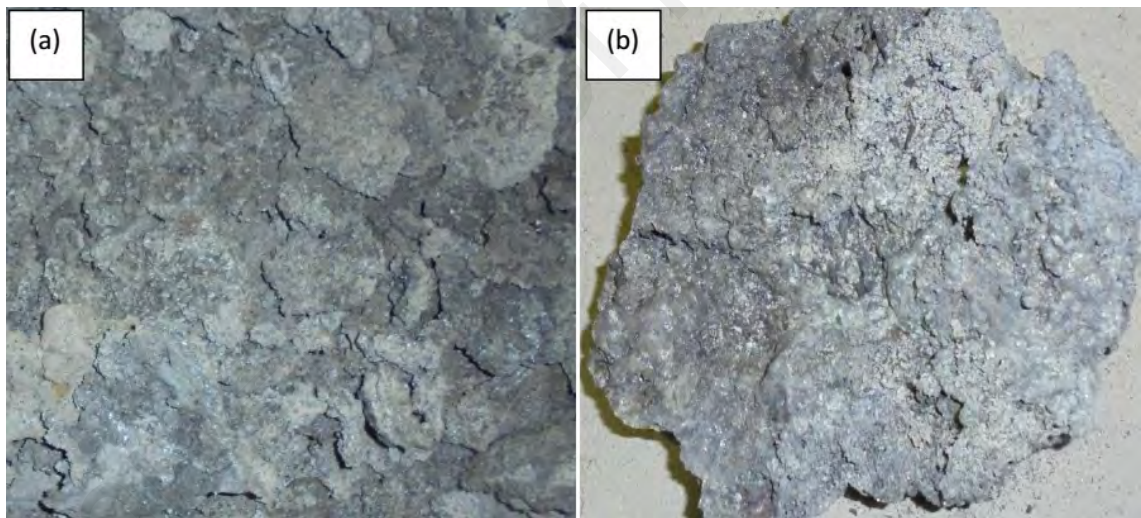


**Figure 4.1:** Photographs of (a) bulk quantity and (b) a big chunk of POC



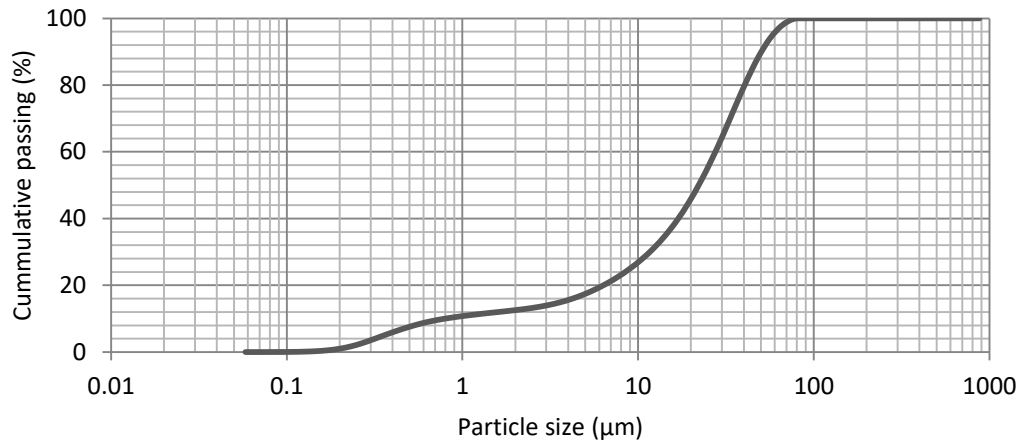


**Figure 4.2:** Particle size of POCP

SEM image obtained from POCP and FA is presented in the **Figure 4.3 (a) and (b)**, respectively. The POCP particles are irregular in shape, and has a micro porous cellular structure as compared to FA which are uniformly distributed spherical granules with smooth surface (Li et al., 2012). The pore is marked as 'A' in **Figure 4.3(a)**. The network type fibre is indicated as 'B' in tubular structure of POCP. This is due to the unburned carbon particles, as identified in the literature (Chandara et al., 2010). Fly ash is a by-product of coal-based power plant which is widely used as a cementitious material in concrete construction.

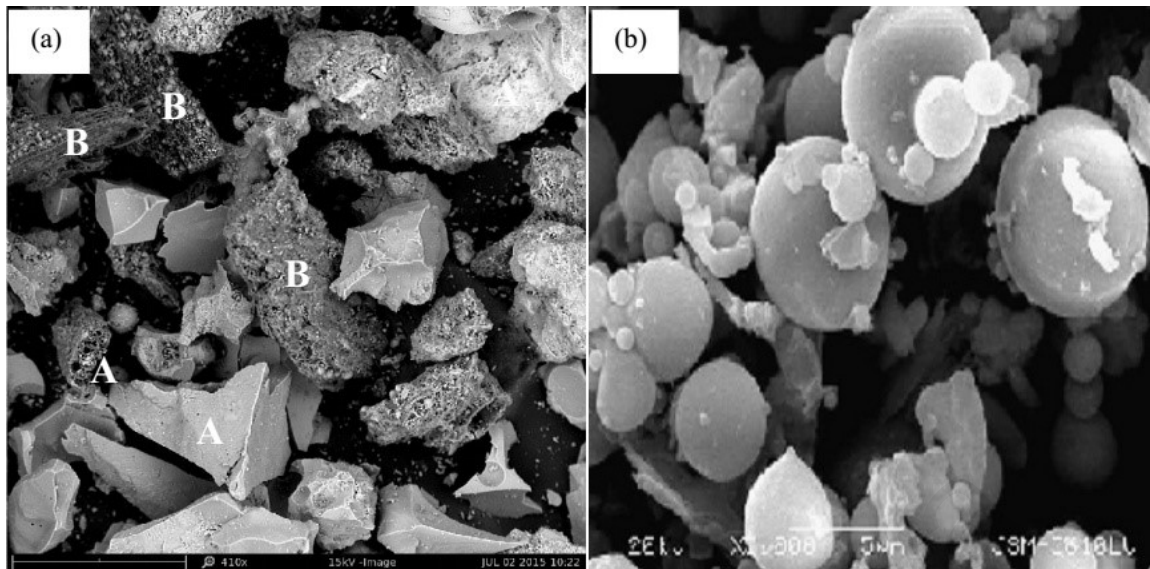


**Figure 4.3:** Morphological differences of (a) POCP and (b) FA (Li et al., 2012)

#### 4.2.2 Chemical Characteristics

The chemical composition of POCP is presented in the **Table 4.2**. POCP consist of silica, alumina and potassium oxides. Previous research also found the similar its oxides in composition. However, the chemical compositions are not consistent due to the variation its exhibits. These variations were observed for POCP samples obtained from different locations in Malaysia. The variation of the chemical composition in POCP depends on the feeding ratio in boiler, the burning temperature and operating conditions of boiler, and the geological condition of the respective area where the palm oil tree was planted (Kanadasan et al., 2015).

The micrograph of POCP is presented in **Figure 4.4**. From FESEM-EDX analysis the predominant elements in the POCP sample presented in **Table 4.1** comprised of oxygen, silicon, potassium, calcium, magnesium and, in a smaller amount of sodium, manganese, aluminum, sulfur, phosphorous and iron.

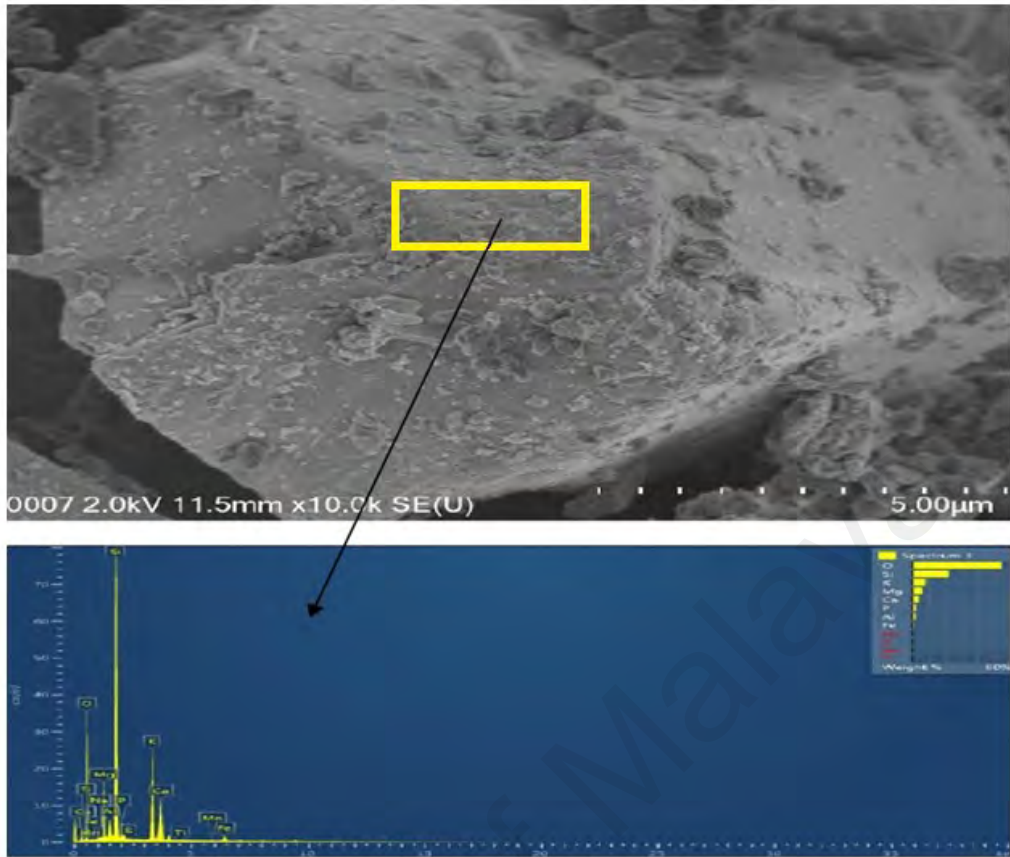


**Figure 4.4:** FESEM-EDX micrograph of POCP

University of Malaya

**Table 4.1:** FESEM-EDX results of POCP

Elements	Line Type	Apparent Concentration	k Ratio	Wt%	Wt% Sigma	Atomic %	Standard Label
O	K series	91.70	0.30857	55.02	0.13	69.68	SiO <sub>2</sub>
Na	K series	0.22	0.00094	0.15	0.03	0.13	Albite
Mg	K series	9.73	0.06450	6.44	0.05	5.37	MgO
Al	K series	2.64	0.01897	1.60	0.03	1.20	Al <sub>2</sub> O <sub>3</sub>
Si	K series	44.04	0.34894	22.19	0.08	16.01	SiO <sub>2</sub>
P	K series	3.84	0.02150	1.76	0.03	1.15	GaP
S	K series	0.13	0.00110	0.07	0.01	0.04	FeS <sub>2</sub>
K	K series	21.11	0.17879	7.80	0.04	4.04	KBr
Ca	K series	10.25	0.09158	3.98	0.03	2.01	Wollastonite
Ti	K series	0.08	0.00083	0.04	0.01	0.02	Ti
Mn	K series	0.15	0.00149	0.06	0.01	0.02	Mn
Fe	K series	2.26	0.02262	0.89	0.02	0.32	Fe
Total:				100.00		100.00	

Chemical composition is important to assess the variability of a material in terms of oxide ingredients, particularly when used as mineral additions in cementitious systems or in any kind of industrial applications. **Table 4.1** presents the chemical compositional differences between POCP and commonly used waste materials in cement-based applications.

**Table 4.2:** Chemical compositions of POCP and commonly used waste materials

Chemical Composition	POCP	FA <sup>a</sup>	POFA <sup>b</sup>	GBFS <sup>c</sup>
SiO <sub>2</sub> (%)	63.90	54.35	48.9	31.75
Al <sub>2</sub> O <sub>3</sub> (%)	3.89	14.33	2.71	14.48
Fe <sub>2</sub> O <sub>3</sub> (%)	3.30	7.08	6.54	0.60
MgO (%)	3.37	2.46	2.74	9.08
CaO (%)	6.93	3.07	13.89	36.44
SO <sub>3</sub> (%)	0.21	0.37	1.54	1.94
K <sub>2</sub> O (%)	10.20	1.82	7.13	---
Total (%)	91.8	84.48	83.45	94.29

**Note:** <sup>a</sup>FA (Kocak & Nas, 2014), <sup>b</sup>POFA (Noorvand et al., 2013), <sup>c</sup>GBFS (Wang et al., 2012).

The oxides present in POCP are mainly inorganic. The results of the SiO<sub>2</sub>+Al<sub>2</sub>O<sub>3</sub>+Fe<sub>2</sub>O<sub>3</sub> oxides weight percentage in POCP, POFA, FA and GBFS are 71.09%, 70.56%, 58.15% and 47.12%, respectively. In addition, K<sub>2</sub>O content in POFA and POCP are slightly higher than fly ash due to higher uptake of this oxide by palm oil plants from the soil (Karim et al., 2013). Minor differences are observed in the chemical of POCP and POFA because both materials are produced from the same source. The significant variation in K<sub>2</sub>O, SiO<sub>2</sub>, CaO, Fe<sub>2</sub>O<sub>3</sub> between POCP and GBFS may be due to the sources of their origin. It is clear that the chemical composition of the POCP much resembles that of FA rather than GBFS.

#### 4.2.3 TGA and Organic Carbon

The characterization of carbon content in wastes is important for supplementary cementitious materials. This unburned carbon absorbs water and super plasticizer (SP). In order to maintain the same fluidity of the concrete mix, more SP is needed. In addition, the compressive strength increases through removal of the unburned carbon (Chandara et al., 2011; Chandara et al., 2010). Previous study established that the oil

palm kernel shell used as boiler feed composed of hemicelluloses (1.2%), cellulose (38.6%) and lignin (39.0%), and also contained some extractives (Ninduangdee & Kuprianov, 2013). Lignin is moderately stable at elevated temperatures due to its highly aromatic backbone. A major mass loss (about 40%) of Kraft lignin is observed between 200 and 600°C (Sen et al., 2015a). **Figure 4.5** presents the weight loss steps of POCP.

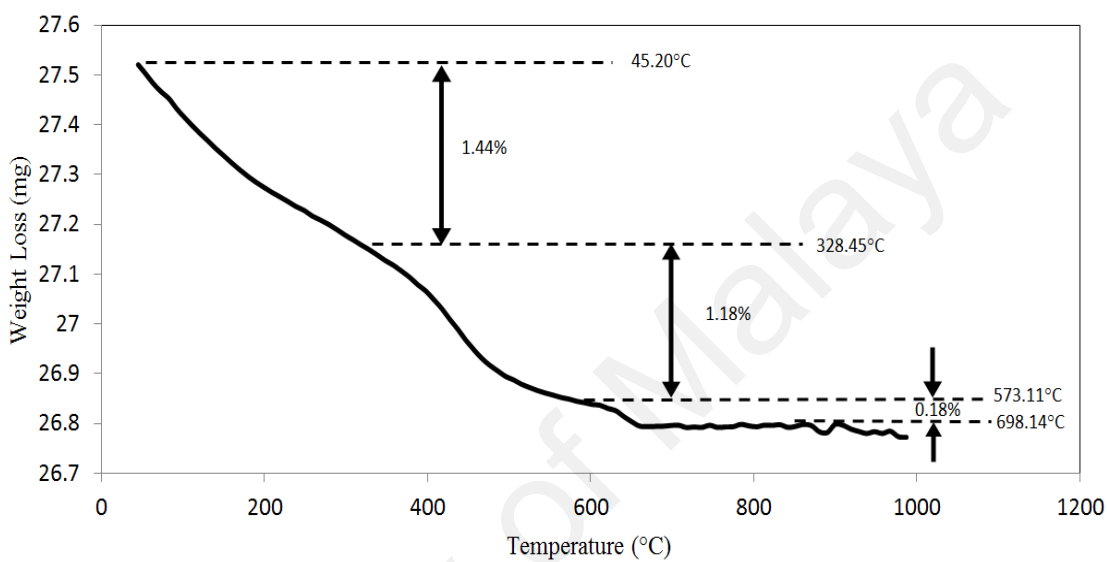


**Figure 4.5:** TGA analysis pattern of POCP

The first major weight loss was observed in the temperature range of 45.20°C to 328.45°C due to degradation of lower molecular weight cellulose and moisture presence in POCP indicated by weight loss of 1.44%. Second highest weight loss of 1.18% was observed in the subsequent step of temperature range from 328.45°C to 573.11°C. This is due to the degradation of lignin and cellulose presence in POCP and minimal contribution through the decomposition of  $\text{CaCO}_3$  (**Equation (4.1)**).



Further minor weight loss was observed within the range of 573.11°C until 698.14°C due to the degradation of the high molecular weight lignin (Lim et al., 2015; Nabinejad

et al., 2015; Ninduangdee & Kuprianov, 2013; Sen et al., 2015b). Moreover, the effect of heat energy also changes the colour of POCP from dark black (**Figure 4.6 (a)**) to grayish brown (**Figure 4.6 (b)**).

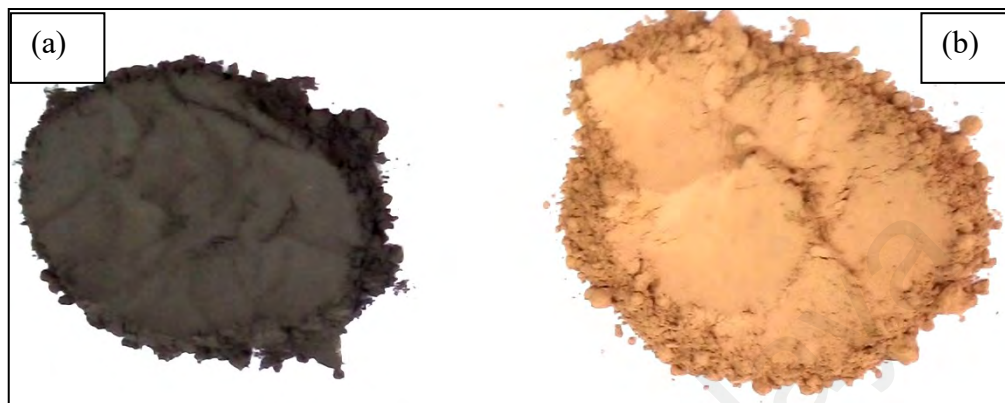


**Figure 4.6:** Colour change, (a) raw and (b) heated at 800°C for 1 hour

The total carbon analysis report of POCP is presented in **Table 4.3**. The organic carbon comes from the palm oil bunch and shell. The material is fed into the boiler randomly with varying proportions of fruit bunch and shell. These wastes contain mainly sugar based polymer like cellulose and hemicelluloses combined with lignin, protein, starch and inorganic phases (Hesas et al., 2013). The composition of fruit bunch and shell comprised of cellulose, hemicelluloses, lignin and extractives as 32.6%, 22.1%, 42.3% and 3.0% by weight, respectively (Lahijani et al., 2012). Factors such as the type of plant, age of the plant, climate condition and processing methods have significant contribution to the carbon-based materials present in the plant. By chemical analysis of the oil palm shell, it was found that 41.33% of TOC was present (Idris et al., 2010). In the current study, TOC in POCP was 2.54%. The presence of organic carbon affects the compressive strength development in cement –based materials.

**Table 4.3:** Total carbon analysis report of POCP

Name of Test	Content (%)
Total Organic Carbon (TOC)	2.54
Inorganic Carbon (IC)	0.063
Total Carbon	2.603

#### 4.2.4 Mineralogical Characteristics

The XRD pattern of POCP shown in **Figure 4.7** indicates the presence of quartz and cristobalite as major peaks at  $2\theta$  angles of  $26.87^\circ$  and  $20.45^\circ$ , respectively. In addition, the amorphisity hump occurs in the angular  $2\theta$  range of  $10^\circ$  to  $35^\circ$  (Kanadasan & Abdul Razak, 2015) and may indicate that the material possesses pozzolanic activity (Wang et al., 2014).

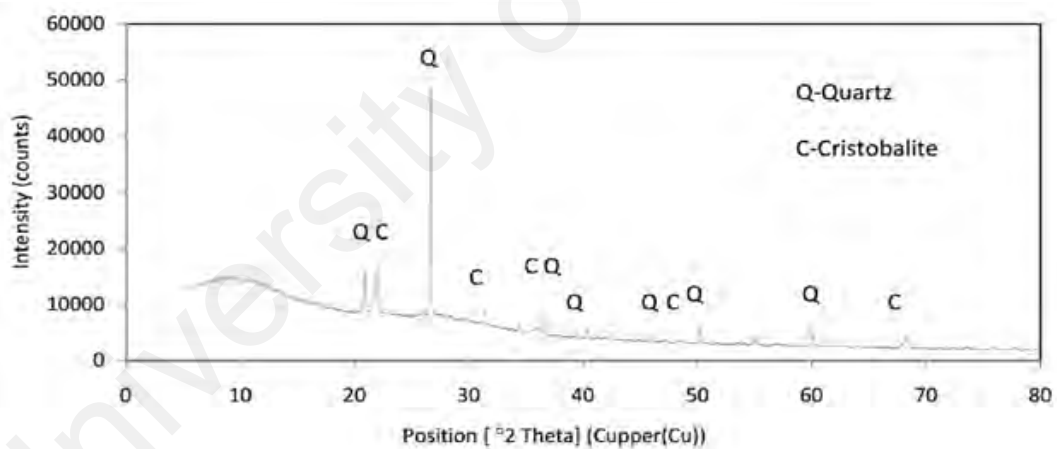


**Figure 4.7:** X-ray diffraction pattern

In addition, previous studies has deduced that the amorphous content in POCP and fly ash is almost similar (Kanadasan & Abdul Razak, 2015). This result indicates the possibility of POCP reacting with  $\text{Ca}(\text{OH})_2$  in the presence of water. However, the rate of pozzolanic reaction is dependent on the intrinsic properties of POCP such as specific surface area, chemical composition and active phase content. The thermodynamic



stability of the phases is an important parameter in the determination of the overall reaction. The principal mineral phases of waste materials such as FA, POFA, POCP and steel slag used commonly in cement-based applications are shown in **Table 4.4**.

**Table 4.4:** Minerals in POCP and common waste material

Name of Materials	Mineralogical Composition	Finding
POCP	Quartz (SiO <sub>2</sub> ), Cristobalite (SiO <sub>2</sub> )	Amorphous phase representing halo present in the 2θ angles range 10-30°
POFA (Chandara et al., 2010)	Quartz (SiO <sub>2</sub> ), Cristobalite (SiO <sub>2</sub> ) and Potassiumaluminumphosphate (K <sub>3</sub> Al <sub>2</sub> (PO <sub>4</sub> ) <sub>3</sub> )	A halo is observed from angles from 20° to 30°, representing an amorphous phase
Fly ash (Kocak & Nas, 2014)	Quartz (SiO <sub>2</sub> ), Hematite (Fe <sub>2</sub> O <sub>3</sub> ), Mullite (3Al <sub>2</sub> O <sub>3</sub> .2SiO <sub>2</sub> ), Albite (NaAlSi <sub>3</sub> O <sub>8</sub> ),Magnesioferrite (MgFe <sub>2</sub> O <sub>4</sub> )	Fly ash has irregular (amorphous) mineralogical structure
Steel Slag (Shi et al., 2004)	Olivine, Merwinite, Dicalcium silicate (C <sub>2</sub> S), Tricalcium silicate (C <sub>3</sub> S), Tetracalcium aluminoferrite (C <sub>4</sub> AF)	It contains phase similar to OPC clinker

The phase composition and the surface area of each phase of additives such as fly ash and POFA affects cement as well as concrete performance. Slag has C<sub>2</sub>S, C<sub>3</sub>S and C<sub>4</sub>AF phases that are similar to OPC clinker, but the percentage is less than OPC. However, the POCP comprised two major phases of SiO<sub>2</sub> i.e. quartz (Q) and cristobalite (C) as shown in **Figure 4.7**. Similar results for another form of waste in the palm oil mill, i.e. POFA was also reported by Chandara et al (2010). The mineralogical composition of POCP much resembles that of fly ash and POFA rather than slag.

#### 4.2.5 Crystallinity of POCP

FTIR spectrum of POCP is shown in **Figure 4.8**. The FTIR analysis also indicates the presence of quartz and cristobalite, which have also been identified by XRD. From FTIR spectrum, these minerals and organic carbon were determined by comparing the observed wave numbers with the available literature. Quartz is one of the significant

minerals and invariably present in POCP. The presence of quartz in the samples can be explained by two bands centered at  $1009\text{ cm}^{-1}$  and  $777\text{ cm}^{-1}$  assigned to stretching and bending vibrations (Si-O) in the  $\text{SiO}_4$  tetrahedra, which are due to the presence of traces of crystalline mineralogical phases (Patil & Anandhan, 2015). A deforming asymmetric band of H-O-H bonds in water component appears at  $1455\text{ cm}^{-1}$ . The main intense peak of Si-O stretching bands was observed in the range of  $1000$  to  $1100\text{ cm}^{-1}$  in most of the agricultural waste. The absorbing or deforming water bands common in agricultural waste occur at  $1650\text{ cm}^{-1}$ . The organic matter of SBA shows a band at  $694\text{ cm}^{-1}$  (Pereira et al., 2015). In the case of POCP, a peak appears at  $2752\text{ cm}^{-1}$ , and may be due to the presence of organic carbon.

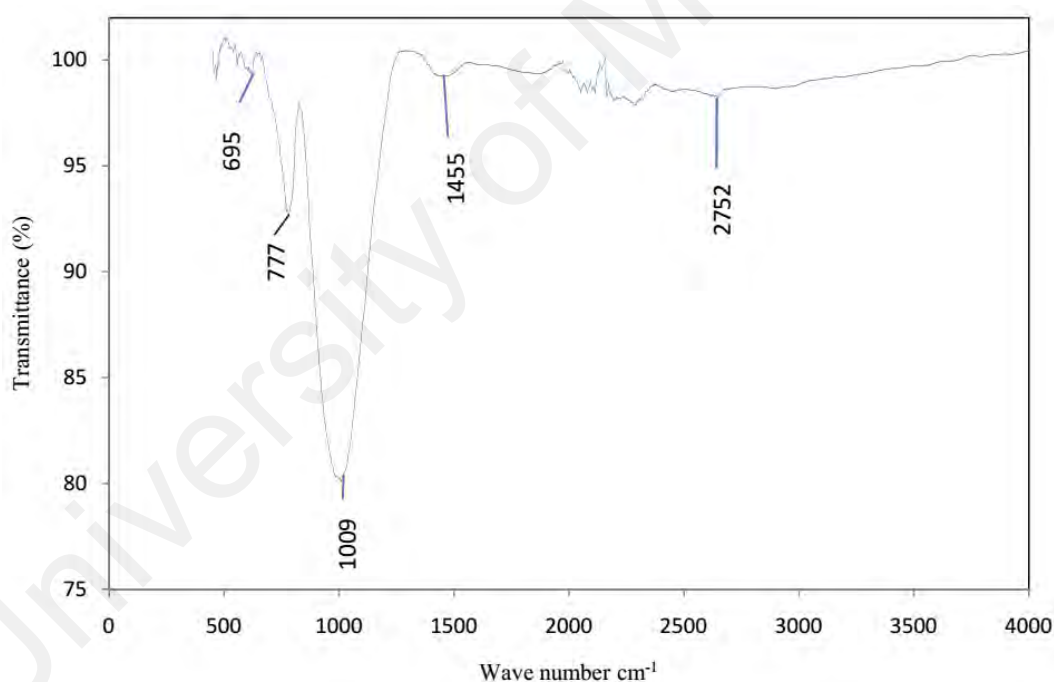


**Figure 4.8:** FTIR spectra of POCP

The crystallinity can be defined as the fraction of crystalline phase in a mixture of crystalline and non-crystalline materials. It refers to degree of disorder. If the crystallinity is less, then the minerals will be in disordered state and if it is high, then the minerals will be considered in an ordered state. The crystalline nature of quartz is

confirmed through the presence of peak around  $695\text{ cm}^{-1}$ . The crystallinity is inversely proportional to the crystallinity index value. The crystallinity index of quartz can be calculated using **Equation (4.2)**.

$$\text{Crystallinity Index} = \frac{I_{777}}{I_{695}} \quad (4.2)$$

where,  $I_{777}$  is the intensity of the absorption band at  $777\text{ cm}^{-1}$  due to the vibration in tetrahedral site symmetry and  $I_{695}$  at  $695\text{ cm}^{-1}$  due to the vibration in octahedral site symmetry by constructing the tangent base lines for these bands (Ramasamy et al., 2011). The stability of tetrahedral symmetry is stronger than the octahedral (Ramasamy et al., 2003; Ramasamy et al., 2011). The structural disorder takes place first in octahedral then tetrahedral. Moreover, quartz is a more stable mineral which is crystallized last compared to other minerals. Therefore, the determination of the crystallinity index of quartz by using the intensity of the bands due to the vibrations in the two symmetries will provide the information about the crystallinity of POCP. From the FTIR data and using Equation 2, the crystallinity index of quartz in POCP is 0.96. This value is within the range of the partial disordered state of quartz (0.75 - 1.00). If this value is more than 1.00 it indicates the completely disordered state of quartz (Parker et al., 1969; Ramasamy et al., 2011). The quartz in POCP is moderately disordered and has an amorphous phase, thus possessing reactivity.

The  $\text{SiO}_2$ ,  $\text{Al}_2\text{O}_3$ ,  $\text{Fe}_2\text{O}_3$ ,  $\text{MgO}$  and  $\text{CaO}$  are the main component of POCP. The  $\text{SiO}_2 + \text{Al}_2\text{O}_3 + \text{Fe}_2\text{O}_3$  oxides percentage is 71.09% in POCP which chemically fulfil the requirement of Class F fly ash. A halo was observed in the XRD spectrum in the angular  $2\theta$  range of  $10^\circ$  to  $35^\circ$  representing pozzolanic reactivity. The TOC in POCP was found to be 2.54% and also contains 0.063% inorganic carbon. The crystallinity index of quartz in POCP is 0.97, which means that the quartz is partially disordered.

### 4.3 Effect of Thermal Activation and Compressive Strength

The effect of heat energy on the physical properties of POCP, i.e. chemical composition, mineralogy, organic carbon and morphology of POCP will be presented and discussed in this section. A comparison of chemical composition between POCP and some waste materials will also be explained. Finally, thermal activated POCP influences on the compressive strength of mortar will also be discussed at the bottom of this section.

#### 4.3.1 Chemical Composition

The chemical composition of POCP, TPOCP and OPC is presented in **Table 4.5**. All the materials used in this experiment are mainly a mixture of inorganic oxides.  $\text{SiO}_2$  is a major oxide present in POCP as well as TPOCP, whereas CaO is the major content in the OPC. The  $\text{SiO}_2$  content in POCP is higher compared with POFA that is 31%, which has been reported by past researchers (Chandara et al., 2010). Previous research found that the composition of  $\text{SiO}_2$ ,  $\text{Al}_2\text{O}_3$ ,  $\text{Fe}_2\text{O}_3$ ,  $\text{K}_2\text{O}$ , CaO and MgO in POFA were 48.9%, 2.71%, 6.54%, 7.13%, 13.89% and 2.74%, respectively (Noorvand et al., 2013). Moreover, the total percentage of  $\text{SiO}_2$ ,  $\text{Al}_2\text{O}_3$  and  $\text{Fe}_2\text{O}_3$  was 74.72% indicating pozzolanic activity, which is higher than POFA as reported (Awal & Hussin, 1997). Differences in chemical composition are observed in POCP and POFA because of burning temperature, operating conditions and retention time of palm oil shell and fibre in the boiler of palm oil mills. The chemical composition variation of POCP was observed in this experiment when heated at 300°C, 580°C and 650°C temperatures for 3 hours. The content of oxides increased with the change in heating temperature from 300°C to 650°C. The POCP and TPOCP are classified as Class F pozzolan as specified by ASTM C 618-12a (ASTM C618-08a, 2008).

**Table 4.5:** Chemical compositions of OPC, POCP and TPOCP

Samples	Chemical Composition (% by weight)							
	SiO <sub>2</sub>	Al <sub>2</sub> O <sub>3</sub>	MgO	Fe <sub>2</sub> O <sub>3</sub>	CaO	K <sub>2</sub> O	TiO <sub>2</sub>	SO <sub>3</sub>
OPC	20.67	5.32	1.49	2.34	64.44	0.10	0.12	3.41
POCP	62.78	3.41	3.52	6.49	6.89	10.54	0.21	0.08
TPOCP <sub>300</sub>	63.07	3.43	3.54	6.52	6.92	10.59	0.21	0.09
TPOCP <sub>580</sub>	64.91	3.53	3.64	6.71	7.12	10.91	0.22	0.11
TPOCP <sub>650</sub>	65.07	3.53	3.65	6.73	7.14	10.94	0.22	0.11

The SiO<sub>2</sub>, Al<sub>2</sub>O<sub>3</sub> and Fe<sub>2</sub>O<sub>3</sub> oxides of wastes such as fly ash, bottom ash, and sugarcane bagasse ash contributes to the pozzolanic activity of concrete. The percentage of these three oxides in POCP, TPOCP<sub>300</sub>, TPOCP<sub>580</sub> and TPOCP<sub>650</sub> were 72.68%, 73.65%, 75.15% and 75.33%, respectively. The thermal activation effect on the chemical composition of POFA, clay, POCP and paper sludge is shown in **Table 4.6**.

**Table 4.6:** Change in chemical composition through thermal activation

Name of wastes	Activation condition	Name of oxides	Content before activation	Content after activation	% of increase	Refs.
POFA	500°C for 1 h	SiO <sub>2</sub>	61.85	67.09	8.47	(Chandara et al., 2010)
		Al <sub>2</sub> O <sub>3</sub>	5.65	6.12	8.32	
		Fe <sub>2</sub> O <sub>3</sub>	5.46	5.92	8.42	
Paper sludge	600°C - 650°C for 2 h	SiO <sub>2</sub>	12.89	26.2	103.26	(Ferreiro et al., 2013)
		Al <sub>2</sub> O <sub>3</sub>	8.30	16.98	104.58	
		Fe <sub>2</sub> O <sub>3</sub>	0.33	0.65	96.96	
		CaO	23.20	47.65	105.38	
POCP	580°C for 3 h	SiO <sub>2</sub>	62.78	64.91	3.39	Present study
		Al <sub>2</sub> O <sub>3</sub>	3.41	3.53	3.51	
		Fe <sub>2</sub> O <sub>3</sub>	6.49	6.71	3.39	
Clay	800°C for 2h	SiO <sub>2</sub>	54.98	60.50	10.04	(Alam et al., 2015)
		Al <sub>2</sub> O <sub>3</sub>	17.54	20.33	15.91	
		Fe <sub>2</sub> O <sub>3</sub>	5.33	4.74	11.06	

Thermal activation did not only cause chemical composition, but changes to mineralogy and morphology also occurred at the same time. The thermal activation removes moisture and organic materials. These factors are significantly responsible for the chemical composition change in POCP and POFA (Ferreiro et al., 2013). The highest increment in oxide percentage was observed in paper sludge due to the high content of organic materials, moisture and carbonate. The chemical decomposition of organic materials and carbonate compounds take place through thermal activation (Chandara et al., 2010). Kaolin in clay is converted to metakaolin through thermal activation. It is apparent that the chemical composition of POCP is changed through thermal activation and the percentage of increase in oxide content is significantly lower compared to paper sludge, clay and POFA.

#### 4.3.2 Total Organic Carbon

The organic and inorganic carbon present in the POCP and TPOCP are given in **Table 4.7**. The TOC in POCP, TPOCP<sub>300</sub>, TPOCP<sub>580</sub> and TPOCP<sub>650</sub> are found to be 3.54%, 3.50%, 0.064% and 0.063%, respectively. The organic carbon comes from the palm oil fruit bunch, fibre and shell due to incomplete burning in the boiler of palm oil mill. The TOC content also depends on the availability on the oxygen and incineration retention time in the boiler. These waste materials consist of sugar based polymer like cellulose and hemicelluloses which combine with lignin, protein, starch and inorganic phases (Hesas et al., 2013). The composition of cellulose, hemicelluloses, lignin and extractives are 32.6%, 22.1%, 42.3% and 3.0% in palm oil plants (Lahijani et al., 2012). The factors such as age of plant, climate condition, soil composition, water quality of area where the plants are grown have a significant effect on the carbon based-materials in the plants. From the analysis of the OPS shell, it was found that TOC was 41.33% (Idris et al., 2010). In the current study, TOC in POCP was found to be 3.54%. This

organic carbon is as a result of incomplete burning of shell and fibre in the boiler. The incomplete burning is due to the availability of oxygen and retention time of waste in burning zone of the boiler.

**Table 4.7:** Total carbon in POCP and TPOCP

Samples	TOC (%)	Inorganic carbon (IC) (%)
POCP	3.54	0.063
TPOCP <sub>300</sub>	3.50	0.058
TPOCP <sub>580</sub>	0.064	0.052
TPOCP <sub>650</sub>	0.063	0.049

It was observed that a big reduction occurred in TOC of TPOCP<sub>580</sub> and TPOCP<sub>650</sub> however, only in significant change of inorganic carbon was observed through thermal activation of POCP. In addition, the organic carbon reduction through the thermal treatment also cause of the color change in POCP as presented in **Figure 4.9**.



**Figure 4.9:** Color change due to thermal activation

### 4.3.3 Crystalline Structure of Minerals

XRD has been used not only for the phase identification of crystalline materials, but also provide useful information about the structure of waste material (Snellings et al., 2014). The XRD patterns of the POCP and TPOCP<sub>580</sub> are shown in the **Figure 4.10**. The XRD pattern of both POCP and TPOCP display a sharp peak at angular  $2\theta$  of  $26.64^\circ$  and  $21.96^\circ$  for quartz (Q) and cristobalite (C), respectively. Another peak of Q was observed in the  $2\theta$  of  $20.86^\circ$ . The crystalline  $\text{SiO}_2$  does not react with calcium hydroxide in the presence of water. In addition, a hump occurs in the angular  $2\theta$  range of  $10^\circ$  to  $35^\circ$  and may indicates that both materials possess pozzolanic activity (Chancey et al., 2010; Chandara et al., 2010; Kanadasan & Abdul Razak, 2015). The major peaks identified in the XRD patterns are Q and C while the other peaks are very small in intensity. Minor changes were observed in the peak structure and wideness when POCP was subjected to thermal activation at  $580^\circ\text{C}$  for 3 hours as shown in **Figure 4.10**. The changes in peak structure indicate that the thermal activation has an insignificant effect on the crystalline structure of minerals of POCP. In the literature, it was found that the disorder state of crystalline structure of the wastes by the observation of peak structure and wideness (Alam et al., 2015; Zeyad et al., 2013).



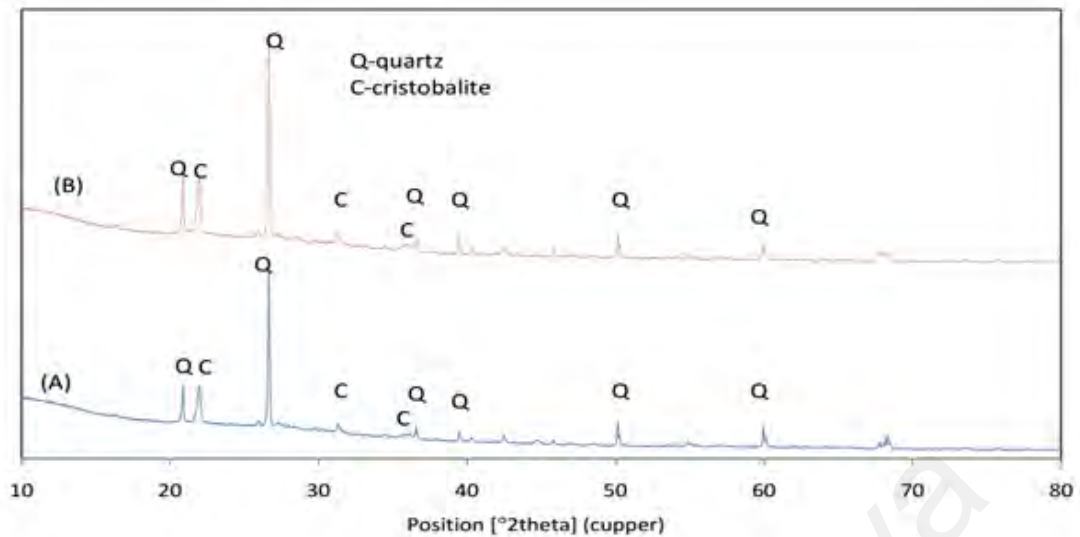


**Figure 4.10:** XRD patterns of (A) POCP and (B) TPOCP<sub>580</sub>

#### 4.3.4 Morphology

SEM micrographs of POCP and TPOCP<sub>580</sub> are presented in **Figure 4.11 (a) and (b)**, respectively. It was found that POCP is porous and irregular in shape. The porous structure is marked as 'A' in **Figure 4.11**. This is due to the unburned carbon particles, as identified in the past literature (Chandara et al., 2010). Organic carbon is removed from POCP by thermal activation. This also changes the morphology of POCP as shown in **Figure 4.11 (b)** for TPOCP<sub>580</sub> sample where the porosity is significantly reduced.

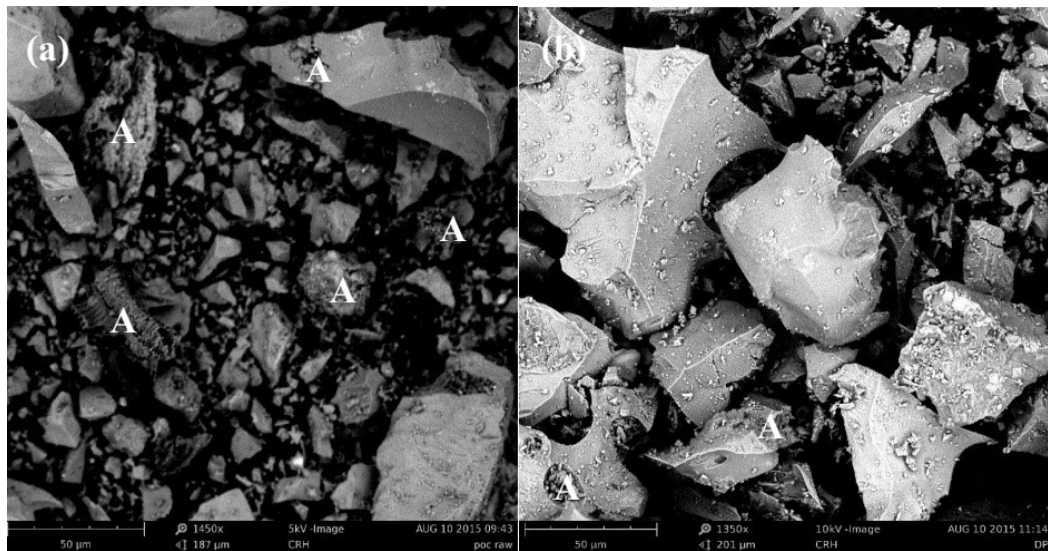


**Figure 4.11:** SEM micrographs of (a) POCP and (b) TPOCP<sub>580</sub>

### 4.3.5 Compressive Strength Development

The compressive strength of POCP and TPOCP cement mortars are presented in **Figure. 4.12**. The compressive strength of POCP and TPOCP mortars increased with curing time. The compressive strength of mortar is one of the major considerations when OPC is partially replaced by new waste materials. The variation of compressive strength between TPOCP<sub>580</sub> and TPOCP<sub>650</sub> is less compared to the variation between TPOCP<sub>300</sub> and TPOCP<sub>580</sub> mortars. The 28<sup>th</sup> day compressive strength of POCP, TPOCP<sub>300</sub>, TPOCP<sub>580</sub> and TPOCP<sub>650</sub> cement mortar samples were 45.9 MPa, 46.5 MPa, 56.3 MPa and 57.3 MPa, respectively.

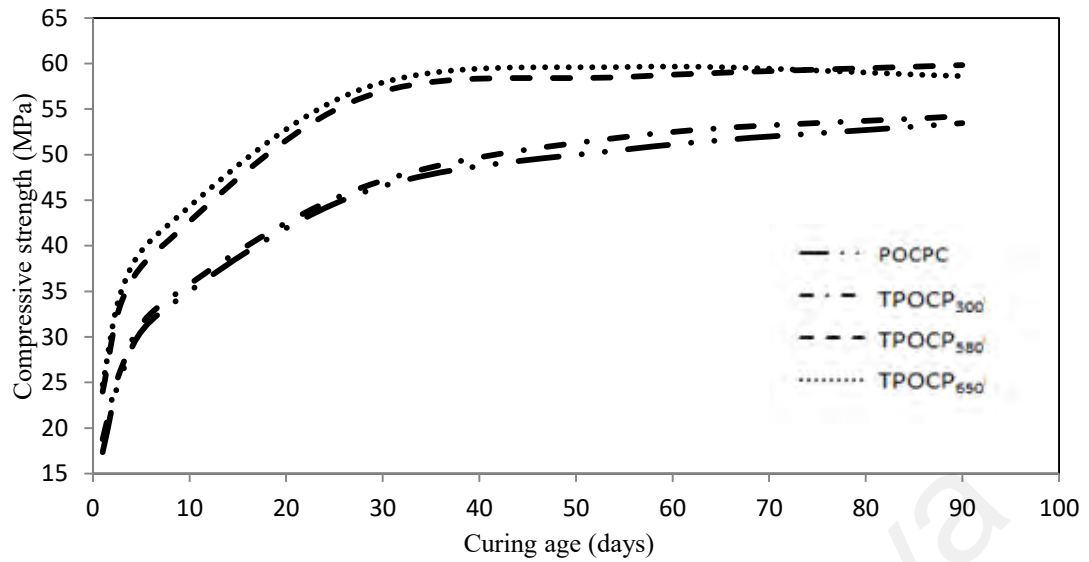


**Figure 4.12:** Effect of thermal activation on compressive strength

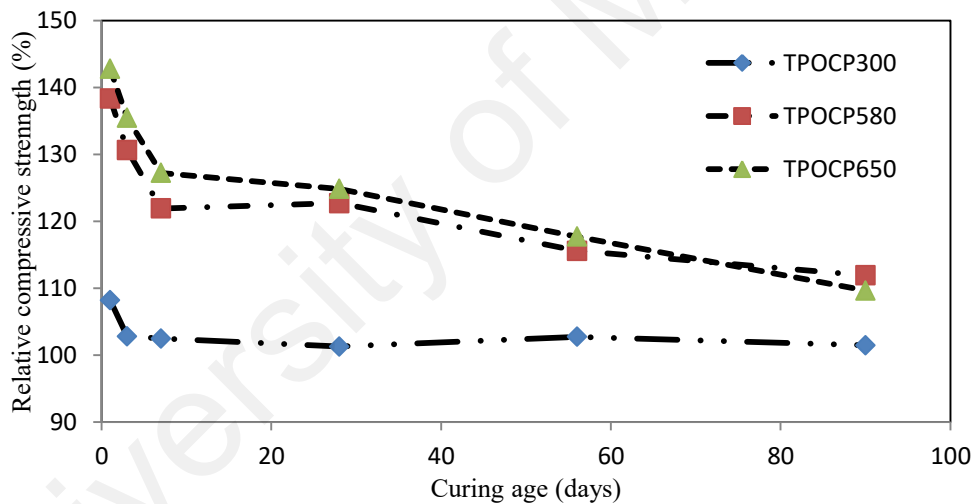


**Figure 4.13:** Comparison of relative compressive strength of TPOCP

**Figure. 4.13** depicts the relative compressive strength of TPOCP mortars at different curing ages compared with POCP mortar. In general, the relative compressive strength of TPOCP mortar is higher than POCP mortar. It is apparent that the relative compressive strength of the POCP<sub>580</sub> and TPOCP<sub>650</sub> mortars was significantly higher compared to TPOCP<sub>300</sub> mortar. The relative compressive strength gain in TPOCP<sub>300</sub> mortar with respect to the POCP mortar are 8.2%, 2.8%, 1.3%, 2.7%, 1.5% of 1, 3, 7,

28, 56 and 90 days, respectively. The compressive strength gain with respect to POCP mortar in TPOCP<sub>580</sub> mortar are 38.4%, 30.7%, 21.9%, 22.7%, 15.6% and 11.9% at curing age of 1, 3, 7, 28, 56 and 90 days, respectively. The relative compressive strength gain for TPOCP<sub>300</sub> mortar was low due to the decomposition of organic compounds of POCP within the temperature range from room temperature to 300°C. However, the relative compressive strength gain for TPOCP<sub>580</sub> mortar was very much higher due to the major decomposition of organic compounds within the temperature range from 300°C to 580°C. The gain of compressive strength in early age is higher compared with later age in TPOCP mortar. The increase of the K<sub>2</sub>O and Na<sub>2</sub>O in TPOCP are the reasons behind the significant development of the early strength (Jawed & Skalny, 1978). The main reason for strength gain in the TPOCP<sub>580</sub> and TPOCP<sub>650</sub> is due to the reduction of TOC from POCP through thermal activation. The reduction of TOC ultimately leads to decrease in the porosity of the POCP particles as well as an increase in the content of inorganic oxides in TPOCP. The reduction of porosity affects the TPOCP mortar matrix properties. Less porous particles of TPOCP in the paste make it much denser. The relative compressive strength variation with the relative air content of mortars is presented in **Figure 4.14**. The compressive strength of 28 days of POCP, TPOCP<sub>300</sub>, TPOCP<sub>580</sub> and TPOCP<sub>650</sub> mortars are 64.2%, 65.0%, 78.8% and 80.2% of OPC mortar. Whereas the air content in TPOCP<sub>300</sub>, TPOCP<sub>580</sub> and TPOCP<sub>650</sub> mortars are 152.0 %, 147.9%, 114.3% and 112.2% of OPC mortar. This clearly shows that the strength gained in TPOCP mortars is due to porosity reduction. Past researches found that the organic carbon of fly negatively influences of air entrainment in concrete (Du & Folliard, 2005; Hill & Folliard, 2006; Hill et al., 1997). The content of alkali metal oxides increases in TPOCP with loss of organic carbon through thermal activation. The air content decrease in TPOCP mortar is due to alkali metals increase and decrease of lignin based organic materials (Association, 1998; Nagi et al., 2007).

Previous researches were found that grounded POFA as well as slag was increased the density of the paste as a result increased compressive strength (Jaturapitakkul et al., 2011; Mo et al., 2015; Tangpagasit et al., 2005). The presence of organic compounds retards the hydration reaction of the cement particles. The effect of TOC reduction in waste containing organic compounds has a significant role in compressive strength development when incorporated as supplementary in cement-based applications.

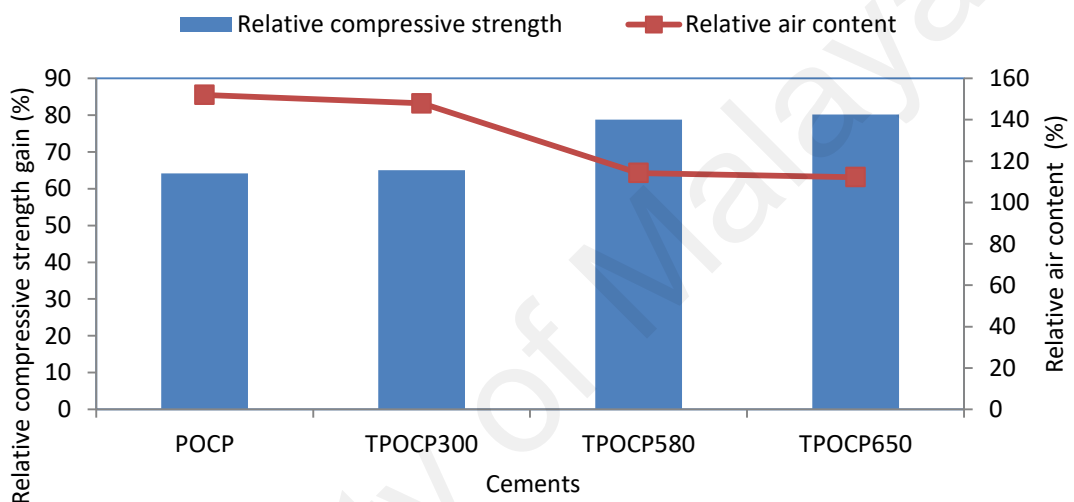


**Figure 4.14:** Relative compressive strength and air content of mortars

Finally, the first major mass loss in TGA pattern was observed in the temperature range from 340°C to 580°C due to degradation of organic compounds present in POCP. The main finding is the reduction of TOC from 3.54% to 0.063% by thermal activation at 580°C for 3 hours. The reduction of TOC ultimately led to an increase of the inorganic oxide content and also reduced porosity through decomposition of organic materials in the POCP. This is the reason behind the higher compressive strength in TPOCP mortar.

#### 4.4 Pozzolanic Reactivity of POCP

The XRD, TGA, FTIR and SEM results of OPC and 30% POCP blended cement paste of different curing ages is presented in graphical form to explain the consumption of  $\text{Ca}(\text{OH})_2$  by active  $\text{SiO}_2$  of POCP. The strength activity index of POCP and some other wastes are presented in a graph for comparison of pozzolanic activity.

##### 4.4.1 Properties of POCP

The pozzolanic activity of waste materials depends on the chemical composition, amorphisity, and particle size of the material (Hamidi et al., 2013; Mirzahosseini & Riding, 2014; Sanjuán et al., 2015). The chemical composition and physical properties of POCP and OPC are shown in **Table 4.8**. The  $\text{SiO}_2$ ,  $\text{Al}_2\text{O}_3$ ,  $\text{Fe}_2\text{O}_3$  and  $\text{K}_2\text{O}$  are the main ingredients of POCP. The active  $\text{SiO}_2$  is the vital oxide to show the pozzolanic activity. The sum of  $\text{SiO}_2$ ,  $\text{Al}_2\text{O}_3$ , and  $\text{Fe}_2\text{O}_3$  in POCP are 70.23%, which fulfilled the standard requirement to indicate the pozzolanic reactivity (C618-08a.).

**Table 4.8:** Chemical composition of POCP

Chemical Composition (%)	OPC	POCP
$\text{SiO}_2$	22.14	60.29
$\text{Al}_2\text{O}_3$	3.84	5.83
$\text{Fe}_2\text{O}_3$	2.98	4.71
$\text{SiO}_2+\text{Al}_2\text{O}_3+\text{Fe}_2\text{O}_3$	28.96	70.83
CaO	65.21	3.27
MgO	1.54	3.76
$\text{SO}_3$	3.22	0.11
$\text{K}_2\text{O}$	0.012	7.79
$\text{P}_2\text{O}_5$	0.012	3.10
$\text{TiO}_2$	0.002	0.13
Specific surface area ( $\text{m}^2/\text{kg}$ )	339	418

A recent work has been conducted on the chemical composition variation of POCP in different areas in Malaysia (Ahmmad et al., 2014, Kanadasan & Razak, 2014, Binti Robani & Chan, 2009, Kanadasan et al., 2015). The variation of the chemical composition in POCP depends on the feeding ratio in a boiler, the burning condition of the boiler, and the geological condition of the respective area where the palm oil tree were grown. The variation of the pozzolanicity basis on chemical composition is presented in **Table 2.4**.

The reactivity of  $\text{SiO}_2$  also depends on its crystalline nature. Only amorphous  $\text{SiO}_2$  can participate in a chemical reaction with portlandite (Uchima et al., 2015). XRD is an apparatus, which is widely used by many researchers to identify amorphisity of a material (Sow et al., 2015). The XRD pattern of POCP is shown in **Figure 4.15**.

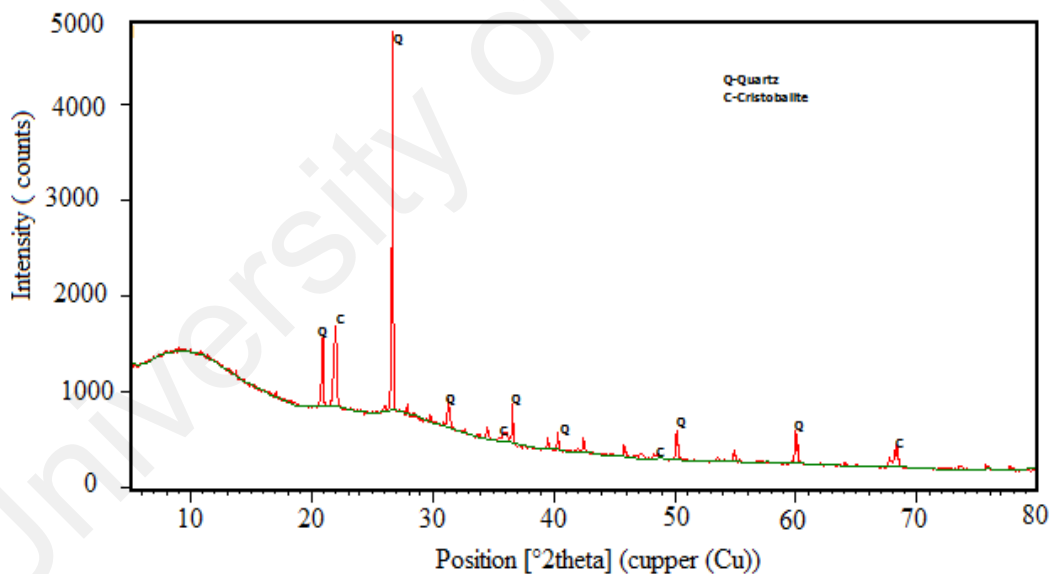


**Figure 4.15:** X-ray diffraction pattern of POCP

The quartz and cristobalite are the major peak was observed at the  $2\theta$  range of  $26.87^\circ$  and  $20.45^\circ$ , respectively. A significant hump was also observed in the angular  $2\theta$  range from  $10^\circ$  to  $35^\circ$ , representing an amorphous phase (Calligaris et al., 2015). The semi quantitative XRD observation was found that quartz, cristobalite, quartz low, gehlenite,

amorphous were present of 20.0%, 2.9%, 0.5%, 31.7% and 39.9%, respectively (Kanadasan & Abdul Razak, 2015). One of the significant parameters of material to show pozzolanic reactivity is its particle size. The particle size distribution of POCP and OPC used in this study is represented in **Figure 4.16**.

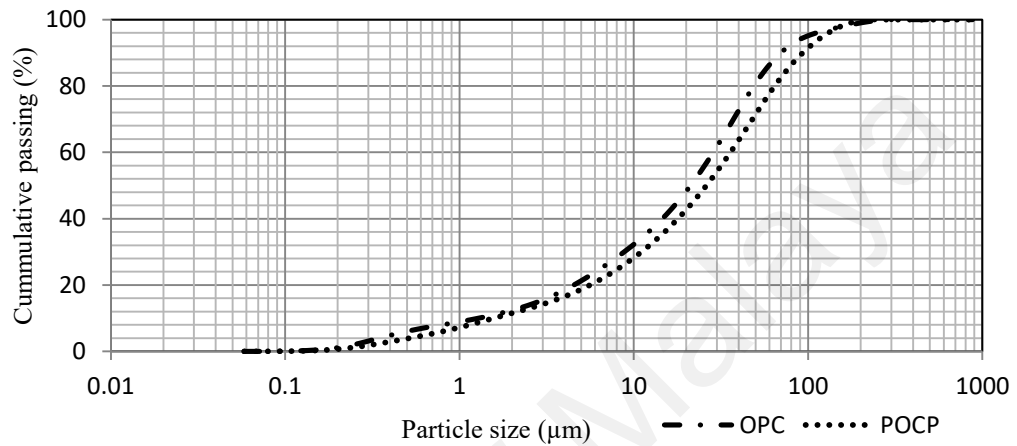


**Figure 4.16:** Particle size distribution of POCP and OPC

The particle size distribution curves of POCP and OPC are almost similar and most of the particle sizes are less than 100 μm. Approximately 50% POCP particles are smaller than 40 μm. Moreover, the specific surface area of OPC and POCP samples are 339 m<sup>2</sup>/kg and 418 m<sup>2</sup>/kg, respectively. POCP has sufficient specific surface area to give pozzolanic activity.



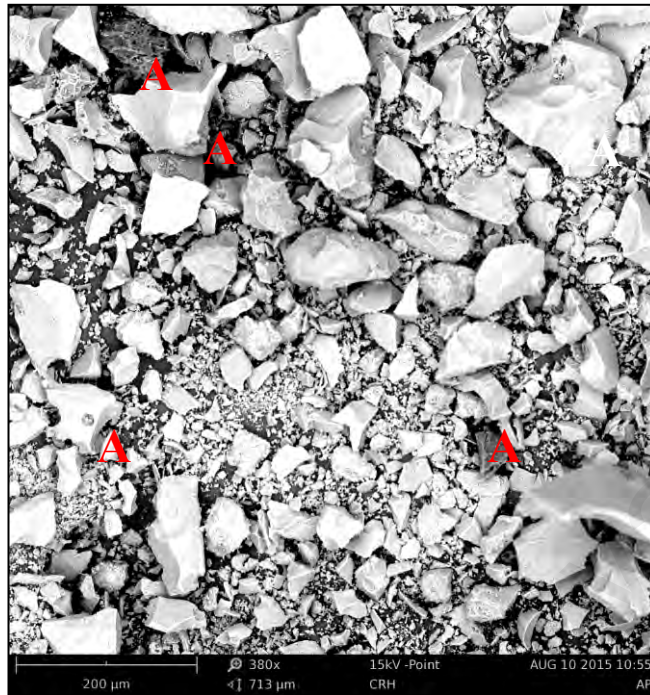


**Figure 4.17:** Micrograph of POCP

The micrograph of POCP is shown in **Figure 4.17**. The morphological analysis found that the POCP contains micro-pores, varies in shapes and sizes. Previous research found that POFA is another form of waste which has micro-pores, varying in shape and size (Khankhaje et al., 2016).

#### 4.4.2 XRD Studies of Pastes

The X-ray diffraction technique is a well-established and very useful tool for the investigation of structural information (Sow et al., 2015). Basically, the interaction of the X-ray with the investigating materials provides important information about the crystalline structure of minerals and types of minerals present. The change in intensity of a characteristic peak of  $\text{Ca}(\text{OH})_2$  at different curing ages for cement paste can also be observed from the XRD patterns. The  $\text{C}_2\text{S}$  (dicalcium silicate or belite),  $\text{C}_3\text{S}$  (tricalcium silicate or alite),  $\text{C}_4\text{AF}$  (tetracalcium alumino ferrite), and  $\text{C}_3\text{A}$  (tricalcium aluminate) are the main phases of pure non-hydrated OPC (Ludwig & Zhang, 2015). During the

hydration reaction, this phase gradually decreases and generates new phase, namely Portlandite and ettringite. The percentage of non hydrated OPC phases and the products of hydration reaction depends on the curing age (reaction time), reaction condition as well as the reactivity of materials blended with OPC. The blended material used is POCP. The assessment of the reactivity of POCP at different curing ages is the objective of the XRD analysis. First observation is the intensity of characteristic peaks of OPC and POCP paste at curing age of 3 days which is shown in **Figure 4.18**.

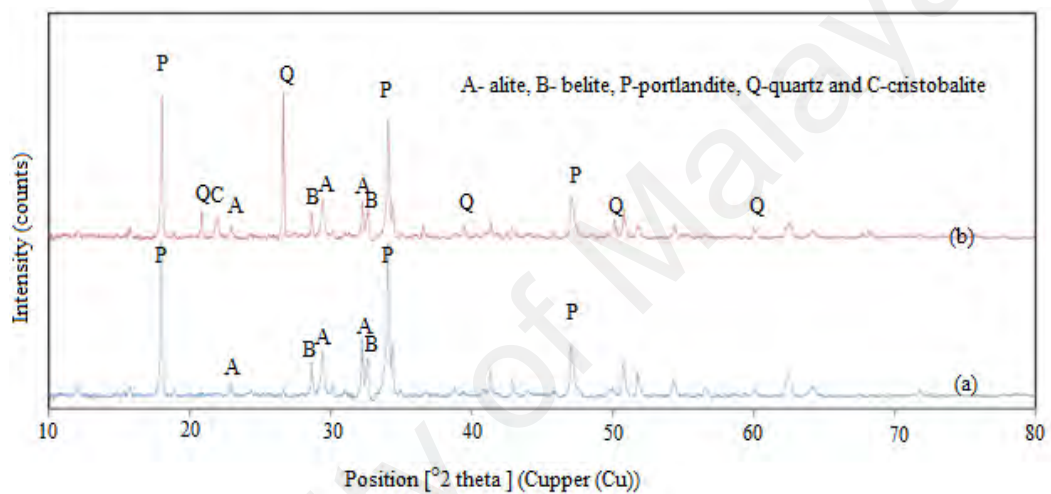


**Figure 4.18:** XRD patterns for (a) OPC and (b) POCP paste cured in 3 days

The quartz and cristobalite are the main peaks of POCP, which remained none reacted in a POCP paste at the curing age of 3 days. Moreover, the non-reacted  $C_2S$  and  $C_3S$  phases of clinker and Portlandite phase were also observed in POCP and OPC paste after 3 days hydration. The  $C_2S$  and  $C_3S$  phases do not have sufficient time for complete hydration reaction. The intense peak of hydration product such as Portlandite was observed at  $2\theta$  of  $18.14^\circ$ . The intensity of Portlandite, non-reacted alite, and belite phases is lower in POCP compared with OPC at curing age of 3 days due to the dilution effect (Khalil et al., 2014).

Second observation is the difference in intensity of characteristic peaks of OPC and POCP at curing age of 28 days which is shown in **Figure 4.19**. It was found that the  $C_2S$  and  $C_3S$  of OPC did not completely take part in the hydration reaction. The reaction rate of  $C_2S$  and  $C_3S$  phase are slow in the presence of water. Moreover, the peak of the quartz and cristobalite were also observed in XRD patterns. The intensity of Portlandite peaks in XRD patterns of the OPC and POCP paste increases with reaction time. The peak intensity of  $C_2S$  and  $C_3S$  phases in OPC and POCP pastes is comparatively lower at the curing age of 28 days compared with 3 days.

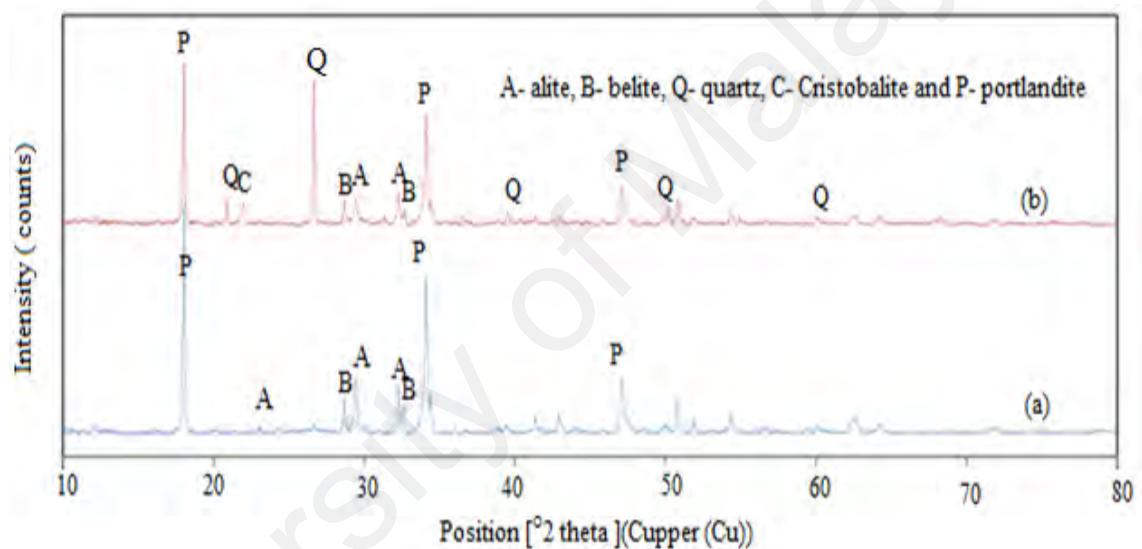


**Figure 4.19:** XRD patterns of OPC and POCP paste of curing age in 28 days

Third observation is the peak intensity of hydration products as well as none reacted phases such as  $C_2S$ ,  $C_3S$  of the curing age of 90 days which is represented in **Figure 4.20**. The intensity of  $C_2S$  and  $C_3S$  peaks is decreased more significantly at curing age of 90 days while the intensity of Portlandite is increased in the POCP paste. Moreover, the intensity of the quartz and cristobalite peaks becomes lower at 90 days of curing time for the POCP paste.

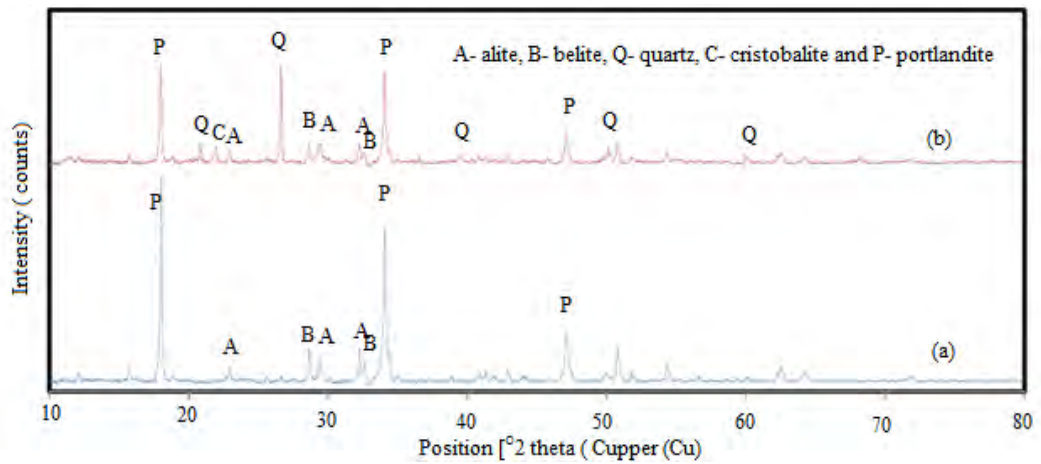


**Figure 4.20:** XRD patterns for OPC and POCPC paste cured in 90 days

Finally, a comparison is done with the intensity of the  $C_2S$  and  $C_3S$  phases and product of the hydration reaction of OPC and POCPC paste i.e. Portlandite for the curing age of 3 days to 90 days. This observation ultimately leads to evaluate the participation of POCPC in chemical reaction with Portlandite. The pozzolanic reaction is basically an acid-based reaction between calcium hydroxide, also known as Portlandite ( $Ca(OH)_2$ ) and silicic acid ( $H_4SiO_4$  or  $Si(OH)_4$ ). The product of this reaction is C-S-H gel. The characteristic peak of the Portlandite was observed in the  $2\theta$  range of  $18.14^\circ$ . The difference in intensity of Portlandite peak between OPC and POCPC pastes at curing ages of 90 days was 9383 counts, which are higher than the curing age of 3 days with the value of 1029 counts. The gap in intensity of Portlandite peak between OPC and POCPC paste at curing ages of 3 days is lower than 28 days. The comparative analysis of the intensity gap of Portlandite peak indicates pozzolanic activity shown by POCPC is at curing age of 3 to 90 days. This observation supports the argument that  $Ca(OH)_2$  is consumed during the pozzolanic reaction (Ashraf et al., 2009). Moreover, the intensity of cristobalite peak decreases with reaction time and almost disappeared at the curing age of 90 days. This observation also supports the participation of POCPC in pozzolanic reaction with  $Ca(OH)_2$  and form C-S-H gel (Khalil et al., 2014).

#### 4.4.3 Thermogravimetric Analysis

The pozzolanic activity of a material is mainly investigated based on the mass loss at two points in thermogravimetric analysis. First, the dehydration of the C-S-H gel takes place at the temperature range of 100°C to 180°C. Second mass loss of the dehydroxation of  $\text{Ca(OH)}_2$  occurs in the temperature range of 450-520°C (Arora et al., 2016; Uchima et al., 2015). The mass loss of OPC and POCPC paste at the curing age of 3 days in the temperature range from 45°C to 1000°C are shown in **Figure 4.21**. The mass loss due to dehydroxation of calcium hydroxide at the temperature range from 400°C to 500°C is lower in POCPC compared with OPC paste. This is due to the less consumption of  $\text{Ca(OH)}_2$  by POCPC and small amount of the  $\text{Ca(OH)}_2$  formed as a result of hydration reaction. The lower amount of  $\text{Ca(OH)}_2$  formation is due to dilution effect when 30% of OPC was replaced by POCPC (Khalil et al., 2014). Moreover, mass loss in the temperature range from 105°C to 180°C is higher in POCPC paste compared with OPC paste cured in 3 days. This mass loss is related to the dehydration of C-S-H gel and the evaporation of the water which is present in the micro pore of POCPC. The SEM micrograph confirmed the presence of micro pores in POCPC. The mass loss related to the  $\text{Ca(OH)}_2$  and C-S-H gel in TGA shows that the pozzolanic activity of POCPC is not significant at curing age of 3 days.

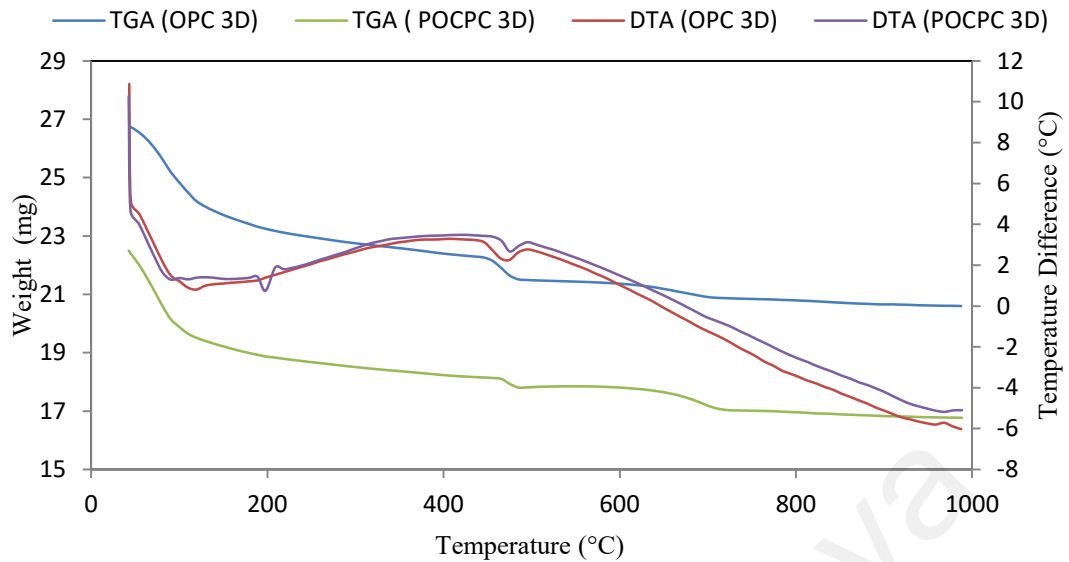


**Figure 4.21:** TGA curve of OPC and POCPC paste cured in 3 days

The mass loss of OPC and POCPC paste at the curing ages of 90 days is shown in the **Figure 4.22**. The mass loss related to the dehydratation of  $\text{Ca(OH)}_2$  at curing age of 90 days of POCPC paste is lower compared with OPC paste. The mass loss in the temperature range of 100-180°C for OPC and POCPC paste is very similar because more C-S-H gel is produced in POCPC which filled up the micro pores of POCPC particles. As a result, the water in the micropores of POCPC matrix was reduced.

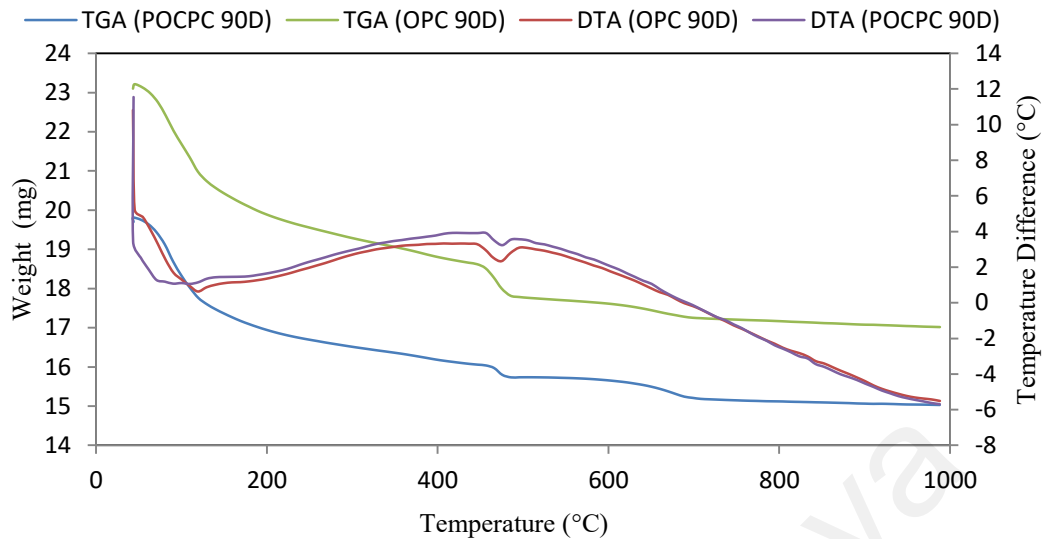


**Figure 4.22:** TGA for OPC and POCPC paste cured in 90 days

A comparative assessment of the concentration difference of the  $\text{Ca(OH)}_2$  at different curing age confirms the pozzolanic activity of POCP (Hamidi et al., 2013). The mass loss difference of OPC and POCPC paste due to dehydratation of  $\text{Ca(OH)}_2$  at curing age of 3 days in the temperature range from  $450^\circ\text{C}$  to  $520^\circ\text{C}$  is 1.25 %, which is lower than the mass loss difference, i.e. 1.86% at curing age of 90 days. It is noticeable that  $\text{Ca(OH)}_2$  takes part in the chemical reaction with POCP. The mass loss for  $\text{Ca(OH)}_2$  at curing age of 3 days is lower for 90 days of OPC paste as well as in POCPC paste. This result confirmed that the  $\text{C}_2\text{S}$  and  $\text{C}_3\text{S}$  did not hydrate completely at curing age of 3 days. XRD data in this study also support that none reacted phases of OPC have a higher intensity peak in OPC and POCPC paste at the curing age of 3 days rather than the 90 days. The comparative assessment found that the higher mass loss difference was observed at the curing age of 90 days, which confirms the participation of  $\text{Ca(OH)}_2$  in chemical reaction with active  $\text{SiO}_2$  of POCP (Ashraf et al., 2009; Khalil et al., 2014). This indicates that POCP is a pozzolanic material.

#### 4.4.4 FTIR Analysis

The FTIR spectra of POCPC and OPC paste of curing ages 90 days is shown in **Figure 4.23**. The strong vibration bands are due to the O-H bond of Portlandite ( $\text{Ca(OH)}_2$ ) which is observed at wavelength of  $3641\text{cm}^{-1}$  and another small peak was also observed at  $539\text{cm}^{-1}$  (Moraes et al., 2015). The intensity of O-H peak in POCPC paste is lower than OPC paste. This result predicts that the concentration of  $\text{Ca(OH)}_2$  in POCPC paste is less than in OPC paste. This result is also supported by the XRD and TGA data. The main vibration bands associated with Si-O bond were at  $956\text{cm}^{-1}$ . This band is attributed to the formation of C-S-H gel due to the pozzolanic reaction (Moraes et al., 2015). The intensity of this band in POCPC paste is stronger than in OPC paste. Both observations confirm that POCPC is a pozzolanic material.

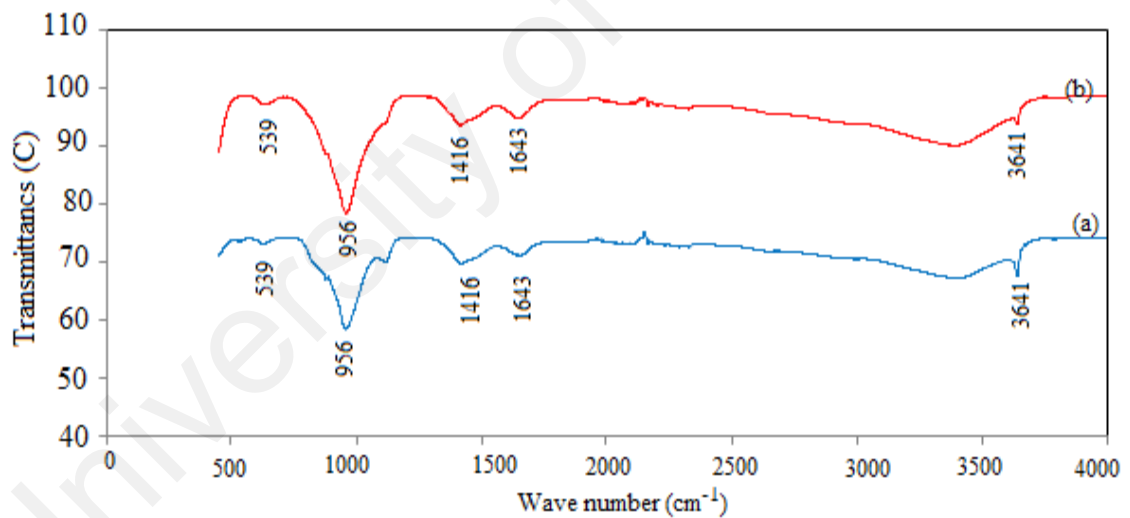


**Figure 4.23:** FTIR analysis of (a) OPC and (b) POCPC paste cured in 90 days

#### 4.4.5 Microstructure Analysis

FESEM observation was also conducted to evaluate the pozzolanic activity of POCPC. **Figure 4.24** shows the FESEM micrograph for OPC paste and 30% POCPC blended cement paste at the curing age of 90 days. The hydration products were mainly in



crystalline and amorphous phase of Portlandite (CH) and C-S-H gel, respectively. The FESEM micrograph of **Figure 4.24 (b)** clearly shows that an amorphous gel is formed due to the pozzolanic reaction of POCP. A dense matrix structure was obtained and the presence of hydrated lime was not apparent. The micro pores of POCP particles were filled by the C-S-H gel. The FTIR and TGA data also confirms the formation of C-S-H gel due to pozzolanic reaction of POCP.

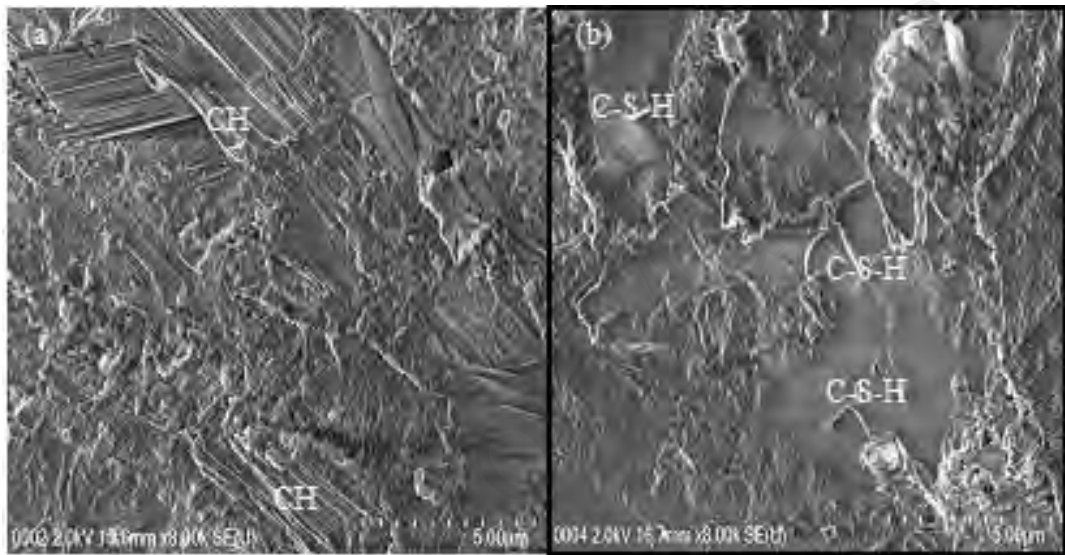


**Figure 4.24:** Micrographs of (a) OPC and (b) POCP pastes cured in 90 days

#### 4.4.6 Strength Activity Index (SAI)

A number of researchers have used the strength activity index method for the determination of the pozzolanic properties of different materials (Alam et al., 2015; Lim et al., 2015). The strength activity index of the waste material can be calculated according to ASTM method using **(Equation 4.3)**,

$$\text{Strength Activity Index(SAI)} = \frac{A}{B} \times 100 \quad (4.3)$$

where, A and B represent the average compressive strength of POCP and control mortar, respectively. The strength activity index of POCP is measured by comparing the

compressive strength of ordinary Portland cement (control mortar) and POCP mortar. The dilution factor is the cause for the decrease in compressive strength in POCP mortar. The compressive strength of POCP mortar at curing age of 7 days and 28 days were 76% and 87% of OPC mortar, respectively, which fulfilled the standard ASTM C 311-13 for pozzolanic activity. The increase in SAI at 28 days may be accredited to the reaction of active phase with CH produced as a result of cement hydration. It is observed that the addition of POCP caused a decrease in the compressive strength at the curing age of 7 days due to the dilution effect and delay of pozzolanic reaction. After 28 days, the mortar containing POCP further increases up to 75% in SAI due to the pozzolanic reaction of POCP. Thus, it can be considered as a pozzolanic material (Lim et al., 2015).

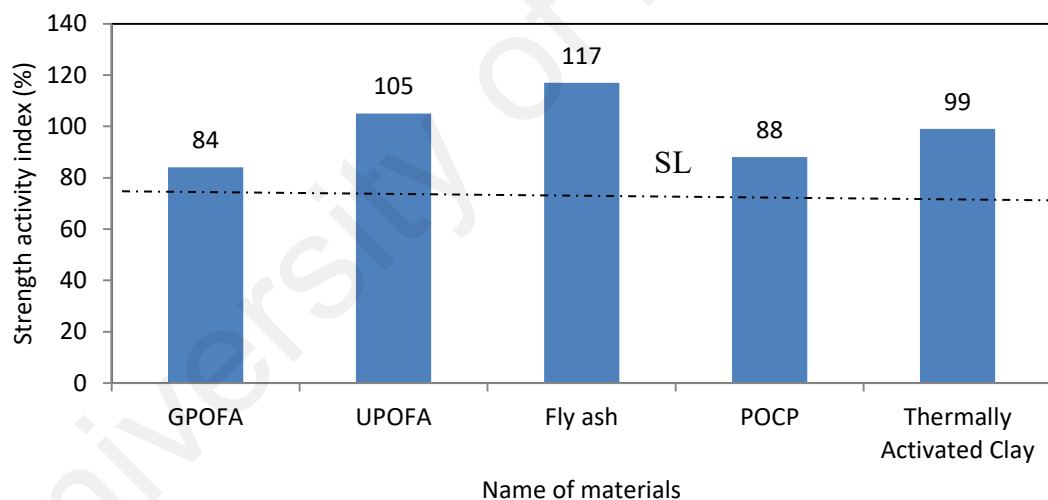


**Figure 4.25:** Strength activity indexes (28 days) of waste materials

A comparative assessment of the strength activity index of ground POFA (GPOFA) (Lim et al., 2015), ultrafine POFA (UPOFA) (Lim et al., 2015), fly ash (Jaturapitakkul et al., 1999), POCP and thermally activated clay is represented in **Figure 4.25**. The horizontal dotted line (SL) in **Figure 4.25** indicates the lower limit of the standard for a pozzolanic material. The strength activity index of POCP is between GPOFA and

UPOFA. The pozzolanic activity of UPOFA is higher compared to GPOFA may be due to small particle size and the reduction of organic carbon in UPOFA (Lim et al., 2015). The specific surface area of POCP and GPOFA were 418 and 493.5 m<sup>2</sup>/kg, respectively. The strength activity index of POCP is slightly higher than GPOFA. This may be due to the difference of chemical composition and amorphisity. Moreover, the strength activity index of fly ash and activated clay is higher than POCP. This is due to the active amorphous phase content in fly ash, and the clay becomes amorphous through the thermal activation.

The pozzolanic activity of POCP is confirmed by the means of XRD, TGA, and FTIR studies of OPC and 30% of POCP blended cement paste at the curing age of 3 days, 28 days and 90 days. Moreover, the strength activity index result also shows the pozzolanic activity of POCP. POCP is a pozzolanic material. The strength activity index assessment found that pozzolanic activity of POCP is lower than fly ash, UPOFA, and activated clay but higher than GPOFA.

#### **4.5 Fresh and Hardened Properties**

The effect of POCP on basic properties of cement, i.e. setting time, water for normal consistency, soundness, viscosity and compressive strength is explained in details. The benefit of the incorporation of POCP which reduce cost and greenhouse gas is also discussed. The contribution of POCP in preserving the natural resource will be described in this section.

##### **4.5.1 Characteristics of Materials**

The properties of OPC and POCP are presented in **Table 4.9**. The specific surface area and specific gravity of POCP were 434 m<sup>2</sup>/kg and 2.14g/cc, respectively, while the values for OPC are 531m<sup>2</sup>/kg and 3.13 g/cc, respectively. The main phases of OPC can

be calculated according to the Brogue equation. The  $\text{Al}_2\text{O}_3/\text{Fe}_2\text{O}_3$  ratio of Portland cement was 2.55 which is greater than the standard limit of 0.64. The cement used in the present experimental study comprises of Tricalcium silicate/Alite ( $\text{C}_3\text{S}$ ) -57.21%, Dicalcium silicate/Belite ( $\text{C}_2\text{S}$ ) -16.65%, Tricalciumaluminate /Aluminate ( $\text{C}_3\text{A}$ ) - 9.88% and Tetracalcium alumino ferrite/ Ferrite  $\text{C}_4\text{AF}$  -6.87%. The summation of  $\text{C}_3\text{S}$  and  $\text{C}_2\text{S}$  was 73.86 %, which greater than the ASTM standard limit of 70%. POCP is the mixture of inorganic oxides with a minor fraction of organic matter. ASTM C 618 standard method is used to categorize as a fly ash 'C' or 'F'. Fly ash of 'C' class contains high calcium because it is normally derived from lignite coal, whereas fly ash of 'F' class comes from bituminous coal and contains low calcium. The chemical composition, moistures and loss of ignition analysis confirm that POCP belongs to Class 'F' fly ash.

**Table 4.9:** Properties of OPC and POCP

<b>Chemical Composition (%)</b>	<b>OPC</b>	<b>POCP</b>	<b>Class F fly ash ASTM C-618 requirements</b>	<b>Class C fly ash ASTM C-618 requirements</b>
$\text{SiO}_2$	21.34	59.21	N/A	N/A
$\text{Al}_2\text{O}_3$	5.13	5.56	N/A	N/A
$\text{Fe}_2\text{O}_3$	2.98	6.90	N/A	N/A
$\text{SiO}_2 + \text{Al}_2\text{O}_3 + \text{Fe}_2\text{O}_3$	29.45	71.67	>70	>50
CaO	64.56	5.23	N/A	N/A
MgO	1.13	3.45	N/A	N/A
$\text{SO}_3$	2.41	2.31	<5.0	<5.0
$\text{Na}_2\text{O}$ equivalent	0.12	16.23	N/A	N/A
$\text{P}_2\text{O}_5$	0.03	0.03	N/A	N/A
$\text{TiO}_2$	0.01	0.14	N/A	N/A
TOC	--	3.45	N/A	N/A
Moisture	0.52	0.23	<3.0	<3.0
Loss of ignition (LOI)	1.35	4.10	6	6
Insoluble residue (IR)	0.65	36.23	N/A	N/A

The particle size is one of the significant factors of supplementary materials, which influences the rheological properties of the paste and compressive strength of mortars. The particle sizes of POCP and OPC are shown in **Figure 4.26**. The particle size of Portland cement of this experiment is found to be similar with that of POCP.

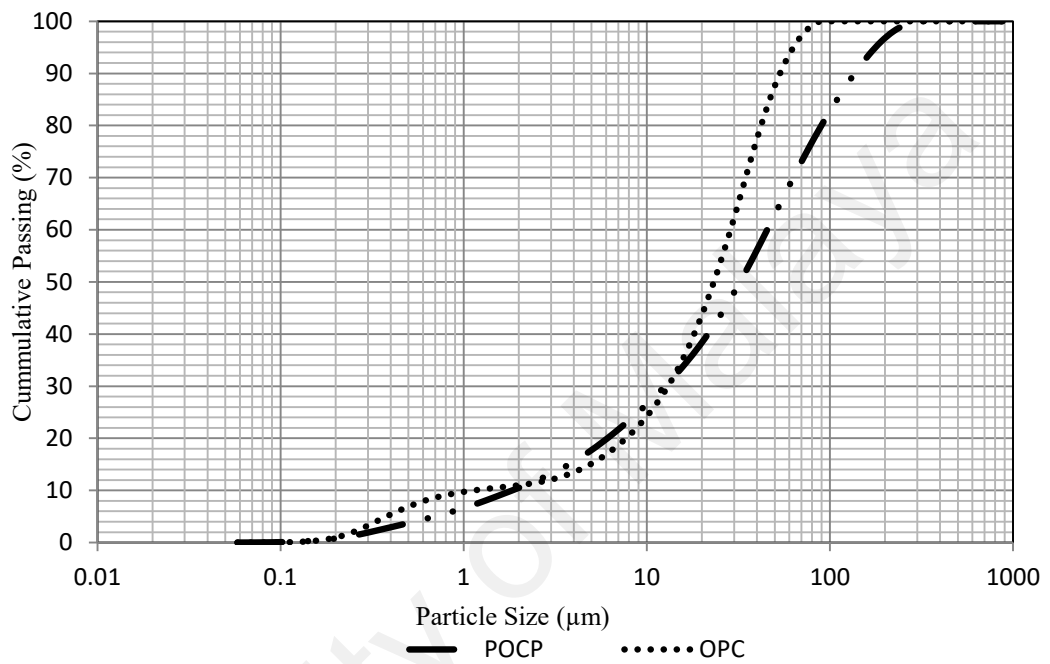


**Figure 4.26:** Particle size of OPC and POCP

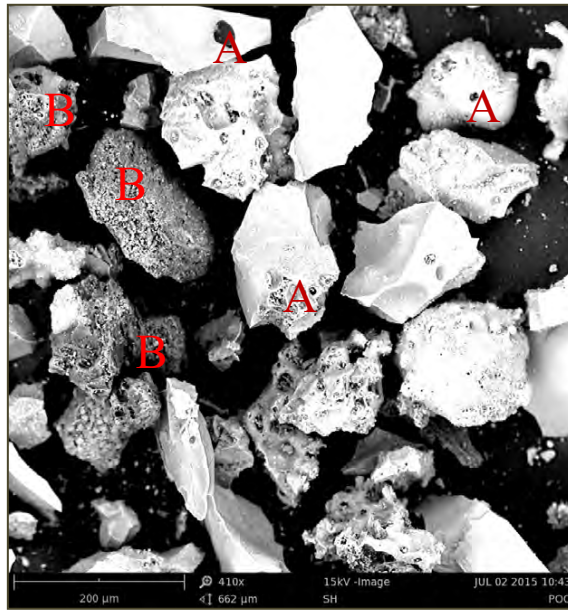


**Figure 4.27:** Micrograph of POCP

The micrograph of POCP is shown in **Figure 4.27**. The POCP particles are irregular in shape and have a micro porous cellular structure. The pore is marked as ‘A’ and the network type fibre as ‘B’ in **Figure 4.27**. The irregular shape and micro pore structure is due to the unburned carbon particles.

## **4.5.2 Rheological Properties**

### **4.5.2.1 Consistency**

The quantity of water for normal consistency of blended cement depends on the chemical composition, fineness and porosity of the added materials. The relative water demands of POCP blended cement at different replacement level is shown in **Figure 4.28**.

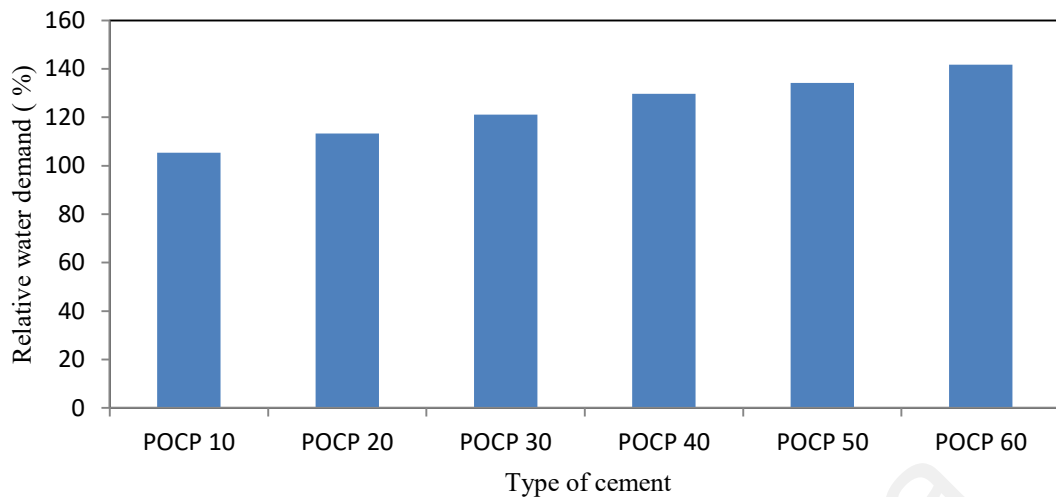


**Figure 4.28:** Relative water demand in POCP blended cements

Water demand increases with replacement level of OPC by POCP. The water for normal consistency of POCP10, POCP20, POCP30, POCP40, POCP50 and POCP60 were 105.3%, 113.3%, 121.1%, 129.7%, 134.2% and 141.7% of OPC, respectively. The water for normal consistency is a physical observation of the early state of hydration. An initial flocculation of cement particle takes place quickly after adding the water. The water demand is related to the physical features and chemical composition of POCP. SEM observation shows that POCP is irregular in shape, size and have lots of micro pores. Free bulk water is a function to fill the micro pore of POCP particles. The physically absorbed water bounded with outer surfaces and pore walls. The substitution of OPC by POCP increased the micro pore vacant space as a result increase in the water demand.

#### 4.5.2.2 Setting time of cement paste

The setting time is a basic requirement of cement standard. According to ASTM standard the setting time shall be lower or equal to 375 minutes for OPC cement. The setting time of OPC and POCP blended cement paste are presented in **Figure 4.29**. The initial time (IST) and final setting time (FST) increased with addition of POCP.

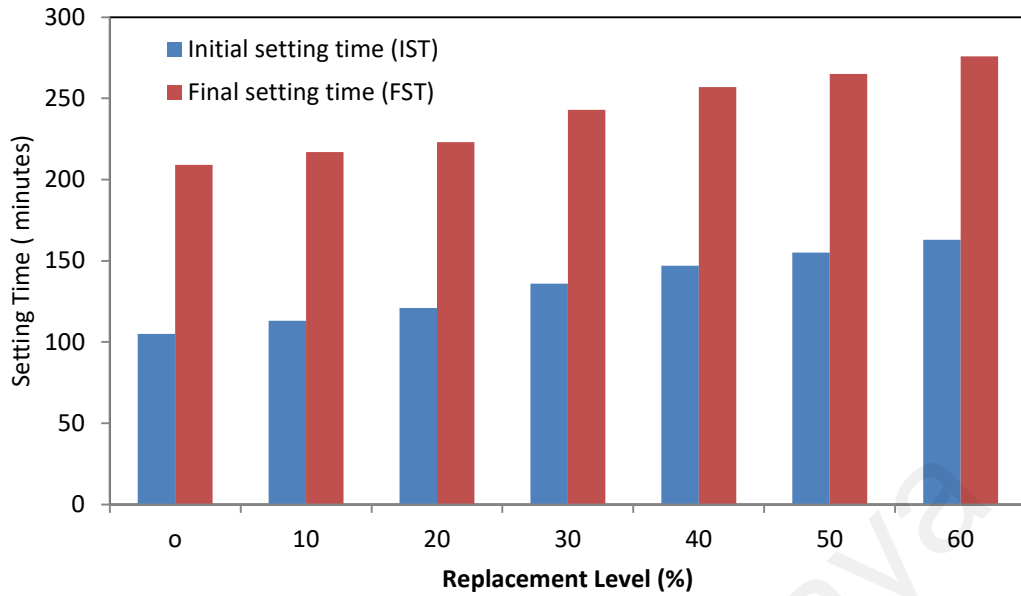


**Figure 4.29:** Effect of POCP on setting behaviour

The setting time increase with the replacement level of OPC by POCP. The setting time is controlled by the addition gypsum ( $\text{CaSO}_4 \cdot 2\text{H}_2\text{O}$ ). Moreover, the  $\text{C}_3\text{A}$ ,  $\text{C}_2\text{S}$  and  $\text{C}_3\text{S}$  phase of OPC cement reacted quickly with water and became hard within a few seconds. The function of gypsum is to delay the hydration reaction time of phases by forming ettringite as shown in **Equation (4.4)**.



The early reaction rate of cement depends on the ionic species ( $\text{Ca}^{+2}$ ,  $\text{SO}_4^{-2}$ ,  $\text{OH}^-$  and  $\text{CO}_3^{-2}$ ) available to make barriers over the grains of the aluminate and ferrite phases. The availability and activity of these ions are governed by some factors, such as allocation of  $\text{Al}_2\text{O}_3$  in the clinker phases, the particle size and quality and quantity of the gypsum. In the case of blended cement, the setting time also depends on the active  $\text{Al}_2\text{O}_3$  present in the POCP waste materials. The early reaction rate of blended cement is retarded due to the existence of POCP particles in OPC particles and reduction in  $\text{C}_3\text{S}$ ,



and  $C_3A$  phase in the blended cement. These are the reasons behind the reduction of the setting time in POCP blended cement.

#### 4.5.2.3 Viscosity of cement paste

The rheological properties of blended cement paste depend on the water to cement ratio, particle size, mineral composition, condition of measurement, mixing time and temperature (Autier et al., 2013; Montes et al., 2013; Chandara et al., 2010; Grzeszczyk & Janowska-Renkas, 2012). The rheological data of the OPC and POCP blended cement paste at different replacement levels are depicted in **Figure 4.30** and **Figure 4.31**.

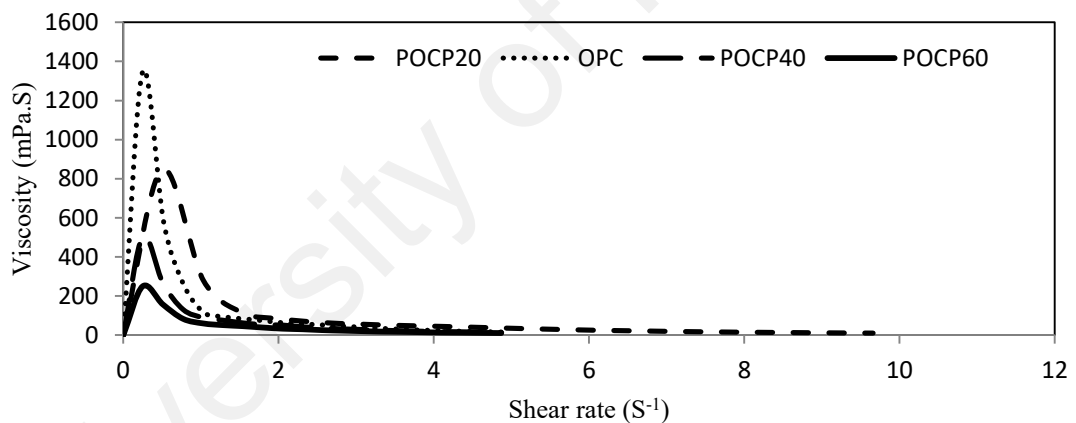


**Figure 4.30:** Viscosity related with shear rate (running time-60 seconds)

**Figure 4.30** shows that the viscosity value increases with shear rate, then falls sharply and remains a constant value in the rest of the range. The maximum viscosity value for OPC, POCP20, POCP40 and POCP 60 was found to be 1347.94, 847.35, 502.4 and 249.8 m Pa.S, respectively. The maximum value of approximate mixing time

is around 6 seconds. The variation of viscosity of POCP blended cements as well as OPC is due to their difference in chemical composition.

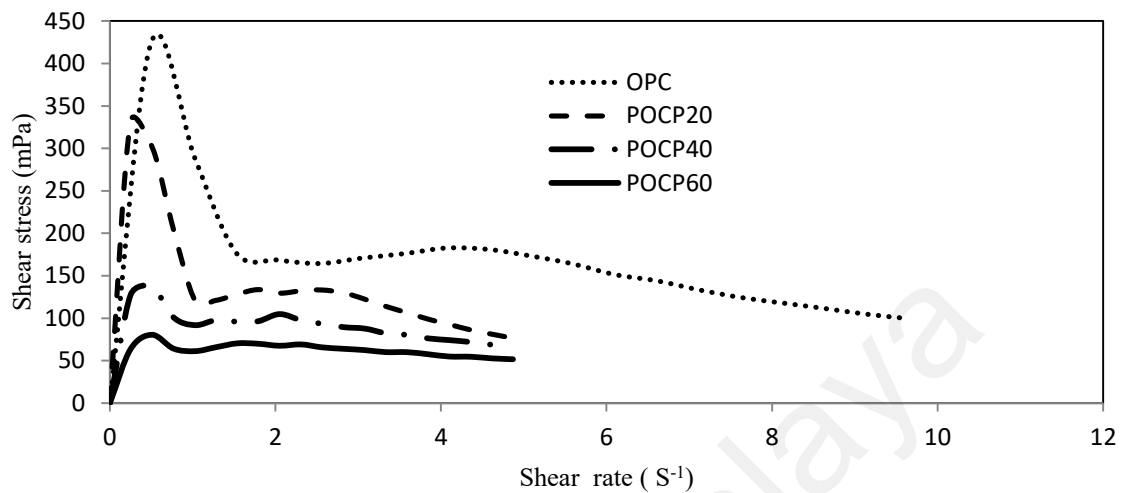


**Figure 4.31:** Shear stress related to shear rate (running time 60 seconds)

**Figure 4.31** shows the relationship between shear stress and the rate of OPC and POCP blended cement paste at running time of 60 seconds. The high shear stress was observed for OPC and then gradually decreases with replacement level of OPC by POCP. The maximum value of shear rate with respect of shear stress was observed at the running time of the Viscometer of 6 seconds for OPC and POCP20 and 9 seconds for POCP40 and POCP60, respectively. The maximum shear stress value for OPC, POCP20, POCP40 and POCP 60 are found to be 424.84, 331.72, 137.24 and 80.48 MPa, respectively. The  $C_3A$  and  $C_3S$  of OPC clinker are mainly responsible for the early hydration reaction. This active ingredients decrease in POCP blended cement paste.

### 4.5.3 Volume Stability

The value of volume expansion is found very low which around 0.2 mm (**Figure 4.32**). The volume stability of POCP blended cement up to 60% replacement

levels of OPC is lower compared with the standard value of 10 mm. The excess amounts of the f-CaO, MgO and SO<sub>3</sub> are responsible for the expansion of the cement paste. The free lime reacts with water resulting in increased the expansion (Chandara et al., 2010). This is the primary causes of the crack formation in the concrete. The volume expansion rates of POCP blended cement paste are found higher than that of OPC which is due to surplus MgO in POCP blended cement as shown in **Table 4.9** (Kocak & Nas, 2014).

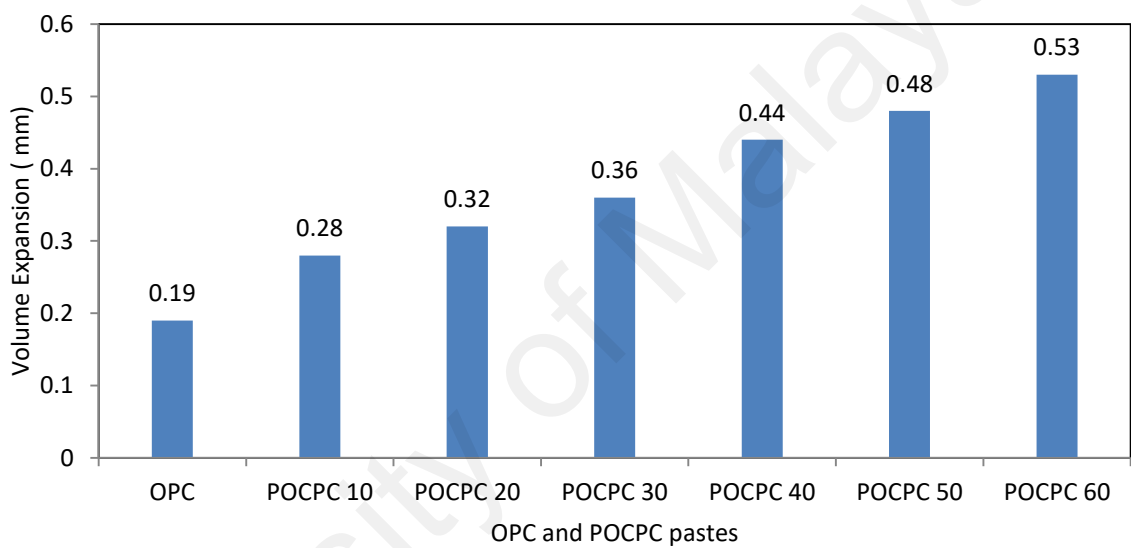


**Figure 4.32:** Volume expansion of POCP blended cements

Although the expansion of POCP blended cement is slightly higher, it fulfills the requirement of the ASTM standard of 10 mm (ASTM Standard, 2000).

#### 4.5.4 Compressive Strength

The assessment of compressive strength of a mortar is a significant factor for introducing a new supplementary cementitious material and its application in concrete. Therefore, the compressive strength of Portland and POCP blended cement mortars are revealed in **Figure 4.33**. From **Figure 4.33**, the compressive strength of the POCP blended cement mortars was found to increase with the reaction time or curing time, but

decreased with the replacement levels of OPC by POCP. The compressive strength of OPC, POCP10, POCP20, POCP30, POCP40, POCP50 and POCP60 are 78.3, 65.6, 62.4, 53.1, 46.1, 37.7 and 29.5 MPa, respectively.

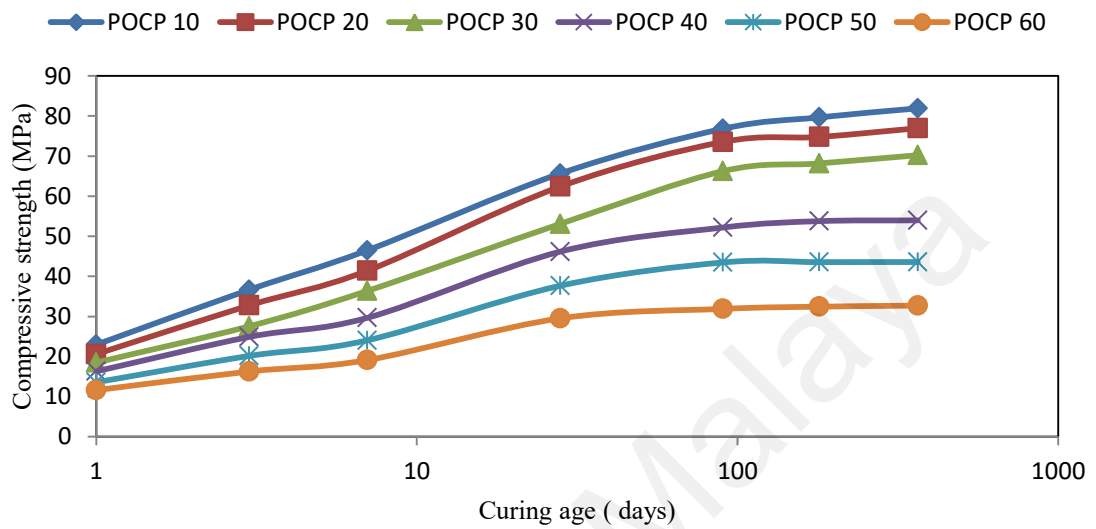


**Figure 4.33:** Effect of POCP on compressive strength

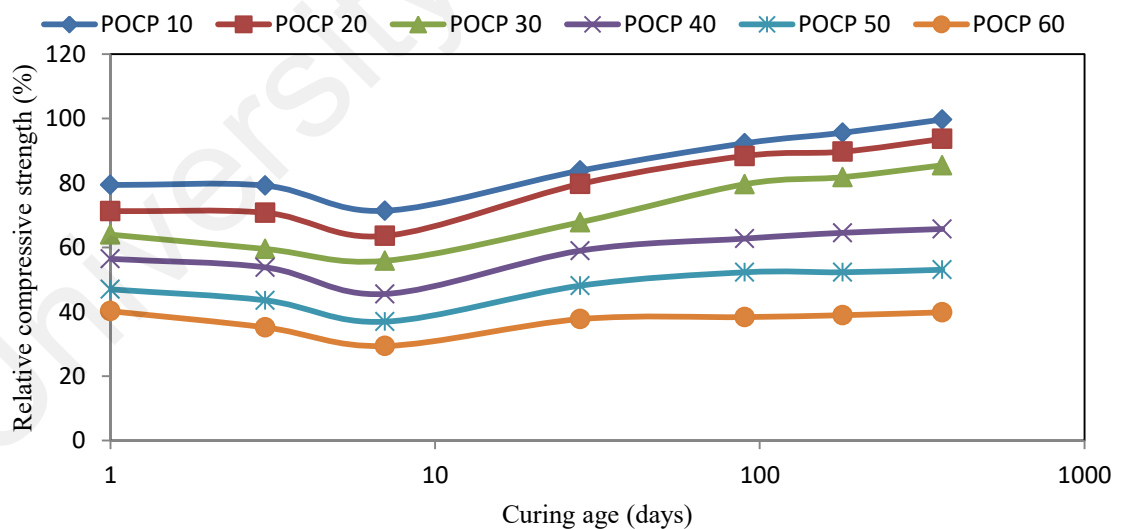


**Figure 4.34:** Relative compressive strength of cements

Admixtures have two type of effects on blended cement, viz., nucleation and packing effect. The packing effect is a physical interaction in which small particle place inside

the cement particle which increase overall matrix density thereby increasing the compressive strength. However, this effect largely depends on particle size. Meanwhile, since POC particle is more porous than OPC, they have no significant contribution on strength development. On the other hand, the nucleation effect arises when the small particles are dispersed in the blended cement paste and take part in the cement hydration reaction. These effects are responsible for progressive strength development and also depend on active surface of  $\text{SiO}_2$ . Literature survey shows that the compressive strength decrease with replacement level of OPC using wastes, which is due to lowering of the content active phase of  $\text{C}_2\text{S}$ ,  $\text{C}_3\text{S}$  and  $\text{C}_3\text{A}$  (Conesa et al., 2008; Segui et al., 2012). **Figure 4.34** shows that the relative compressive strength of POCP blended cement with respect to OPC decrease up to 7 days and gradually increase. The excess alkali metal oxide content in POCP is responsible for early strength development. The strength development from 7 to 365 days is mainly due to the pozzolanic activity of POCP.

#### 4.5.5 Flexural Strength

The effect of POCP on flexural strength in 28 days with corresponding replacement level is shown in **Figure 4.35**. The flexural strength of POCP blended cements decreases with the replacement levels. The effectiveness of POCP particle depends on the bonding energy between aggregate with of the paste. This bonding energy reduces with replacement level of OPC with POCP. The variation of flexural strength at different replacement levels is an indication for the interaction of POCP in the transition zone. Moreover, the irregular shape porous and fibrous nature of POCP is also responsible for the effectiveness in paste-aggregate interface.

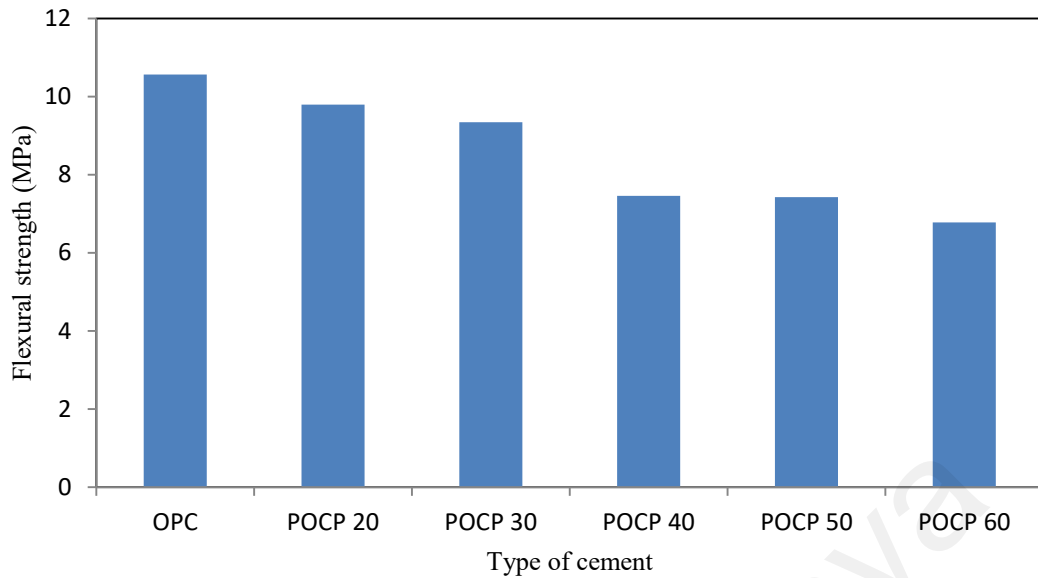


**Figure 4.35:** Effect of POCP on flexural strength

#### 4.5.6 Cost and Compressive Strength

The feasibility of POCP as cementitious materials in cement production is predominately related to the cost of incorporation of the POCP. One of the main focus of the present research work is to evaluate the economic aspects of incorporation of POCP in composite cement when compared with OPC. The Palm Oil Clinker is discarded in abundance from palm oil mill in Malaysia that is mostly used for the covering of potholes on roads. One of the drawbacks of the utilization of OPC in concrete is its high cost. The main cost is related to fuel for burning the raw materials at a temperature range of 340°C to 1750°C in a kiln to produce main phases, viz.,  $C_2S$ ,  $C_3S$  and  $C_3A$  of cement. **Figure 4.36** shows that the economic benefit for incorporation of POCP and the relative compressive strength of standard age.

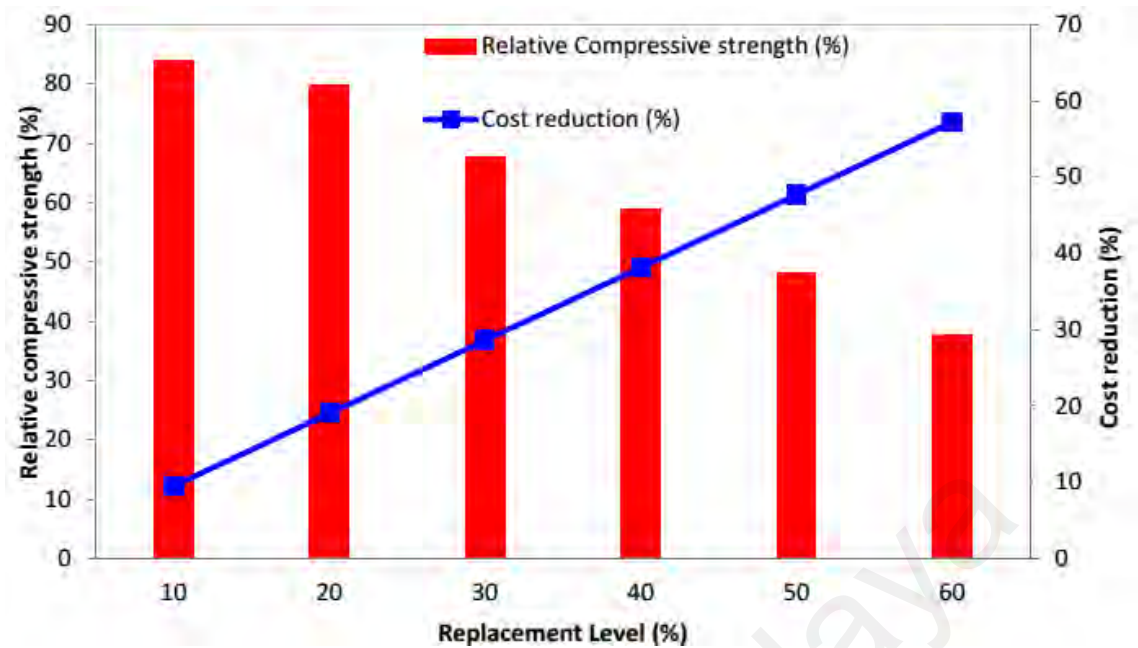


**Figure 4.36:** Cost and compressive strength of cements

The cost-benefit analysis has been done based on the prices of the OPC and palm oil clinker in local markets in Malaysia. The prices of OPC and palm oil clinker were found to be as 0.44RM/kg and 0.02RM/kg, respectively. **Figure 4.36** shows that the cost and the relative compressive strength of POCP blended cement decreases with the replacement level. The incorporation of POCP in cement decreases the cost. The cost saving factor with compressive strength expresses the engineering economic index. The potential user of blended cement can easily select the expected compressive strength of cement and its corresponding expenditure. The utilization of palm oil clinker is found to be economically viable (Chen et al., 2016; Kanadasan & Razak, 2015).

#### 4.5.7 Greenhouse Gas Reduction and Compressive Strength

**Figure 4.37** shows the relationship between the greenhouse emission of POCP blended cements and the compressive strength at 28 days for different replacement level of OPC. The calculation was performed by setting up some boundaries for current practice of palm oil mill. Traditionally, palm oil clinker is dumped in the open land

without any treatment, which is currently being used directly in blended cement production without any pre-processing. The carbon dioxide emission for POCP blended cement production is calculated based on the UNEP and Mineral Products Association guidelines (Association, 2012; Jones et al., 2011; Thomas et al., 2000). The carbon dioxide emission in the primary process of POCP is zero because it is a by-product of palm oil mill. The CO<sub>2</sub> emission related to the transport of POCP is 0.156 kg/km for diesel vehicles and the average distances of palm oil mill to cement factory is considered to be about 50 km. The CO<sub>2</sub> emissions are 0.95 tonnes per tonne of OPC production.

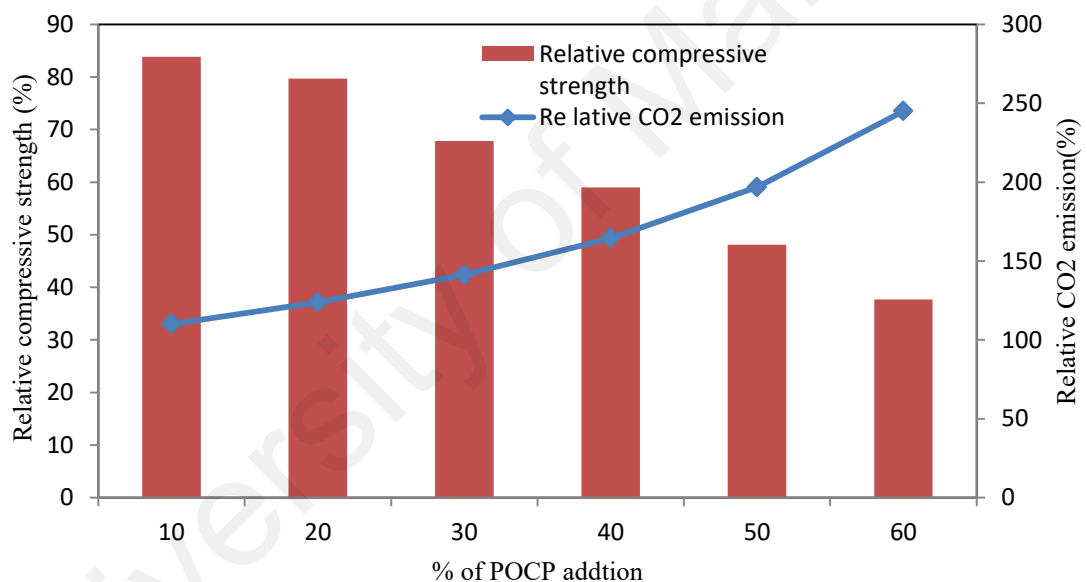


**Figure 4.37:** CO<sub>2</sub> reduction and compressive strength of cements

However, the POCP incorporation lowers the emission by 25.6% at the 10% replacement level of OPC. In literature, it was found that the basic oxygen furnace slag was used as supplementary materials for carbon dioxide reduction (Chen et al., 2016). The overall utilization of supplementary materials in cement reached up to 34.2% in 2016 which reduced CO<sub>2</sub> emission by 312 Mt CO<sub>2</sub> as compared to the 2013 level of CO<sub>2</sub> emission (Kajaste & Hurme, 2016). Therefore, incorporation of POCP as a



supplementary cementitious material would be a potential way to reduce CO<sub>2</sub> emissions in the grinding stage of composite cement production. This is a significant outcome of the present research from the viewpoint of environmental safety.

#### **4.5.8 Natural Resource Conservation**

The utilization of POCP in cement production is a prospective approach in saving the natural resource of OPC clinker. This approach not only offers an environmental friendly treatment of waste, but also convert the waste into a resource. Palm oil clinker is produced in large quantity as a by-product of palm oil industry in Malaysia. As may be noted, solid waste management is a vital issue in Malaysia, particularly in the urban areas. There are many challenges in the disposal system of solid waste, including land shortage, economical problem and lack of public awareness. The cement industry in Malaysia can play an important role in converting the palm oil mill waste (POCP) into a resource that would otherwise cause multiple problems like water pollution, alternation of soil composition and air pollution. **Figure 4.38** presents the saving of the natural resources of OPC by using the POCP as supplementary material in blended cement.

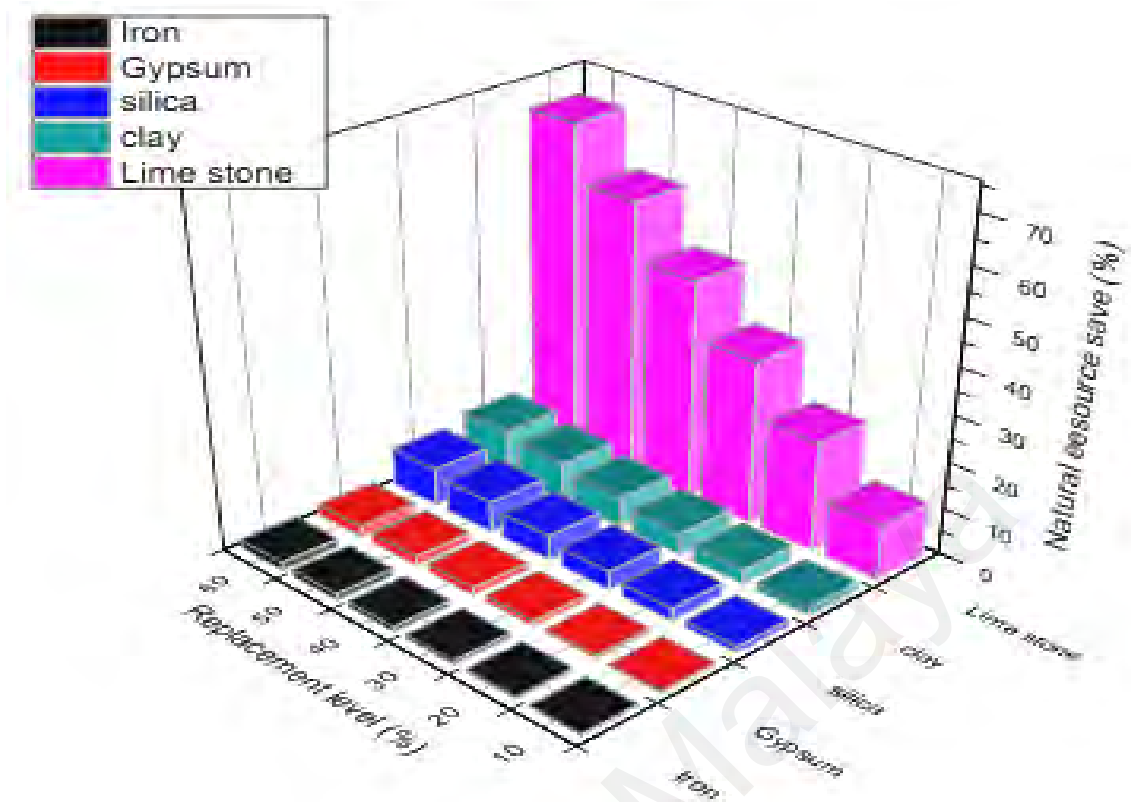


**Figure 4.38:** Natural resource conservation at different replacement levels

OPC clinker is a composite mixture of different oxides which comes from the natural raw materials. The phases of the OPC clinker usually consist of  $\text{CaO}$ ,  $\text{SiO}_2$  and  $\text{Al}_2\text{O}_3$ , which are produced as a result of physico-chemical change of the limestone, quartz and the clay or shale in a kiln. The natural resources conservation is calculated based on the data presented in the literature (Hewlett et al., 2003). The composition of raw mixed, i.e. limestone, clay, Iron ore and silica shale of OPC clinker is considered as 78.00%, 11%, 2% and 9%, respectively in the current study. Previous studies show that the clinker was produced with approximately 64% of raw materials by weight (Hewlett et al., 2003). This is mainly due to the calcination of limestone. A composition of 96% clinker and 4% gypsum for OPC production is considered in this calculation. The 96% clinker is produced from 117% limestone, 16.5% clay, 3% iron ore and 13.5% silica shale. The analysis found that the limestone, clay, Iron ore, silica shale and gypsum

saved are 35.1%, 4.95%, 0.9%, 4.05% and 1.2%, respectively at 30% incorporation of POCP in OPC.

The setting time, water demand and soundness increased with replacement level of OPC by POCP, but remain within the limit of the ASTM standard. The incorporation of POCP reduces the cost, greenhouse gas emission and save the natural resource significantly.

#### 4.6 Radiological Hazards

The first part of this section will discuss the characterization result of the radionuclide present in POCP and POFA, and then calculate the different radiological hazard indicators. At the last part of this section, comparison will be made the radiological risk of POCP with POFA and coal fly ash for its possible use as ingredient for building materials.

##### 4.6.1 Radionuclide in POC and POFA

Recently, POC and POFA have found diversified application in concrete construction. Therefore, it is essential to observe the possible radiological risk caused by the  $^{226}\text{Ra}$ ,  $^{232}\text{Th}$  and  $^{40}\text{K}$  radionuclides to the population for incorporation of palm oil mill waste in concrete construction. The activity levels of  $^{226}\text{Ra}$ ,  $^{232}\text{Th}$  and  $^{40}\text{K}$  in POC and POFA are shown in **Table 4.10**. The activity concentration in POC samples was found to be in the range of  $7.01\pm 0.12$  to  $5.56\pm 0.23$  (average:  $6.40\pm 0.25$ ),  $4.87\pm 0.14$  to  $4.21\pm 0.03$  (average:  $4.53\pm 0.09$ ) and  $604.23\pm 2.18$  to  $570.56\pm 1.88$  (average:  $583.90\pm 1.95$ )  $\text{Bq kg}^{-1}$  for  $^{226}\text{Ra}$ ,  $^{232}\text{Th}$  and  $^{40}\text{K}$ , respectively. Similarly, the activity levels of  $^{226}\text{Ra}$ ,  $^{232}\text{Th}$  and  $^{40}\text{K}$  in POFA sample varied from  $9.03\pm 0.21$  to  $6.98\pm 0.29$  (average:  $8.10\pm 0.33$ ),  $7.98\pm 0.19$  to  $6.14\pm 0.12$  (average:  $7.02\pm 0.15$ ) and  $413.01\pm 1.78$  to  $498.02\pm 2.31$  (average:  $446.65\pm 2.30$ )  $\text{Bq kg}^{-1}$ , respectively. The differences in the

activity concentration between the POC and POFA samples is due to the radioactive mineral content, origin of materials, the geochemical and geological parameter of soil from where up taking the radionuclides by the palm oil plants and generating process in palm oil mill, among other factors (Kumari et al., 2015; Peppas et al., 2010). The difference in activity concentrations of  $^{226}\text{Ra}$  and  $^{232}\text{Th}$  among the palm oil mill wastes are insignificant. One possible reason might be because both wastes originate from the same source. The activity concentration of  $^{226}\text{Ra}$  and  $^{232}\text{Th}$  in palm oil mill waste were found to be lower than the world average value of  $50 \text{ Bq kg}^{-1}$  (Asaduzzaman et al., 2015). By contrast, the activity concentration of  $^{40}\text{K}$  in POFA is somewhat lower than the POC which may be due to the differences in particle size of raw POC and POFA (Peppas et al., 2010). Moreover, the  $^{40}\text{K}$  activity concentration in POC is greater than the world average value of  $500 \text{ Bq kg}^{-1}$  (Asaduzzaman et al., 2015). The activity level of thorium was found to be higher than radium, which may be due to the reason that the abundance of thorium is greater than radium in the soil of Malaysia which is presented in **Table 2.5** in page 39.

**Table 4.10:** Radioactivity of  $^{226}\text{Ra}$ ,  $^{232}\text{Th}$  and  $^{40}\text{K}$  in POC and POFA

Samples	Activity Concentration ( $\text{Bq Kg}^{-1}$ )		
	$^{226}\text{Ra}$	$^{232}\text{Th}$	$^{40}\text{K}$
POC 1	6.89±0.28	4.46±0.09	570.73±1.86
POC 2	6.90±0.29	4.53±0.09	570.56±1.88
POC 3	5.85±0.28	4.40±0.09	572.73±1.98
POC 4	7.01±0.12	4.87±0.14	598.56±2.10
POC 5	5.56±0.23	4.21±0.03	604.23±2.18
POC 6	6.23±0.27	4.76±0.11	586.62±1.67
$\bar{X} \pm S_x$	<b>6.40±0.62</b>	<b>4.53±0.04</b>	<b>583.90± 14.91</b>
POFA 1	8.16±0.34	6.14±0.12	440.79±2.01
POFA 2	7.74±0.35	6.41±0.13	449.79±2.12
POFA 3	7.95±0.38	7.13±0.13	456.90±2,01
POFA 4	8.75±0.42	7.98±0.19	421.43±1.98
POFA 5	9.03±0.21	7.56±0.21	498.21±2.31
POFA 6	6.98±0.29	6.91±0.10	413.01±1.78
$\bar{X} \pm S_x$	<b>8.10±0.73</b>	<b>7.02±0.69</b>	<b>446.66±30.19</b>
World Average value	50	50	500

**Note:**  $\bar{X}$  denotes for average value and  $S_x$  stand for standard deviation.

For safe utilization of as a building material, the radium equivalent activity ( $\text{Ra}_{\text{eq}}$ ) must be kept lower than the value of  $370 \text{ Bq kg}^{-1}$  (Ghose et al., 2012; Monika Gupta & Chauhan, 2012).

#### 4.6.2 Potential Radiological Hazard

The relative contribution of  $^{226}\text{Ra}$ ,  $^{232}\text{Th}$  and  $^{40}\text{K}$  to  $\text{Ra}_{\text{eq}}$  in POC and POFA samples is presented in **Figure 4.39**. It was observed that the contribution of  $^{226}\text{Ra}$ ,  $^{232}\text{Th}$  and  $^{40}\text{K}$  is 1.08%, 0.76 % and 98.16%, respectively in POC. The relative contribution was

1.75% from  $^{226}\text{Ra}$ , 1.52% from  $^{232}\text{Th}$  and 96.72% from  $^{40}\text{K}$  in POFA. Also,  $^{40}\text{K}$  was the major contributor to the  $R_{\text{eq}}$  in both of the palm oil mill wastes.

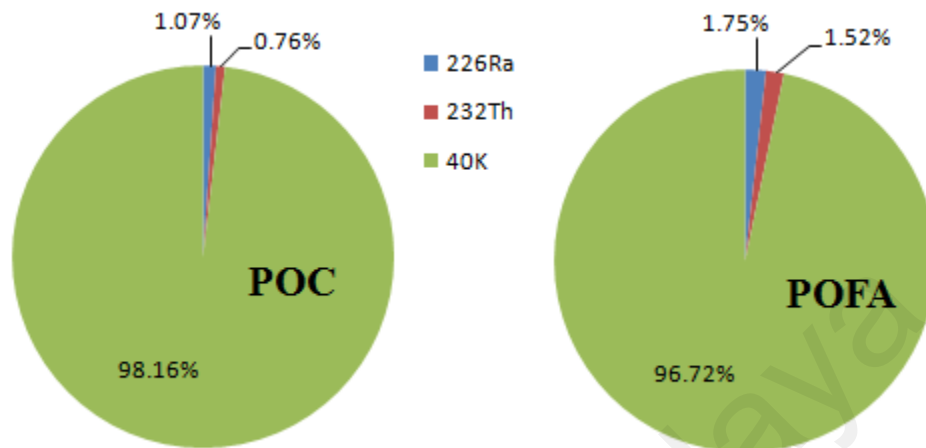


**Figure 4.39:** Relative contributions of  $^{226}\text{Ra}$ ,  $^{232}\text{Th}$  &  $^{40}\text{K}$  to  $R_{\text{eq}}$  in POC & POFA

The outdoor absorbed dose rate of POC and POFA varied from 30.7 to 28.84  $\text{nGy h}^{-1}$  (average: 29.64  $\text{nGy h}^{-1}$ ) and 29.16 to 24.33  $\text{nGy h}^{-1}$  (average: 26.69  $\text{nGy h}^{-1}$ ), respectively. Since, earth originated materials are mostly used for the construction of buildings; gamma exposure in indoor environments is generally greater than outdoor gamma exposure.

Since, one of the target of this work is to assess the radiological feasibility for the incorporation of palm oil mill waste in concrete, their radiological effects on indoor air environment is important. The average indoor absorbed dose rate of  $41.49 \pm 0.91$  and  $36.81 \pm 2.25$   $\text{nGy h}^{-1}$  was obtained for POC and POFA, respectively. The resulting values obtained were within the world range of 20 to 200 ( $\text{nGy h}^{-1}$ ), and lower compared to the population-weighted average value of 84 ( $\text{nGy h}^{-1}$ ) (United Nations. Scientific Committee on the Effects of Atomic Radiation, 2008; Solak et al., 2012). While, the annual effective dose for POC and POFA samples ranged from 0.21 to 0.19  $\text{mSv y}^{-1}$  (average: 0.20  $\text{mSv y}^{-1}$ ) and 0.23 to 0.18  $\text{mSv y}^{-1}$  (average: 0.18  $\text{mSv y}^{-1}$ ), respectively.

These values are very much lower than the ICRP (1990) suggested upper limit of  $1(\text{mSv y}^{-1})$  (Gupta & Chauhan, 2011; Monika Gupta & Chauhan, 2012; Kobeissi et al., 2013; Protection, 1991; Rahman et al., 2013).

For construction material, exemption dose limit of  $0.3 \text{ mSvy}^{-1}$  satisfy the  $\gamma$ -index of  $I_{\gamma} \leq 0.5$ , while the maximum dose limit of  $1 \text{ mSvy}^{-1}$  corresponds to  $\gamma$ -index of  $I_{\gamma} \leq 1$ . Therefore, material with  $I_{\gamma} \geq 1$  should not be used in the construction of the building to avoid unnecessary radiation hazard originate from building. For all POC and POFA samples, gamma index ( $I_{\gamma}$ ) was found as  $I_{\gamma} < 0.5$  which indicates that the contributions of  $\gamma$ -dose from the palm oil mill wastes (POC and POFA used as ingredient of building material) were below the exemption dose limit of  $0.3 \text{ mSvy}^{-1}$  and thus can be used as a component of building material. The values alpha index of POC and POFA were found to be significantly lower than the suggested limit of 1 for internal exposure (Asaduzzaman et al., 2015; Gupta & Chauhan, 2011; Monika Gupta & Chauhan, 2012; Khandaker et al., 2012; Solak et al., 2012).

The external ( $H_{\text{ex}}$ ) and internal ( $H_{\text{in}}$ ) hazard indexes are frequently used for the characterization of construction materials. For all POC and POFA samples (**Table 4.11**) analyzed in this work, the  $H_{\text{ex}}$  and  $H_{\text{in}}$  hazard indexes were noticed to be lower than the suggested limit of 1 (Arabi et al., 2008; Ghose et al., 2012; Khandaker et al., 2012; Kobeissi et al., 2013). Thus, in the radiological point of view, these palm oil waste materials are safer to use as an ingredient of construction of dwellings.

**Table 4.11:** Indicators of radiological hazard of POC and POFA

Samples	Radium equivalent activity (Bq kg <sup>-1</sup> )	Absorbed dose rate (nGy h <sup>-1</sup> )		Annual effective dose (mSv y <sup>-1</sup> )	Alpha index	Gamma index	Hazard index	
		D <sub>out</sub>	D <sub>in</sub>				E <sub>in</sub>	I <sub>γ</sub>
POC 1	57.16	29.28	40.98	0.20	0.24	0.03	0.15	0.17
POC 2	57.26	29.32	41.04	0.20	0.24	0.03	0.15	0.17
POC 3	56.26	28.84	40.37	0.19	0.23	0.03	0.15	0.17
POC 4	60.10	30.72	43.00	0.21	0.24	0.04	0.16	0.18
POC 5	58.05	29.88	41.83	0.21	0.24	0.02	0.16	0.17
POC 6	57.80	29.80	41.72	0.20	0.24	0.03	0.16	0.17
$\bar{X} \pm S_X$	<b>57.81±1.29</b>	<b>29.64±0.65</b>	<b>41.49±0.91</b>	<b>0.20±0.004</b>	<b>0.24±0.005</b>	<b>0.03±0.003</b>	<b>0.16±0.003</b>	<b>0.17±0.004</b>
POFA 1	50.84	25.55	35.77	0.18	0.20	0.04	0.14	0.16
POFA 2	51.49	25.88	36.24	0.18	0.21	0.04	0.14	0.16
POFA 3	53.28	26.71	37.39	0.18	0.21	0.04	0.14	0.17
POFA 4	52.57	26.14	36.59	0.18	0.21	0.04	0.16	0.18
POFA 5	58.13	29.16	40.82	0.20	0.23	0.05	0.13	0.15
POFA 6	48.62	24.33	34.06	0.23	0.19	0.03	0.14	0.16
$\bar{X} \pm S_X$	<b>52.49±3.20</b>	<b>26.69±1.61</b>	<b>36.81±2.25</b>	<b>0.18±0.01</b>	<b>0.21±0.01</b>	<b>0.04±0.004</b>	<b>0.14±0.01</b>	<b>0.16±0.1</b>

**Note:**  $\bar{X}$  denotes for average value and  $S_X$  stand for standard deviation.



### 4.6.3 Comparison of Radiological Hazard

The activity concentrations of  $^{226}\text{Ra}$ ,  $^{232}\text{Th}$  and  $^{40}\text{K}$  of palm oil mill wastes are in contrast with the literature values of coal fly ash and bottom ash determined in Malaysia and other countries (**Table 4.12**). The average radioactivity activity levels of  $^{226}\text{Ra}$  and  $^{232}\text{Th}$  in palm oil mill wastes were significantly lower compared to the coal fly ash, whereas the level of  $^{40}\text{K}$  for POC and POFA samples was compared with the available data in the literature for fly ash. There is large variation of radioactivity concentrations from country to country, one power plant to another in the same country, which could be due to the differences in minerals, geographical and geological condition of the area from where the material originate (Ademola & Onyema, 2014; Amin et al., 2013; Asaduzzaman et al., 2015; Mamta Gupta et al., 2013; Kovler et al., 2012; Lu et al., 2012; Peppas et al., 2010). This information is significant for incorporation of newly introduce waste materials as a supplementary material in concrete. It is clear from the **Table 4.12** that palm oil mill wastes are more suitable than coal fly ash from the view of radiological hazards to use as ingredient for building materials.

**Table 4.12:** Radioactivity of  $^{226}\text{Ra}$ ,  $^{232}\text{Th}$ ,  $^{40}\text{K}$  in POC, POFA and Fly Ash.

Samples, origin	Mean activity concentration (Bq kg <sup>-1</sup> )			Radium equivalent activity (Bq kg <sup>-1</sup> )	Refs.
	$^{226}\text{Ra}$	$^{232}\text{Th}$	$^{40}\text{K}$		
POFA, Selengor, Malaysia	8.10	7.02	446.66	52.49	Present
POC, Selengor, Malaysia	6.40	4.5	583.90	57.74	Present
Bottom Ash, west of Kapar, Malaysia	138.7	108	291.2	315.39	(Amin et al., 2013)
Fly ash, Megalopolis, Greece	1004	56	470	1120.15	(Peppas et al., 2010)
Fly ash, Studstrup, Denmark	161	156	583.9	428.77	(Peppas et al., 2010)
Fly ash, Dadri (U.P.) India	118.6	147.3	352	356.11	(Mamta Gupta et al., 2013)
Fly ash, Dhaka, Bangladesh	117.8	157.3	1463.3	455.08	(Khandoker Asaduzzaman et al., 2015)
Fly ash, Orji River Thermal Power plant, Nigeria	40.8	49.1	321	135.64	(Ademola & Onyema, 2014)
Fly ash, Eastern black sea region, Turkey	38	50	204	125.12	(Ademola & Onyema, 2014)
Fly ash, Xi'an coal-fired power plants, China	67.6	74.3	225.3	191.07	(Lu et al., 2012)

**Note:** Standard safe limit is lower than 370 Bq kg<sup>-1</sup>.

#### 4.7 Heavy Metal Levels and Potential Leaching Risk

The heavy metals create many health problems as well as contaminate the environment. This section presents the characterization of heavy metals and potential risk of the incorporation of POC in cement-based applications.

## **4.7.1 Characterization of Heavy Metal**

### **4.7.1.1 FESEM-EDX studies**

The FESEM-EDX report of POC sample is presented in **Figure 4.40**. The POC sample was coated with carbon trapping. The magnification of micrograph of POC sample is the order of 100  $\mu$ m. The goal of the FESEM - EDX analysis was to find out the heavy metal content in a particular point of the micrograph. Results show that the As, Ba, Cu, Zn, V, Se, Cr, Ni, Pb, Ag and Cd metals were present in POC.

University of Malaysia

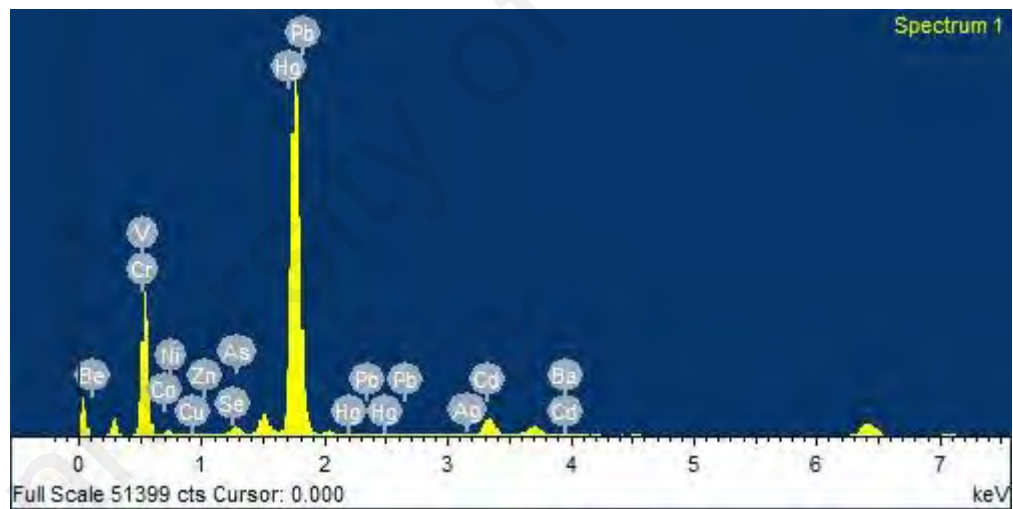
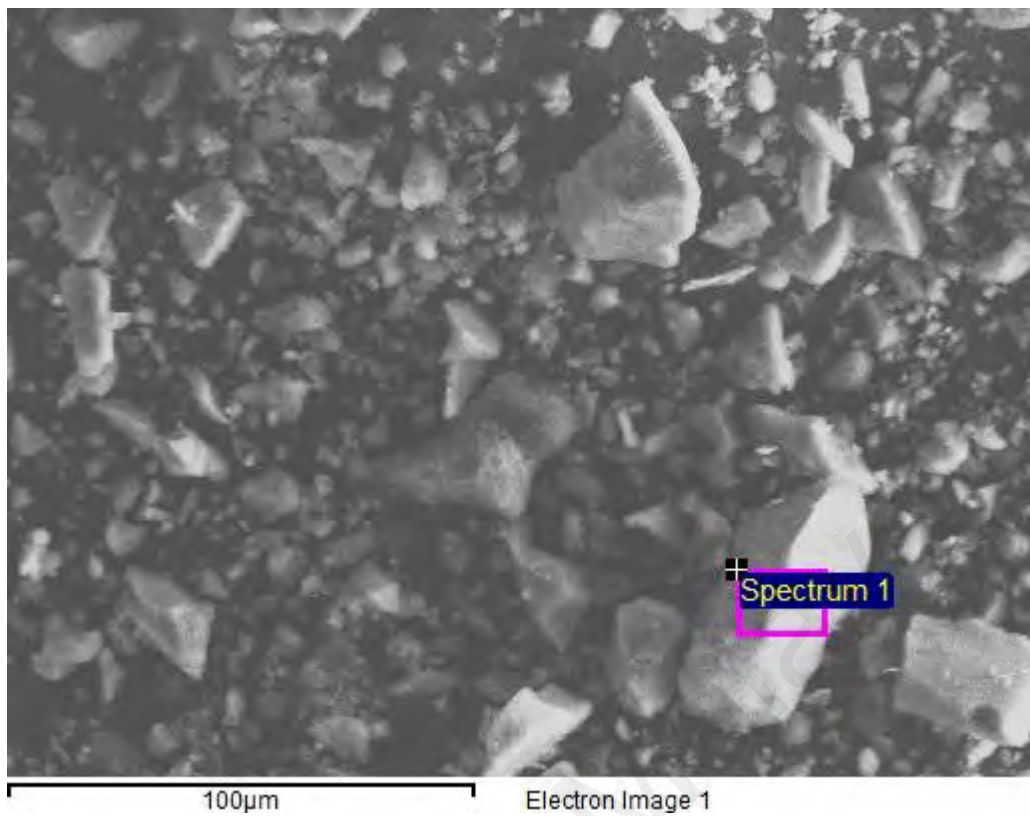


**Figure 4.40:** FESEM-EDX of POC

#### 4.7.1.2 Mineral analysis

The XRD pattern of POC is shown in **Figure 4.41**. The result reveals that quartz ( $\text{SiO}_2$ ) has the major peak with its high content. This indicates that the main mineral in the POC is quartz. The second major peak as observed in the XRD pattern is the cristobalite which is another form of  $\text{SiO}_2$  mineral. The crystallographic structure of the

quartz and cristobalite are hexagonal and tetragonal, respectively. The intensity of quartz and cristobalite are 41442.21 and 9890.63 counts, respectively at the two theta angle of 26.64° and 21.96°, respectively. The wider background in the XRD pattern at 2 theta ranges of 10° to 35° indicates that the crystalline phase is present with amorphous phase in POCP. An amorphosity hump was observed which could be due to the glassy phase present in POC.

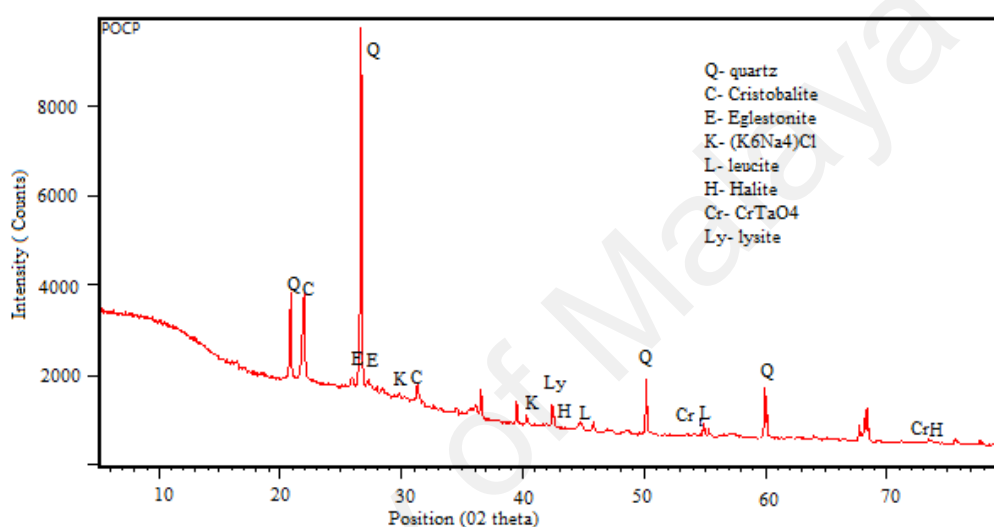


**Figure 4.41:** Mineral analysis of POC

The mineral eglesonite ( $\text{Hg}_{96}\text{C}_{148}\text{O}_{32}\text{H}_{16}$ ) is associated with Hg, O<sub>2</sub>, H and Cl, and the crystal lattice is cubic. It contains some minor minerals such as ( $\text{K}_6\text{Na}_4$ ) Cl, Lucite, Halite ( $\text{Na}_4\text{Cl}_{14}$ ),  $\text{CrTaO}_4$  and lysite in POC. Elatossite ( $\text{CuFeO}_2$ ) which is a mineral of Cu is also present in the studying material. Traces of Stbilitate-Ca, a calcium containing minerals, is also present in the materail. The alloy of the Co, Ni and S is identified in POC. The analysis of the XRD data shows that a number of inorganic minerals are present in POC. These minerals might have been procured from the soil or water by the root of the palm oil tree. The amount of minerals are very minor in the palm oil shell or fibres. The content of minerals is enriched or reformed in POC through the combustion in the boiler of palm oil mill. In literature, it was found that POC contain 39.9 %

amorphous phases (Kanadasan & Abdul Razak, 2015). The sustaining power of heavy metals in POC matrix depends on the bonding force in minerals and stability at different environmental conditions. The composition of mineral in POC depends on the feeding ratio in the boiler of palm oil mill, geological condition of the area where palm oil was grown and burning condition (Kanadasan et al., 2015). The mineralogical composition of fly ash also depends on the type of waste burned and also the burning conditions. Generally, the minerals, i.e. quartz, mulite, magnesioferrite, anorthite, anhydrite, hematite are present in fly ash (Haiying et al., 2010). There is a significant variation in the mineralogical composition of POC and fly ash, although both are produced through the burning process.

#### 4.7.1.3 ICP-MS studies

The heavy metal concentration in the POC is shown in the **Table 4.13**. The sequence of the total concentration of heavy metal in the POC is in the order of As> Ba> Cu> Zn> V> Se> Be> Cr> Ni> Pb> Ag> Cd. The result shows that POC is mainly composed of As, Ba and Cu metals. The concentration of As metal is much higher than other elements. The amount of four fractions of sequential extraction method is of the total concentration of heavy metals and its recovery as given in the **Table 4.13**. The analysis results of the metal concentration in direct digestion and sequential extraction methods in POC are similar. The recovery of heavy metals in sequential extraction method lies in the range of 90.82 % to 113.73%. The variation in concentration that was obtained by direct digestion and a sequential extraction process is in the order of 5% only. The results obtained from both methods are found to be close. This ensures that the results are legitimate and up to the EPA-TCLP standards.

**Table 4.13:** Total concentration of targeted metals of POC

<b>Elements</b>	<b>Direct Digestion Method (mg/kg)</b>	<b>Sequential Extraction (mg/kg)</b>	<b>Recovery (%)</b>
Be	5.13	4.66	90.82
V	11.02	10.60	96.18
Cr	2.65	2.72	102.72
Ni	1.93	2.16	111.74
Cu	45.43	46.34	101.10
Zn	11.84	11.23	94.86
As	1507	1318.87	87.52
Se	6.5	5.83	89.62
Ag	0	0	0
Cd	0	0	0
Ba	81.97	77.2	105.60
Pb	1.76	1.96	111.16

**Table 4.14:** Comparison of heavy metals among different ashes

Element (mg/kg)	POCP (current study)	BFB-boiler FA	Coal Fly ash	MSWI FA	Heavy fuel FA	Coal FA	Waste filter bags FA
Be	5.13	<1.0	-	-	-	-	-
V	11.02	-	-	-	31000	-	-
Cr	2.65	332±1.7	54-103	232.0–716.2	146.0	464.0-74.0	26.35-164.10
Ni	1.93	-	26-63	140.7–378.6	7100	-	48.35-9477.60
Cu	45.43	21.1±0.0	40-83	728.0–2162.0	92.5	101.0-55.0	20.40-83.17
Zn	11.84	4010±13.9	29-124	2088.0–14129.0	247.0	150.0-98.0	5621.80-88974.65
As	1507	7.6<1.00.3	-	-	-	90.0-27.0	-
Se	6.5	<3.0	-	-	-	ND	-
Ag	0	-	-	-	-	2.1-ND	-
Cd	0	0.50±0.1	-	83.67–525.0	-	26-24	17.70-77.20
Ba	81.97	350.7±4.5	-	-	-	195.0-148.0	-
Pb	1.76	4.9±0.02	10-56	782.6–9901.0	78.0	ND	1517.95-44054.55

**Note:** BFB-boiler FA (Pöykiö et al., 2016), Coal Fly ash (Sushil & Batra, 2006), MSWI FA (Pan et al., 2013), Heavy fuel FA (Al-Degs et al., 2014), Coal FA, (Yilmaz et al., 2015) and waste filter bags FA (Zhou et al., 2013).

The heavy metals in POC and some common ashes which are commonly being used in cement-based application are tabulated in **Table 4.14**. A lot of variation is observed in heavy metals of different ashes even though all were produced through the burning process. 5.15 mg/kg Beryllium (Be) is contained in POC which is higher than BFB-boiler ash (Pöykiö et al., 2016). However, the heavy vanadium fuel fly ash is composed 31000 mg/kg vanadium metals that were very far from other ashes. Chromium is a very toxic metal. The Cr, Ni, Zn, Ba and Pb content in POC is significantly lower than other ashes. The Cd and Ag are absent in POC. Arsenic was higher in POC compared with



the rest of the ashes. The soil in this area may contain excess amount of arsenic minerals. Most of the toxic metals are comparatively lower in POC.

## **4.7.2 Potential Leaching Risk**

### **4.7.2.1 Leaching behaviour studies**

The USEPA Method 1311 is widely used as an authentic leaching test procedure. While the TCLP mostly used for characterization of hazards, it sometimes is used to measure the impact of waste in ground water as well as a worst case condition of municipal waste for land filling. The sequence of the leaching concentration of heavy metals from POC is in the order of As> Ni> Cu> Zn> V> Be> Cr> Se which are not similar by content to the metals order like As> Cu> Zn> V> Se> Be> Cr> Ni> Pb> Ag> Cd. The leaching behaviour of waste depends on the chemical stability of metals in waste matrix. Generally, the leaching concentration of heavy metals is largely related to its' content in waste, but the relation is not linear. The leaching value of the As, Be were 0.89 and 4.56 mg/L, respectively, which is very close the limiting value of 5 and 1 mg/L, respectively stipulated in the standard. POC is produced as the burning of palm waste at a temperature range of 500-800°C. The oxide of Arsenic is vaporized easily at this temperature. This study and previous literature confirms the higher presences of K<sub>2</sub>O in POC. Potassium reacts with arsenic and form mineral in gaseous condition at the burning system of palm oil mill and produce an amorphous mineral at the time of cooling. This may be caused because of the highest concentration of Arsenic in POC. The concentration of Ni, Cu and Zn is much lower compared with standard values. These metals can easily be volatilized from palm oil waste at the incineration time. The incomplete burning may responsible for their presences in POC. The leaching value of the Cr, Ag, Cd and Pb are 0.04, 0.00, 0.00 and 0.01 mg/L, respectively. These metals may be vaporized in this temperature or redistributed in a stable mineral form

which cannot leach in leaching conditions. The previous studies found that the leaching concentration of As, Cu, Zn, Cr, Ni, Pb, Ag and Cd were in the range of 0.15-0.63, 0.12-82, 4.3-2217, <0.1-4.3, 0.80-38 and 0.15-2960 mg/L, respectively in different fly ashes (Al-Degs et al., 2014; C.-S. Chen et al., 2016; Jegadeesan et al., 2008; Shi & Kan, 2009; Xie & Zhu, 2013). This variation is due to the origin of waste, type of wastes, incineration condition, etc. The leaching concentrations of heavy metals from POCP are obtained within standard limit and values are comparatively lower than municipality waste incineration ash. This research shows the limitation of the TCLP method for general leachability assessment (Halim et al., 2003; Xie & Zhu, 2013). Therefore, the TCLP results need to be further justified to confirm the environmental safety.

#### **4.7.2.2 Speciation studies**

Four step sequential extraction method was used in this study to measure the speciation of heavy metals of the POC. The name of the extracting portion is the acid soluble (R1), reducible (R2), oxidizable (R3) and residual (R4). Recall that POC is often dumped in open land or used for covering potholes on the road near the palm oil mills. Thus, there is a possibility to contaminate surface water through the leaching of metals from POC. The leaching of heavy metal of waste material depends on its' bonding energy in the matrix as well as leaching condition (Haiying et al., 2010; Singh & Lee, 2015; Wu et al., 2015). The speciation analysis of POC provides the idea about the capability of POC fraction to leach in different environmental conditions. The weak bonded metal of POC can be released and converted to free positive ions that can be used biologically. The heavy metal in acid soluble fraction is potentially influenced on its' mobility (Singh & Lee, 2015). Therefore, the significant mobility of the positive metal ion imposes a greater risk of contamination of the ground water as well as surface water or soil composition. The speciation of heavy metals is shown in **Figure 4.42**.

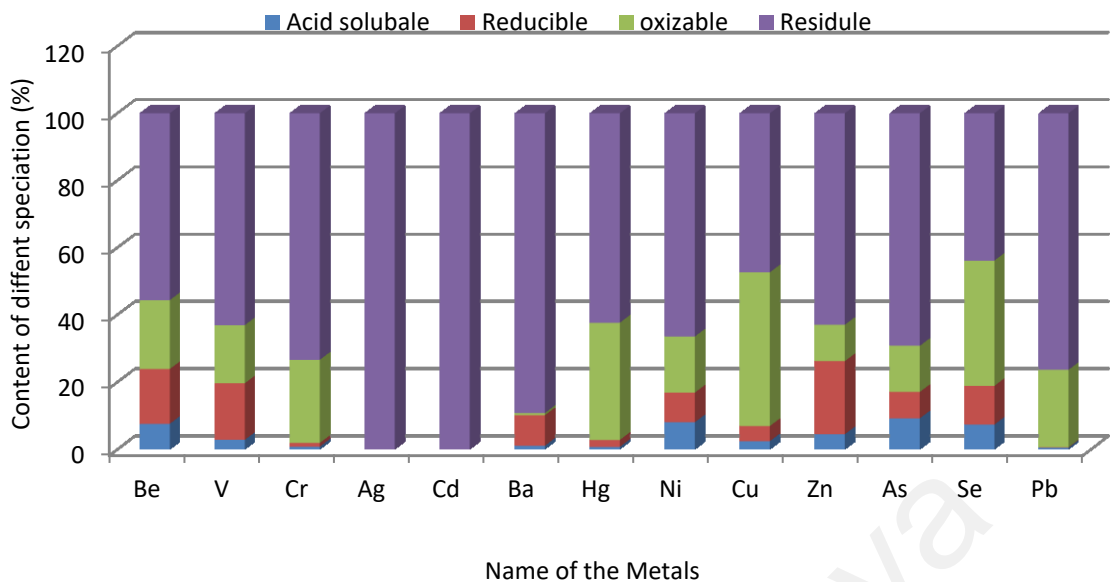


**Figure 4.42:** Speciation of targeted metals of POC

As shown in **Figure 4.42** the acid-soluble fraction of the metals follows the order of As (9.27%)> Ni (8.09%)> Be(7.63%)> Zn(4.53%)> Se(3.78%)> V(2.86%)> Cu(2.47) > Ba(1.09%)> Cr(0.84%)> Pb(0.51%). The acid soluble fraction of POC is in the range from 0.0% to 9.27%. The As, Ni and Be containing minerals or alloy are unstable in the presence of acid. The small amount of V, Se, Cu and Acr also liberate from the POC matrix in acidic solution. The other metals did not interact with an acidic solution. The consideration of As, Ni and Be leaching toxicity is predominant for utilization of POC in concrete construction where acid rain is infrequent. This part of the metal is easily movable and bioavailable that can leach easily and contaminate surface water.

The reducible fraction of metals follows the ; Zn (21.73%) > V (16.80%) > Be (16.26%) > Se (11.50%) > Ba (9.06%) > Ni (8.81%) > As (7.81%) > Cu (4.49%) > Cr (1.10%) > Pb (0.15%). In addition, the oxidizable part of heavy metals in POC as sequences of Cu (45.69%) > Se (37.25%) > Cr (24.68%) > Pb(23.0%) > Be (20.47%)> V(17.27%) > Ni(16.67%) >As(13.71%)> Zn(10.80%)> Ba(0.65%). The acid soluble parts are less stable than the reducible and oxidizable parts of metals in the POC matrix.

Ag(0%) and Cd(0%) are totally absent in the acid soluble, reducible and oxidizable fraction. The heavy metals may be free from POC when external environmental condition change which make it bioavailable.

The residual parts in POC are mainly quartz minerals, which are stable in normal environmental condition. The residual parts in POC of Be, V, Cr, Ag, Cd, Ba, Ni, Cu, Zn, As, Se and Pb are 55.62%, 463.06%, 73.36%, 100%, 100%, 89.18%, 66.42%, 47.33%, 62.94%, 69.19%, 43.86% and 76.33%, respectively. The major fraction of most of the targeted metals is released on residual condition.

#### 4.7.2.3 Potential risk studies

The potential risk of heavy metal leaching of POC is shown in the **Figure 4.43**. If the hydration energy exceeds the existing bonding strength of POC matrix in that case POC enters into the solution. Otherwise, POC is deposited as residue at the bottom of the vessel. The reactivity depends on the dissolving capability of metals in the medium. The bioavailability and potential leaching toxicity risk of POC for incorporation in concrete construction or disposed through land filling largely associated with the dissolving capacity of metals in an environmental condition. The Risk Assessment Code (RAC) is a ratio of the acid soluble parts and total fractions (Wang et al., 2015). The risk is categorized into five classes based on the value of RAC. The value of RAC of Cr, Ag, Cd and Pb was 0.84%, 0%, 0% and 0.51 %, respectively. The RAC values of these metals are less than 1 %. Consequently, these metals cannot cause contamination to the environment. If the percentage falls within the range of 1-10%, 11-30%, 31-50% and more than 50% are designated as low risk, medium risk and high risk, respectively to the environment. The metals of Ba(1.09%), Ni(8.09%), Cu(4.62%), Be(7.63%), V (2.85%), Zn(4.53%), As(9.27%) and Se(7.38%) belongs to the class of low risk (Pan et al., 2013; Wang et al., 2015). There are no metals in high or medium hazard range to the

environment of POC. The RAC value of As and Be are higher compared to Ni, Cr, V, Se metals.

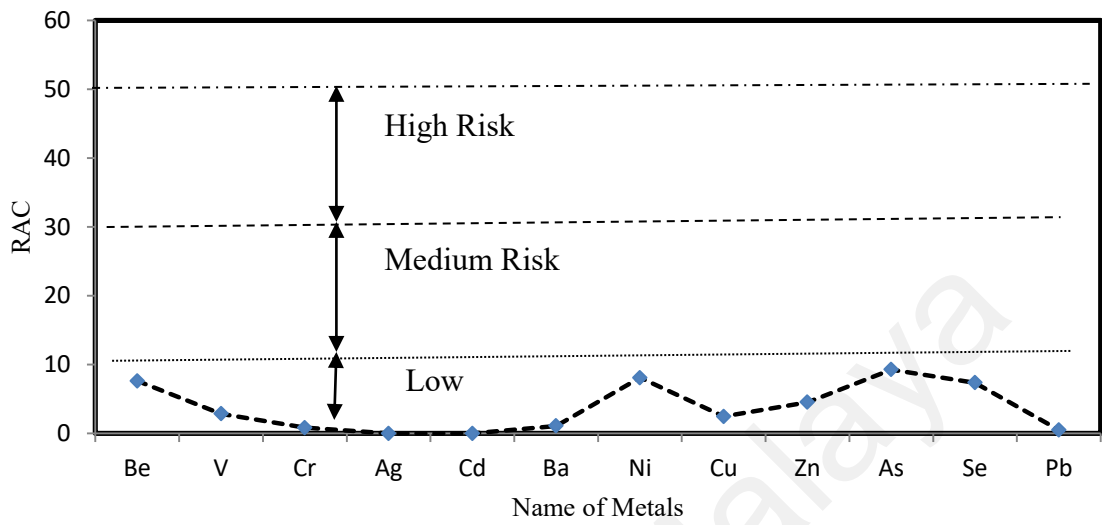


**Figure 4.43:** Potential heavy metal leaching risk of POC

University of Malaysia

## CHAPTER 5: CONCLUSIONS AND RECOMMENDATIONS

### 5.1 Introduction

The present research was conducted to explore the feasibility of palm oil clinker powder (POCP) as a supplementary cementitious material in cement-based applications. Palm oil clinker is a waste material of palm oil mill which is obtained as a result of incomplete combustion of palm oil shell and fibre in the boiler. In current practice, this waste is dumped in open land or is often used for covering potholes on the road which leads to environmental pollution. The feasibility assessment was planned to provide an overview of the technical and environmental issues related to the utilization of this waste material in cement-based applications. The experimental and analytical data were used to explain the feasibility of POCP. Finally, some suggestions for the future research are also included.

### 5.2 Characterization of POCP

The first objective of this study is to characterize the palm oil clinker powder for utilization as a supplementary cementitious material in cement-based applications. An elaborate characterization of POCP sample which was collected from Dengkil, Malaysia has been evaluated. The experimental results were compared with the data available in the literature regarding other supplementary cementitious materials, i.e. POFA, FA and GBFS which had been used in cement-based applications.

The results showed that the POCP is composed of several oxides, viz.,  $\text{SiO}_2$ ,  $\text{Al}_2\text{O}_3$ ,  $\text{Fe}_2\text{O}_3$ ,  $\text{MgO}$  and  $\text{CaO}$  oxides. The percentage of  $\text{SiO}_2 + \text{Al}_2\text{O}_3 + \text{Fe}_2\text{O}_3$  oxides is 71.09% in POCP which chemically satisfy the requirement of Class F fly ash. Microstructure analysis confirms that the particle of POCP is irregular in shape, and it contains small

pores. The result showed that POCP is blackish in colour while fibrous materials are also present. TGA and TOC observation found that organic carbon is present in POCP. POCP was found to contain 2.54% along with 0.063% inorganic carbon. An amorphisity halo was observed in the XRD pattern in the angular  $2\theta$  range of  $10^\circ$  to  $35^\circ$ . Moreover, two bands centered at  $1009$  and  $779\text{ cm}^{-1}$  were assigned to stretching and bending vibrations (Si-O) which are due to the presence of traces of crystalline mineralogical phases such as quartz and cristobalite in POCP. The crystallinity index of quartz in POCP is 0.97, which means that the quartz is partially disordered.

The results were compared with the data which are available in literature of POFA, FA and GBFS. The results of the  $\text{SiO}_2+\text{Al}_2\text{O}_3+\text{Fe}_2\text{O}_3$  oxides weight percentage in POCP, POFA, FA and GBFS are 71.09 %, 70.56 %, 58.15 % and 47.12%, respectively. On the basis of chemical composition, the percentage of the three oxides to indicate pozzolanicity is highest for POCP and POFA when compared to FA and GBFS. Also, it was observed from SEM image that POCP particles are irregular in shape and has a micro porous cellular structure as compared to FA which are uniformly distributed spherical granules with a smooth surface (Li et al., 2012). The quartz and cristobalite are the major minerals present in POCP. Similar results was reported Chandara et al (Chandara et al., 2010) for other palm oil mill waste i.e. POFA. Slag has  $\text{C}_2\text{S}$ ,  $\text{C}_3\text{S}$  and  $\text{C}_4\text{AF}$  phases that are similar to OPC clinker, but the percentage is less than OPC. The mineralogical composition of POCP much resembles that of fly ash and POFA rather than slag. The characterization data of this research disclose possible new ideas to for future researches for diversified applications of palm oil clinker.

### **5.3 Chemical Interaction of POCP in Cement-Based Applications**

The chemical interaction, i.e. organic carbon effect and pozzolanic activity of POCP in cement-based applications is the second objective of this research which was

identified through micro analytical techniques. The results were compared with other waste materials which has a chemical interaction at the time of cement-based applications.

The thermal activation process changes the characteristic properties of POCP, therefore their influences on the compressive strength development have been studied. The percentage of inorganic oxide increased in POCP through thermal activation. The increment rate of  $\text{SiO}_2$ ,  $\text{Al}_2\text{O}_3$  and  $\text{Fe}_2\text{O}_3$  in  $\text{TPOCP}_{580}$  were 3.4%, 3.5% and 3.4%, respectively. The chemical composition of POCP changed through thermal activation and the percentage of increase in oxide content was significantly lower compared to paper sludge, clay and POFA. SEM observation found that fibres materials removed and reduced the porosity. The color of POCP changes from black to gray through the thermal activation. Thermal activation had an insignificant influence on the crystalline structure of the minerals. The main finding of the work was the reduction of TOC from 3.54% to 0.063% by thermal activation at 580°C for 3 hours. The relative compressive strength gain of  $\text{TPOCP}_{580}$  mortar was 38.4 %, 30.7%, 21.9%, 22.7%, 15.6% and 11.9% compared to POCP mortar at the curing ages of 1, 3, 7, 28, 56 and 90 days, respectively. This is mainly due to the reduction of organic carbon, which leads to reduced porosity of the matrix. The compressive strength development through the thermal activated POCP as supplementary material is an important finding for optimum incorporation of this waste in cement-based application without compromise with respect to the compressive strength.

The pozzolanic activity of POCP has also been examined in this research by investigating the microstructure properties as well as strength activity index. The XRD pattern shows that the difference in  $\text{Ca}(\text{OH})_2$  peak intensity between OPC and POCP paste at the curing age of 3 days is lower than the curing age of 28 days and 90 days.



The intensity difference between 3 and 90 days are more pronounced than between 3 and 28 days. This indicates that the consumption of  $\text{Ca}(\text{OH})_2$  by POCP at the curing age of 90 days is effective. This is a clear indication of the pozzolanic activity of POCP. This result is also supported by the TGA, FTIR and FESEM observations. The strength activity index result also shows that the pozzolanic activity of POCP is lower than fly ash, UPOFA and activated clay and higher than GPOFA. This finding is very much positive to encourage the utilization of POCP as cementitious materials.

#### **5.4 Effect of POCP Characteristics on Fresh and Hardened Properties of Cement**

The determination of the effect of POCP on the fresh and hardened properties of cement is a requirement by the ASTM, EN standards for introducing a new waste material as supplementary cementitious material. The fresh properties which includes water for normal consistency, setting time, viscosity and volume expansion, and hardened properties such as, compressive and flexural strength of POCP blended cement were observed up to 60% replacement levels. Additionally, the cost, greenhouse gas emission and resource conservation aspect of incorporation of POCP in blended cement was also investigated through a mini ball mill scale experiment.

The following conclusions were drawn from the findings in the experiments. The water for normal consistency of POCP10, POCP20, POCP30, POCP40, POCP50 and POCP60 were 105.3%, 113.3%, 121.1%, 129.7%, 134.2% and 141.7% of OPC, respectively. The setting time value is placed within ASTM standard limits up to 60% replacement levels. The viscosity of POCP blended cement is lower than OPC cement paste. The expansion of POCP blended cement is placed within the range of 0.19-0.53 mm which is significantly lower than the standard limit of 10 mm. The compressive and flexural strength of POCP blended decreases with replacement level of OPC. The POCP incorporation in OPC can save about 25% of the cost compared to the OPC.

POCP incorporation will lower the CO<sub>2</sub> emission by 25.36% at 30% replacement level of OPC. The limestone, clay, Iron ore, silica shale and gypsum saved are 35.1%, 4.95%, 0.9%, 4.05% and 1.2%, respectively at 30% replacement of the OPC. The cement user can easily select their demanded quality of POCP blended cement and related cost, greenhouse gas emission and resource conservation.

### **5.5 Radiological Hazard and Heavy Metal Leaching Risk**

The radiological hazard and heavy metal leaching risk due to the incorporation of POCP as an ingredient of building materials has been determined in this research for the confirmation of the environmental safety. Radioactivity is a major problem for utilization of fly ash in cement-based applications. In the present study, the radiological hazard indices were compared with fly ash and POFA. Additionally, the heavy metal leaching risk was also compared with other waste materials which has been used as an ingredient of concrete construction.

The radium equivalent activities of POC and POFA were found in the range of 48.62 to 60.10 Bq kg<sup>-1</sup> which is significantly lower than the recommend safe limit of 370 Bq kg<sup>-1</sup>. The absorbed dose rates and corresponding annual effective dose rate in an indoor environment originated from palm oil mill waste were considerably less than the recommended value of ICRP (1990). The radium equivalent of POCP and POFA were found to be significantly lower from coal fly ash. Additionally, the data reported herein can be regarded as base values for the distributions of natural series of radionuclides in POCP and POFA in the studied region and may be used as reference information for environmental radioactivity monitoring with the intent of minimizing population exposure to ensure a safer living environment.

The heavy metal characterization data confirmed that the As, Ba, Cu, Zn, V, Se, Cr, Ni, Pb, Ag and Cd metals are present in POCP. The sequence of the total concentration of heavy metal in POC are in the order of As> Ba> Cu> Zn> V> Se> Be> Cr> Ni> Pb> Ag> Cd. The average heavy metal content in POCP was comparatively lower than fly ash as reported in data available in the literature. The leaching concentration of As and Be were 4.56 and 0.83 mg/L, which are close to the standard limit of 1 and 5 mg/L, respectively. The leaching concentration of heavy metals was obtained within standard limit and the values are comparatively lower than municipality waste incineration ash. Risk code analysis confirmed that all the metals which are present in POC are placed in a low risk area. This observation confirms that POCP is environmentally safe to be used in cement-based applications.

## **5.6 Conclusions**

The experimental observations of this indicates that POCP is a feasible supplementary cementitious materials which can be used in cement-based applications. This waste is more appropriate to be used as supplementary cementitious compared to fly ash from the point of radiological hazard and heavy metal leaching risk. Also, it serves as a better alternative to convert the POCP waste into a resource, i.e. new supplementary cementitious materials rather than throwing in open land or a landfill site which cause of environmental pollution. These findings indicate that the use of POC has benefits which includes lower carbon footprint concrete, cleaner environment, sustainable use of waste material; reduction in greenhouse gas as well as cost compared to Portland cement, and conservation of natural resource.

## 5.7 Recommendations

Comparing several studies from past literatures, it was found that, there are some factors that are needed more attention to be paid in future works. More experimental and theoretical research is encouraged in order to attain the consistent function of POCP in cement-based applications. There are still a number of questions and further enhancement that can be predicted for the incorporation of POCP in cement-based applications. Therefore, the following points are worth further investigation:

1. The characteristic properties, i.e. chemical composition, TOC, thermal behaviour of POCP are not consisted even through the sample was collected from the same factory at different time. Attention should be given to investigate the effect of different factory sample in cement-based application. Furthermore, more attention should be drawn to find there is need to developed a method for making the consistent quality of POCP of different palm oil mills.
2. The thermal activation effect on POCP was run in this experiment up to 650°C. The high temperature effect on POCP properties is not clear in this study. The XRD patterns show that the heat energy does not change the crystalline structure, significantly. But, the change of amorphous content was not investigated so far and their influence on the pozzolanic activity.
3. The thermal activated POCP effect of the rheological and mechanical properties of cement at different replacement level was not measured in this study.
4. The heavy metals level and leaching toxicity were measured for samples which were collected from only a specific area of Malaysia. The heavy metal type and its level depend on the geological condition of the sample collecting area. The heavy metal leaching toxicity of POCP sample which is collected from all over Malaysia can be investigated for environmental safety.

5. Literature found that radioactivity level in Malaysian earth materials varies from area to area. Therefore, knowledge on, the radioactivity level of the whole Malaysian POCP is important in order to ensure the safety of health for incorporation of palm oil mill waste in concrete construction.
6. Additionally, there is significant amount of  $K_2O$  present in POCP and it may be possible to activate this alkali oxides for utilization in the geopolymer.

University of Malaya

## REFERENCES

- Ademola, J. A., & Onyema, U. C. (2014). Assessment of Natural Radionuclides in Fly Ash Produced at Orji River Thermal Power Station, Nigeria and the Associated Radiological Impact. *Natural Science*, 6(10), 752-759.
- Adesanya, D. A., & Raheem, A. A. (2009). Development of corn cob ash blended cement. *Construction and Building Materials*, 23(1), 347-352.
- Ahmad, H., Sofian, M., & Noor, M. N. (2007). Mechanical properties of palm oil clinker concrete, 1st Engineering Conference on Energy and Environment, 27-28 December 2007, Kuching, Sarawak.
- Ahmad, N., Jaafar, M., & Alsaffar, M. (2015). Natural radioactivity in virgin and agricultural soil and its environmental implications in Sungai Petani, Kedah, Malaysia. *Pollution*, 1 (3), 305-313.
- Ahmad, N., Jaafar, M. S., Bakhsh, M., & Rahim, M. (2015). An overview on measurements of natural radioactivity in Malaysia. *Journal of Radiation Research and Applied Sciences*, 8(1), 136-141.
- Ahmmad, R., Jumaat, M. Z., Alengaram, U. J., Bahri, S., Rehman, M. A., & Hashim, B. H. (2015). Performance evaluation of palm oil clinker as coarse aggregate in high strength lightweight concrete. *Journal of Cleaner Production*, 112(1), 566-574.
- Ahmmad, R., Jumaat, M. Z., Alengaram, U. J., Bahri, S., Rehman, M. A., & Hashim, H. (2015). Performance evaluation of palm oil clinker as coarse aggregate in high strength lightweight concrete. *Journal of Cleaner Production*, 30, 1-9.
- Ahmmad, R., Jumaat, M. Z., Bahri, S., & Islam, A. B. M. S. (2014). Ductility performance of lightweight concrete element containing massive palm shell clinker. *Construction and Building Materials*, 63, 234-241.
- Azura, A., Fauziah, C.I., & Samsuri, A. W. (2012). Cadmium and Zinc Concentrations in Soils and Oil Palm Tissues as Affected by Long-Term Application of Phosphate Rock Fertilizers. *Soil and Sediment Contamination: An International Journal*, 21(5), 586-603.
- Al-Degs, Y., Ghrir, S., Khoury, A., Walker, H., Gavin M., Sunjuk, M., & Al-Ghouthi, M., A. (2014). Characterization and utilization of fly ash of heavy fuel oil generated in power stations. *Fuel Processing Technology*, 123, 41-46.
- Alam, S. (2014). Assessment of pozzolanic activity of thermally activated clay and its impact on strength development in cement mortar. *RSC Advance.*, 5(8), 6079-6084.
- Alam, S. (2015). Assessment of pozzolanic activity of thermally activated clay and its impact on strength development in cement mortar. *RSC Advances*, 5(8), 6079-6084.

- Alam, S., & Gul, S. (2015). Correction: Assessment of pozzolanic activity of thermally activated clay and its impact on strength development in cement mortar. *RSC Advances*, 5(14), 10680-10680.
- Alharbi, W. R., AlZahrani, J. H., & Adel, G. E. A. (2011). Assessment of radiation hazard indices from granite rocks of the southeastern Arabian Shield, Kingdom of Saudi Arabia. *Australian Journal of Basic and Applied Science*, 5(6), 672-682.
- Almayahi, B. A., Tajuddin, A. A., & Jaafar, M. S. (2012a). Effect of the natural radioactivity concentrations and  $^{226}\text{Ra}/^{238}\text{U}$  disequilibrium on cancer diseases in Penang, Malaysia. *Radiation Physics and Chemistry*, 81(10), 1547-1558.
- Almayahi, B. A., Tajuddin, A. A., & Jaafar, M. S. (2012b). Radiation hazard indices of soil and water samples in Northern Malaysian Peninsula. *Applied Radiation and Isotopes*, 70(11), 2652-2660.
- Adrián, A., Almenares, R. S., Betancourt, S., & Leyva, C. (2015). Pozzolanic Reactivity of Low Grade Kaolinitic Clays: Influence of Mineralogical Composition. *Calcined Clays for Sustainable Concrete*, 10, 339-345.
- Adrian, A., Fernandez, R., Quintana, R., Scrivener, K. L., & Martirena, F. (2015). Pozzolanic reactivity of low grade kaolinitic clays: Influence of calcination temperature and impact of calcination products on OPC hydration. *Applied Clay Science*, 108, 94-101.
- Amin, N., Alam, S., & Gul, S. (2016). Effect of thermally activated clay on corrosion and chloride resistivity of cement mortar. *Journal of Cleaner Production*, 111, 155-160.
- Amin, Y. M., Khandaker, M. U., Shyen, A. K. S., Mahat, R. H., Nor, R. M., & Bradley, D. A. (2013). Radionuclide emissions from a coal-fired power plant. *Applied Radiation and Isotopes*, 80, 109-116.
- Apriantoro, N. H., Ramli, A. T., & Sutisna, S. (2013). Activity concentration of  $^{238}\text{U}$ ,  $^{232}\text{Th}$  and  $^{40}\text{K}$  based on soil types in Perak state, Malaysia. *Earth Science Research*, 2(2), 1-22.
- Arora, A., Sant, G., & Neithalath, N. (2016). Ternary blends containing slag and interground/blended limestone: Hydration, strength, and pore structure. *Construction and Building Materials*, 102, 113-124.
- Aruntaş, H. Y., Gürü, M., Dayı, M., & Tekin, I. (2010). Utilization of waste marble dust as an additive in cement production. *Materials & Design*, 31(8), 4039-4042.
- Asaduzzaman, K., Khandaker, M. U., Amin, Y.M, & Bradley, D.A. (2016). Natural radioactivity levels and radiological assessment of decorative building materials in Bangladesh. *Indoor and Built Environment*, 25(3), 1-10.
- Asaduzzaman, K., Khandaker, M. U., Amin, Y. M., & Mahat, R. (2015). Uptake and distribution of natural radioactivity in rice from soil in north and west part of peninsular malaysia for the estimation of ingestion dose to man. *Annals of Nuclear Energy*, 76, 85-93.

- Asaduzzaman, K., Mannan, F., Khandaker, M. U., Farook, M. S., Elkezza, A., Amin, Y. B. M., ...Kassim, H. B. A. (2015). Assessment of Natural Radioactivity Levels and Potential Radiological Risks of Common Building Materials Used in Bangladeshi Dwellings. *Plos One*, *10*(10), 1-16.
- Asavapisit, S., & Ruengrit, N. (2005). The role of RHA-blended cement in stabilizing metal-containing wastes. *Cement and Concrete Composites*, *27*(7), 782-787.
- Ashraf, M., Khan, A. N., Ali, Q., Mirza, J., Goyal, A., & Anwar, A. M. (2009). Physico-chemical, morphological and thermal analysis for the combined pozzolanic activities of minerals additives. *Construction and Building Materials*, *23*(6), 2207-2213.
- Association, Mineral Products (APM). (2012). Fact Sheet 18 [Part 1] Embodied CO<sub>2</sub> of UK Cement, Additions and Cementitious Material: Mineral Products Association Gillingham, UK.
- Association, Portland Cement (APC). (1998). Control of air content in concrete. *Concrete Technology Today*, *19*(1), 1-8.
- ASTM C618-08a. (2008). Standard Specification for Coal Fly Ash and Raw or Calcined Natural Pozzolan for Use in Concrete. *Annual Book of ASTM Standards*: West Conshohocken, USA.
- ASTM C 231M-14. (2014). Standard Test Method for Air Content of Freshly Mixed Concrete by the Pressure Method: ASTM C231/C231M-14. ASTM International: West Conshohocken, USA.
- ASTM C618-08a (2013). Standard Specification for Coal Fly Ash and Raw or Calcined Natural Pozzolan for use in Concrete. ASTM International.
- Aswood, M. S., Jaafar, M. S., & Bauk, S. (2013). Assessment of radionuclide transfer from soil to vegetables in farms from Cameron highlands and Penang, (Malaysia) using neutron activation analysis. *Applied Physics Research*, *5*(5), 73-85.
- Atiş, C. D. (2005). Strength properties of high-volume fly ash roller compacted and workable concrete, and influence of curing condition. *Cement and Concrete Research*, *35*(6), 1112-1121.
- Autier, C., Azema, N., Taulemesse, J. M., & Clerc, L. (2013). Mesostructure evolution of cement pastes with addition of superplasticizers highlighted by dispersion indices. *Powder Technology*, *249*, 282-289.
- Awal, A. S. M. A., & Hussin, M. W. (1997). The effectiveness of palm oil fuel ash in preventing expansion due to alkali-silica reaction. *Cement and Concrete Composites*, *19*(4), 367-372.
- Aziz, R. A., Rahim, S. A., Sahid, I., & Idris, W. M. R. (2015). Speciation and Availability of Heavy Metals On Serpentinized Paddy Soil and Paddy Tissue. *Procedia-Social and Behavioral Sciences*, *195*, 1658-1665.



- Azrina, A., Khoo, H. E., Idris, M. A., Amin, I., & Razman, M. R. (2011). Major inorganic elements in tap water samples in Peninsular Malaysia. *Malaysian Journal of Nutrition*, 17(2), 271-276.
- Bahurudeen, A., & Santhanam, M. (2015). Influence of different processing methods on the pozzolanic performance of sugarcane bagasse ash. *Cement and Concrete Composites*, 56, 32-45.
- Bai, C., Deng, X. Li, J., Jing, Y., & Jiang, W. (2014). Preparation and properties of mullite-bonded porous SiC ceramics using porous alumina as oxide. *Materials Characterization*, 90, 81-87.
- Bartoňová, L. (2015). Unburned carbon from coal combustion ash: An overview. *Fuel Processing Technology*, 134, 136-158.
- Beretka, J., & Mathew, P. J. (1985). Natural radioactivity of Australian building materials, industrial wastes and by-products. *Health Physics*, 48(1), 87-95.
- Burgos-Montes, O., Alonso, M. M., & Puertas, F. (2013). Viscosity and water demand of limestone-and fly ash-blended cement pastes in the presence of superplasticisers. *Construction and Building Materials*, 48, 417-423.
- Chancey, R. T., Stutzman, P. J., Maria C.G., & Fowler, D. W. (2010). Comprehensive phase characterization of crystalline and amorphous phases of a Class F fly ash. *Cement and Concrete Research*, 40(1), 146-156.
- Chandara, C., Azizli, K. A. M., Ahmad, Z. A., Hashim, S. F. S., & Sakai, E. (2012). Heat of hydration of blended cement containing treated ground palm oil fuel ash. *Construction and Building Materials*, 27(1), 78-81.
- Chandara, C., Azizli, K. A. M., Ahmad, Z. A., Hashim, S. F. S., & Sakai, E. (2011). Analysis of mineralogical component of palm oil fuel ash with or without unburned carbon. *Advanced Materials Research*, 173, 7-11.
- Chandara, C., Sakai, E., Azizli, K. A. M., Ahmad, Z. A., & Hashim, S. F. S. (2010). The effect of unburned carbon in palm oil fuel ash on fluidity of cement pastes containing superplasticizer. *Construction and Building Materials*, 24(9), 1590-1593.
- Chen, C. S., Shih, Y. J., & Huang, Y. (2016). Recovery of lead from smelting fly ash of waste lead-acid battery by leaching and electrowinning. *Waste Management*, 52, 212-220.
- Chen, K. W., Pan, S. Y., Chen, C. T., Chen, Y. H., & Chiang, P. C. (2016). High-gravity carbonation of basic oxygen furnace slag for CO<sub>2</sub> fixation and utilization in blended cement. *Journal of Cleaner Production*, 150, 350-360.
- Chuan, L. F. (2015). Innovative Cement Additives Quality Improvers in Sustainable Cement and Concrete. *Sains Malaysiana*, 44(11), 1599-1607.
- Conesa, J. A., Gálvez, A., & Fullana, A. (2008). Decomposition of paper wastes in presence of ceramics and cement raw material. *Chemosphere*, 72(2), 306-311.

- Cordeiro, G. C., & Sales, C. P. (2015). Pozzolanic activity of elephant grass ash and its influence on the mechanical properties of concrete. *Cement and Concrete Composites*, 55, 331-336.
- Coskun, M. (2011). Fundamental pollutants in the European Union (EU) countries and their effects on Turkey. *Procedia-Social and Behavioral Sciences*, 19, 467-473.
- Demis, S., Tapali, J. G., & Papadakis, V. G. (2014). An investigation of the effectiveness of the utilization of biomass ashes as pozzolanic materials. *Construction and Building Materials*, 68, 291-300.
- Du, L., & Folliard, K. J. (2005). Mechanisms of air entrainment in concrete. *Cement and Concrete Research*, 35(8), 1463-1471.
- Đurašević, M., Kandić, A., Stefanović, P., Vukanac, I., Šešlak, B., Milošević, Z., & Marković, T. (2014). Natural radioactivity in lignite samples from open pit mines "Kolubara", Serbia—risk assessment. *Applied Radiation and Isotopes*, 87, 73-76.
- El Arabi, A. M., Ahmed, N. K., & Din, K. S. (2008). Assessment of terrestrial gamma radiation doses for some Egyptian granite samples. *Radiation Protection Dosimetry*, 128(3), 382-385.
- Erdem, T. K., Meral, C., Tokyay, M., & Erdoğan, T. Y. (2007). Use of perlite as a pozzolanic addition in producing blended cements. *Cement and Concrete Composites*, 29(1), 13-21.
- Etetim, D. U. (2013). Well Integrity behind casing during well operation: Alternative sealing materials to cement, Master Thesis, NTNU, Institute for Geovitenskap of Petroleum.
- Fernandez, R., Martirena, F., & Scrivener, K. L. (2011). The origin of the pozzolanic activity of calcined clay minerals: a comparison between kaolinite, illite and montmorillonite. *Cement and Concrete Research*, 41(1), 113-122.
- Ferreiro, S., Frías, M., Villa, R. V., & Rojas, I. S. D. (2013). The influence of thermal activation of art paper sludge on the technical properties of blended Portland cements. *Cement and Concrete Composites*, 37, 136-142.
- Fitos, M., Badogiannis, E. G., Tsvivilis, S. G., & Perraki, M. (2015). Pozzolanic activity of thermally and mechanically treated kaolins of hydrothermal origin. *Applied Clay Science*, 116, 182-192.
- Frías, M., Rojas, M. S. D., García, R., Valdés, A. J., & Medina, C. (2012). Effect of activated coal mining wastes on the properties of blended cement. *Cement and Concrete Composites*, 34(5), 678-683.
- Frías, M., Savastano, H., Villar, E., Rojas, M. I. S. D., & Santos, S. (2012). Characterization and properties of blended cement matrices containing activated bamboo leaf wastes. *Cement and Concrete Composites*, 34(9), 1019-1023.
- Ganesan, K., Rajagopal, K., & Thangavel, K. (2007). Evaluation of bagasse ash as supplementary cementitious material. *Cement and Concrete Composites*, 29(6), 515-524.

- Gao, X., Yu, Q. L., & Brouwers, H. J. H. (2015). Characterization of alkali activated slag-fly ash blends containing nano-silica. *Construction and Building Materials*, 98, 397-406.
- Garcia-Nunez, J. A., Ramirez-Contreras, N. E., Rodriguez, D. T., Silva-Lora, E., Frear, C. S., Stockle, C., & Garcia-Perez, M. (2016). Evolution of palm oil mills into bio-refineries: Literature review on current and potential uses of residual biomass and effluents. *Resources, Conservation and Recycling*, 110, 99-114.
- García, R., Villa, R. V. D., Vegas, I., Frías, M., & Rojas, M. S. D. (2008). The pozzolanic properties of paper sludge waste. *Construction and Building Materials*, 22(7), 1484-1490.
- Gardner, L. J., Bernal, S. A., Walling, S. A., Corkhill, C. L., Provis, J. L., & Hyatt, N. C. (2015). Characterisation of magnesium potassium phosphate cements blended with fly ash and ground granulated blast furnace slag. *Cement and Concrete Research*, 74, 78-87.
- Ghofrani, M., Mokaram, K. N., Ashori, A., & Torkaman, J. (2015). Fiber-cement composite using rice stalk fiber and rice husk ash: Mechanical and physical properties. *Journal of Composite Materials*, 49(26), 3317-3322.
- Ghose, S., Asaduzzaman, K., & Zaman, N. (2012). Radiological significance of marble used for construction of dwellings in Bangladesh. *Radioprotection*, 47(01), 105-118.
- Grzeszczyk, S., & Janowska-Renkas, E. (2012). The influence of small particle on the fluidity of blast furnace slag cement paste containing superplasticizers. *Construction and Building Materials*, 26(1), 411-415.
- Gupta, M., & Chauhan, R. P. (2011). Estimating radiation dose from building materials. *Iranian Journal of Radiation Research*, 9(3), 187-194.
- Gupta, M., Mahur, A. K., Varshney, R., Sonkawade, R. G., Verma, K. D., & Prasad, R. (2013). Measurement of natural radioactivity and radon exhalation rate in fly ash samples from a thermal power plant and estimation of radiation doses. *Radiation Measurements*, 50, 160-165.
- Gupta, M., & Chauhan, R. P. (2012). Estimation of Low-Level Radiation Dose from Some Building Materials Using Gamma Spectroscopy. *Indoor and Built Environment*, 21(3), 465-473.
- Guilherme A. C., Franco, M. K. K. D., Laurence, P. L., Rodrigues, M. S., Beraldo, A. L., Fabiano, Y.,...Cardoso, L. P. (2015). Assessing the pozzolanic activity of cements with added sugar cane straw ash by synchrotron X-ray diffraction and Rietveld analysis. *Construction and Building Materials*, 98, 44-50.
- Ha, T. H., Muralidharan, S., Bae, J. H., Ha, Y. C., Lee, H. G., Park, K. W., & Kim, D. K. (2005). Effect of unburnt carbon on the corrosion performance of fly ash cement mortar. *Construction and Building Materials*, 19(7), 509-515.
- Haiying, Zhang, Y. Z., & Jingyu, Q. (2010). Characterization of heavy metals in fly ash from municipal solid waste incinerators in Shanghai. *Process Safety and Environmental Protection*, 88(2), 114-124.

- Halim, C. E., Amal, R., Beydoun, D., Scott, J. A., & Low, G. (2003). Evaluating the applicability of a modified toxicity characteristic leaching procedure (TCLP) for the classification of cementitious wastes containing lead and cadmium. *Journal of Hazardous Materials*, 103(1), 125-140.
- Hamidi, M., Kacimi, L., Cyr, M., & Clastres, P. (2013). Evaluation and improvement of pozzolanic activity of andesite for its use in eco-efficient cement. *Construction and Building Materials*, 47, 1268-1277.
- Hasanbeigi, A. (2013). Emerging energy-efficiency and CO<sub>2</sub> emission-reduction technologies for cement and concrete production. Retrieved from <https://escholarship.org/uc/item/9td3v9sk>.
- Hesas, R. H., Arami-Niya, A., Daud, W. M. A. W., & Sahu, J. N. (2013). Comparison of oil palm shell-based activated carbons produced by microwave and conventional heating methods using zinc chloride activation. *Journal of Analytical and Applied Pyrolysis*, 104, 176-184.
- Hewlett, P. (2003). *Lea's chemistry of cement and concrete*. Butterworth-Heinemann, Elsevier: London, UK.
- Hill, R. L., & Folliard, K. J. (2006). The impact of fly ash on air-entrained concrete. *Concrete in Focus*, 5(3), 71-72.
- Hill, R. L., Sarkar, S. L., Rathbone, R. F., & Hower, J. C. (1997). An examination of fly ash carbon and its interactions with air entraining agent. *Cement and Concrete Research*, 27(2), 193-204.
- Hossain, K. M. A. (2003). Blended cement using volcanic ash and pumice. *Cement and Concrete Research*, 33(10), 1601-1605.
- Hvistendahl, M. (2007a). Coal ash is more radioactive than nuclear waste. *Scientific American*, 13, 99-103.
- Hvistendahl, M. (2007b). Coal ash is more radioactive than nuclear waste. *Scientific American*. 13, 104-109.
- Ibrahim, H. A., & Razak, H. A. (2016). Effect of palm oil clinker incorporation on properties of pervious concrete. *Construction and Building Materials*, 115, 70-77.
- Idris, S. S., Rahman, N. A., Ismail, K., Alias, A. B., Rashid, Z. A., & Aris, M. J. (2010). Investigation on thermochemical behaviour of low rank Malaysian coal, oil palm biomass and their blends during pyrolysis via thermogravimetric analysis (TGA). *Bioresource Technology*, 101(12), 4584-4592.
- Ilić, B., Radonjanin, V., Malešev, M., Zdujčić, M., & Mitrović, A. (2016). Effects of mechanical and thermal activation on pozzolanic activity of kaolin containing mica. *Applied Clay Science*, 123, 173-181.
- Jacoby, P. C., & Pelisser, F. (2015). Pozzolanic effect of porcelain polishing residue in Portland cement. *Journal of Cleaner Production*, 100, 84-88.

- Jang, J. G., Ahn, Y .B., Souri, H., & Lee, H. K. (2015). A novel eco-friendly porous concrete fabricated with coal ash and geopolymeric binder: Heavy metal leaching characteristics and compressive strength. *Construction and Building Materials*, 79, 173-181.
- Jaturapitakkul, C., Kiattikomol, K., & Songpiriyakij, S. (1999). A study of strength activity index of ground coarse fly ash with Portland cement. *Science Asia*, 25, 223-229.
- Jaturapitakkul, C., Tangpagasit, J., Songmue, S., & Kiattikomol, K. (2011). Filler effect and pozzolanic reaction of ground palm oil fuel ash. *Construction and Building Materials*, 25(11), 4287-4293.
- Jawed, I., & Skalny, J. (1978). Alkalies in cement: a review: II. Effects of alkalies on hydration and performance of Portland cement. *Cement and Concrete Research*, 8(1), 37-51.
- Jegadeesan, G., Al-Abed, S. R., & Pinto, P. (2008). Influence of trace metal distribution on its leachability from coal fly ash. *Fuel*, 87(10), 1887-1893.
- Jones, M. R., McCarthy, M. J., & Newlands, M. D. (2011). *Fly ash route to low embodied CO<sub>2</sub> and implications for concrete construction*. World of Coal Ash Conference, Denver, Colorado, USA.
- Kajaste, R., & Hurme, M. (2016). Cement industry greenhouse gas emissions–management options and abatement cost. *Journal of Cleaner Production*, 112, 4041-4052.
- Kanadasan, J., & Razzak, H. A. (2015). Utilization of Palm Oil Clinker as Cement Replacement Material. *Materials*, 8(12), 8817-8838.
- Kanadasan, J., Fauzi, A. F. A., Razak, H. A., Selliah, P. S. V., & Yusoff, S. (2015). Feasibility studies of palm oil mill waste aggregates for the construction industry. *Materials*, 8(9), 6508-6530.
- Kanadasan, J., & Razak, H. A. (2014). Mix design for self-compacting palm oil clinker concrete based on particle packing. *Materials & Design*, 56, 9-19.
- Kanadasan, J., & Razak, H. A. (2015). Engineering and sustainability performance of self-compacting palm oil mill incinerated waste concrete. *Journal of Cleaner Production*, 89, 78-86.
- Karim, M. R., Zain, M. F. M., Jamil, M., & Lai, F. C. (2013). Fabrication of a non-cement binder using slag, palm oil fuel ash and rice husk ash with sodium hydroxide. *Construction and Building Materials*, 49, 894-902.
- Karim, M. R., Zain, M. F. M., Jamil, M., Lai, F.C., & Islam, M. N. (2012). Strength of mortar and Concrete as influenced by rice husk ash: a review. *World Applied Sciences Journal*, 19(10), 1501-1513.
- Khalil, N. M., Hassan, E. M., Shakhdofa, M. M. E., & Farahat, M. (2014). Beneficiation of the huge waste quantities of barley and rice husks as well as coal fly ashes as additives for Portland cement. *Journal of Industrial and Engineering Chemistry*, 20(5), 2998-3008.

- Khandaker, M. U., Jojo, P. J., Kassim, H. A., & Amin, Y. M. (2012). Radiometric analysis of construction materials using HPGe gamma-ray spectrometry. *Radiation Protection Dosimetry*, 152(1-3), 33-7.
- Khankhaje, E., Hussin, M. W., Mirza, J., Rafieizonooz, M., Salim, M. R., Siong, H. C., & Warid, M. N. M. (2016). On blended cement and geopolymer concretes containing palm oil fuel ash. *Materials & Design*, 89, 385-398.
- Kılıç, A., & Sertabipoğlu, Z. (2015). Effect of heat treatment on pozzolanic activity of volcanic pumice used as cementitious material. *Cement and Concrete Composites*, 57, 128-132.
- Kobeissi, M. A., El-Samad, O., & Rachidi, I. (2013). Health assessment of natural radioactivity and radon exhalation rate in granites used as building materials in Lebanon. *Radiation Protection Dosimetry*, 153(3), 342-351.
- Kocak, Y., & Nas, S. (2014). The effect of using fly ash on the strength and hydration characteristics of blended cements. *Construction and Building Materials*, 73, 25-32.
- Kourounis, S., Tsivilis, S., Tsakiridis, P. E., Papadimitriou, G. D., & Tsibouki, Z. (2007). Properties and hydration of blended cements with steelmaking slag. *Cement and Concrete Research*, 37(6), 815-822.
- Kovler, K. (2011). Legislative aspects of radiation hazards from both gamma emitters and radon exhalation of concrete containing coal fly ash. *Construction and Building Materials*, 25(8), 3404-3409.
- Kovler, K. (2012). Does the utilization of coal fly ash in concrete construction present a radiation hazard? *Construction and Building Materials*, 29, 158-166.
- Kroehong, W. S., T., & Jaturapitakkul, C. (2011). Effect of palm oil fuel ash fineness on packing effect and pozzolanic reaction of blended cement paste. *Procedia Engineering*, 14, 361-369.
- Kumari, R., Kant, K., & Garg, M. (2015). The effect of grain size on radon exhalation rate in natural-dust and stone-dust samples. *Physics Procedia*, 80, 128-130.
- Lahijani, P., Zainal, Z. A., & Mohamed, A. Rn. (2012). Catalytic effect of iron species on CO<sub>2</sub> gasification reactivity of oil palm shell char. *Thermochimica Acta*, 546(0), 24-31.
- Lea, F. M. (1970). *The chemistry of cement and concrete*. Edward Arnold Publishers Limited: London, UK.
- Lee, S. H., Kawakami, A., Sakai, E., & Daimon, M. (2003). The fluidity of cement pastes with fly ashes containing a lot of unburned carbon. *Journal of the Korean Ceramic Society*, 40(3), 219-224.
- Lee, S., Seo, M. D., Kim, Y. J., Park, H. H., Kim, T. N., Hwang, Y., & Cho, S. B. (2010). Unburned carbon removal effect on compressive strength development in a honeycomb briquette ash-based geopolymer. *International Journal of Mineral Processing*, 97(1), 20-25.

- Leong, H. Y., Ong, D. E. L., Sanjayan, J. G., & Nazari, A. (2016). Suitability of Sarawak and Gladstone fly ash to produce geopolymers: A physical, chemical, mechanical, mineralogical and microstructural analysis. *Ceramics International*, 42(8), 9613-9620.
- Li, X., Gan, C., & Hu, B. (2011). Accessibility to microcredit by Chinese rural households. *Journal of Asian Economics*, 22(3), 235-246.
- Li, X., Lv, Y. M. B., Chen, Q., Yin, X., & Jian, S. (2012). Utilization of municipal solid waste incineration bottom ash in blended cement. *Journal of Cleaner Production*, 32, 96-100.
- Li, Y., Liu, C., Luan, Z., Peng, X., Zhu, C., Chen, Z., & Jia, Z. (2006). Phosphate removal from aqueous solutions using raw and activated red mud and fly ash. *Journal of Hazardous Materials*, 137(1), 374-383.
- Lim, N. H. A. S., Ismail, M. A., Lee, H. S., Hussin, M. W., Sam, A. R. M., & Samadi, M. (2015). The effects of high volume nano palm oil fuel ash on microstructure properties and hydration temperature of mortar. *Construction and Building Materials*, 93, 29-34.
- Linak, W. P., Miller, C. A., Seames, W. S., Wendt, J. O. L., Ishinomori, T., Endo, Y., & Miyamae, S. (2002). On trimodal particle size distributions in fly ash from pulverized-coal combustion. *Proceedings of the Combustion Institute*, 29(1), 441-447.
- Lincoln, J. D., Ogunseitan, O. A., Shapiro, A. A., & Saphores, J. M. (2007). Leaching assessments of hazardous materials in cellular telephones. *Environmental Science & Technology*, 41(7), 2572-2578.
- Lu, X., Li, L. Y., Wang, F., Wang, L., & Zhang, X. (2012). Radiological hazards of coal and ash samples collected from Xi'an coal-fired power plants of China. *Environmental Earth Sciences*, 66(7), 1925-1932.
- Ludwig, H., & Zhang, W. (2015). Research review of cement clinker chemistry. *Cement and Concrete Research*, 78, 24-37.
- Malaysia, Agensi Inovasi (MAI). (2011a). National Biomass Strategy 2020: New wealth creation for Malaysia's palm oil industry: Kuala Lumpur, Malaysia.
- Malaysia, Agensi Inovasi (MAI). (2011b). National Biomass Strategy 2020: New wealth creation for Malaysia's palm oil industry: Malaysia, Kuala Lumpur.
- Mirzahosseini, M., & Riding, K. A. (2014). Effect of curing temperature and glass type on the pozzolanic reactivity of glass powder. *Cement and Concrete Research*, 58, 103-111.
- Mo, L., Liu, M., Al-Tabbaa, A., Deng, M., & Lau, W. Y. (2015). Deformation and mechanical properties of quaternary blended cements containing ground granulated blast furnace slag, fly ash and magnesia. *Cement and Concrete Research*, 71, 7-13.

- Moh, Y. C., & Manaf, L. A. (2014). Overview of household solid waste recycling policy status and challenges in Malaysia. *Resources, Conservation and Recycling*, 82, 50-61.
- Mohammadi, A., & Barikani, M. (2014). Synthesis and characterization of superparamagnetic Fe<sub>3</sub>O<sub>4</sub> nanoparticles coated with thiodiglycol. *Materials Characterization*, 90, 88-93.
- Mohammed, H, Sadeek, S., Mahmoud, A. R., & Zaky, D. (2016). Comparison of AAS, EDXRF, ICP-MS and INAA performance for determination of selected heavy metals in HFO ashes. *Microchemical Journal*, 128, 1-6.
- Moraes, J. C. B, Akasaki, J. L., Melges, J. L. P., Monzó, J., Borrachero, M. V., Soriano, L. & Tashima, M. M. (2015). Assessment of sugar cane straw ash (SCSA) as pozzolanic material in blended Portland cement: Microstructural characterization of pastes and mechanical strength of mortars. *Construction and Building Materials*, 94, 670-677.
- Muhammad, B. G., Jaafar, M. S., Rahman, A. A., & Ingawa, F. A. (2012). Determination of radioactive elements and heavy metals in sediments and soil from domestic water sources in northern peninsular Malaysia. *Environmental Monitoring and Assessment*, 184(8), 5043-5049.
- Murad, W., & Siwar, C. (2007). Waste management and recycling practices of the urban poor: a case study in Kuala Lumpur city, Malaysia. *Waste Management & Research*, 25(1), 3-13.
- Nabinejad, O., Sujan, D., Rahman, M. E., & Davies, I. J. (2015). Effect of oil palm shell powder on the mechanical performance and thermal stability of polyester composites. *Materials & Design*, 65, 823-830.
- Nagi, M. (2007). Evaluating air-entraining admixtures for highway concrete. (Vol. 578): Transportation Research Board: Washington D.C. USA.
- Ninduangdee, P., & Kuprianov, V. I. (2013). Study on burning oil palm kernel shell in a conical fluidized-bed combustor using alumina as the bed material. *Journal of the Taiwan Institute of Chemical Engineers*, 44(6), 1045-1053.
- Noorvand, H., Ali, A. A. A., Demirboga, R., Noorvand, H., & Farzadnia, N. (2013). Physical and chemical characteristics of unground palm oil fuel ash cement mortars with nanosilica. *Construction and Building Materials*, 48, 1104-1113.
- Omar, M. (2002). *Natural radioactivity of building materials used in Malaysia*, Proceeding presentation, Radiation Protection and Dosimetry (S61), 554, 347-350.
- Omran, A., Mahmood, A., Aziz, H. Abdul, & Robinson, G. M. (2009). Investigating households attitude toward recycling of solid waste in Malaysia: a case study. *International Journal of Environmental Research*, 3(2), 275-288.
- Öner, M., Erdoğan, K., & Günlü, A. (2003). Effect of components fineness on strength of blast furnace slag cement. *Cement and Concrete Research*, 33(4), 463-469.



- Pan, Y., Wu, Z., Zhou, J., Zhao, J., Ruan, X., Liu, J., & Qian, G. (2013). Chemical characteristics and risk assessment of typical municipal solid waste incineration (MSWI) fly ash in China. *Journal of Hazardous Materials*, *261*, 269-276.
- Parker, T. W. (1969). A classification of kaolinites by infrared spectroscopy. *Clay Minerals*, *8*(2), 135-141.
- Patil, A. G., & Anandhan, S. (2015). Influence of planetary ball milling parameters on the mechano-chemical activation of fly ash. *Powder Technology*, *281*, 151-158.
- Pavlík, Z., Fořt, J., Záleská, M., Pavlíková, M., Trník, A., Medved, I., & Černý, R. (2016). Energy-efficient thermal treatment of sewage sludge for its application in blended cements. *Journal of Cleaner Production*, *112*, 409-419.
- Peppas, T. K., Karfopoulos, K. L., Karangelos, D. J., Rouni, P. K., Anagnostakis, M. J., & Simopoulos, S. E. (2010). Radiological and instrumental neutron activation analysis determined characteristics of size-fractionated fly ash. *Journal of Hazardous Materials*, *181*(1), 255-262.
- Pereira, A., Akasaki, J. L., Melges, J. L. P., Tashima, M. M., Soriano, L., Borrachero, M. V., & Payá, J. (2015). Mechanical and durability properties of alkali-activated mortar based on sugarcane bagasse ash and blast furnace slag. *Ceramics International*, *41*(10), 13012-13024.
- Periathamby, A., Hamid, F. S., & Khidzir, K. (2009). Evolution of solid waste management in Malaysia: impacts and implications of the solid waste bill, 2007. *Journal of Material Cycles and Waste Management*, *11*(2), 96-103.
- Permana, A. S., Towolioe, S. A., N. A., & Ho, C. S. (2015). Sustainable solid waste management practices and perceived cleanliness in a low income city. *Habitat International*, *49*, 197-205.
- Pontes, F. V. M., Bruna, A. D. O., de Souza, E. M. F, Ferreira, F. N., da Silva, L. I. D., Carneiro, M. C, Vaitsman, D. S. (2010). Determination of metals in coal fly ashes using ultrasound-assisted digestion followed by inductively coupled plasma optical emission spectrometry. *Analytica Chimica Acta*, *659*(1), 55-59.
- Porstendörfer, J. (1996). Radon: measurements related to dose. *Environment International*, *22*, 563-583.
- Pöykiö, R., Mäkelä, M., Watkins, G., Nurmesniemi, H., & Olli, D. (2016). Heavy metals leaching in bottom ash and fly ash fractions from industrial-scale BFB-boiler for environmental risks assessment. *Transactions of Nonferrous Metals Society of China*, *26*(1), 256-264.
- Protection, International Commission on Radiological. (1991). *ICRP Publication 60: 1990 Recommendations of the International Commission on Radiological Protection*: Elsevier Health Sciences: USA.
- Radiation, United Nations Scientific Committee on the Effects of Atomic. (2000). Sources and effects of ionizing radiation. UNSCEAR 2000 report to the General Assembly, with scientific annexes. Volume II: Effects. United Nations Publications: USA..

- Radiation, United Nations. Scientific Committee on the Effects of Atomic. (2008). *Effects of ionizing radiation: report to the General Assembly, with scientific annexes* (Vol. 1). United Nations Publications: USA.
- Rafidah, B. R., & Chan, C. M. (2009). *Reusing Soft Soils with Cement-Palm Oil Clinker (POC) Stabilisation*. International Conference on Engineering and Education in the 21st Century: Malaysia.
- Rahman, S. U., Rafique, M., & Jabbar, A. (2013). Radiological hazards due to naturally occurring radionuclides in the selected building materials used for the construction of dwellings in four districts of the Punjab Province, Pakistan. *Radiation Protection Dosimetry*, 153(3), 352-360.
- Rai, A., Prabakar, J., Raju, C.B., & Morchalle, R. K. (2002). Metallurgical slag as a component in blended cement. *Construction and Building Materials*, 16(8), 489-494.
- Ramasamy, V., Anandalakshmi, K., & Pormusamy, V. (2003). Rapid determination of quartz and structural characterisation of feldspars in rocks using FTIR. *Indian Journal of Physics and Proceedings of The Indian Association for The Cultivation of Science-Part A*, 77(4), 347-352.
- Ramasamy, V., Suresh, G., Meenakshisundaram, V., & Ponnusamy, V. (2011). Horizontal and vertical characterization of radionuclides and minerals in river sediments. *Applied Radiation and Isotopes*, 69(1), 184-195.
- Ramli, A. T., Hussein, A. Wahab M. A., & Wood, A. K. (2005). Environmental  $^{238}\text{U}$  and  $^{232}\text{Th}$  concentration measurements in an area of high level natural background radiation at Palong, Johor, Malaysia. *Journal of Environmental Radioactivity*, 80(3), 287-304.
- Ramli, A.T., Apriantoro, N. H., Wagiran, H., Wood, A. K., & Kuan, L. S. (2009). Health risk implications of high background radiation dose rate in Kampung Sungai Durian, Kinta District, Perak, Malaysia. *Global Journal of Health Science*, 1(2), 140-146.
- Ranjbar, N., Behnia, A., Alsubari, B., Birgani, P. M., & Jumaat, M. Z. (2016). Durability and mechanical properties of self-compacting concrete incorporating palm oil fuel ash. *Journal of Cleaner Production*, 112, 723-730.
- Righi, S., & Bruzzi, L. (2006). Natural radioactivity and radon exhalation in building materials used in Italian dwellings. *Journal of Environmental Radioactivity*, 88(2), 158-170.
- Rukzon, S., & Chindaprasirt, P. (2009). Use of disposed waste ash from landfills to replace Portland cement. *Waste Management & Research*, 27(6), 3456-3467.
- Saeed, M. O., Hassan, M. N., & Mujeebu, M. A. (2009). Assessment of municipal solid waste generation and recyclable materials potential in Kuala Lumpur, Malaysia. *Waste Management*, 29(7), 2209-2213.
- Safiuddin, M., Salam, M. A., & Jumaat, M. Z. (2011). Utilization of palm oil fuel ash in concrete: a review. *Journal of Civil Engineering and Management*, 17(2), 234-247.

- Saikia, B. J., Parthasarathy, G. & Sarmah, N. C. (2008). Fourier transform infrared spectroscopic estimation of crystallinity in SiO<sub>2</sub> based rocks. *Bulletin of Materials Science*, 31(5), 775-779.
- Sajedi, F., & Razak, H. A. (2010). The effect of chemical activators on early strength of ordinary Portland cement-slag mortars. *Construction and Building Materials*, 24(10), 1944-1951.
- Saleh, M. A., Ramli, A. T., Alajerami, Y., & Aliyu, A. S. (2013). Assessment of natural radiation levels and associated dose rates from surface soils in Pontian District, Johor, Malaysia. *Journal of Ovonic Research*, 9(1), 17-27.
- Salih, M. A., Farzadnia, N., Ali, A. A. A., & Demirboga, R. (2015). Effect of different curing temperatures on alkali activated palm oil fuel ash paste. *Construction and Building Materials*, 94, 116-125.
- Sanjuán, M. Á., Argiz, C., Gálvez, J. C., & Moragues, A. (2015). Effect of silica fume fineness on the improvement of Portland cement strength performance. *Construction and Building Materials*, 96, 55-64.
- Seddighi, M., Shirini, F., & Mamaghani, M. (2015). Brønsted acidic ionic liquid supported on rice husk ash (RHA-[pmim] HSO<sub>4</sub>): A highly efficient and reusable catalyst for the synthesis of 1-(benzothiazolylamino) phenylmethyl-2-naphthols. *Comptes Rendus Chimie*, 18(5), 573-580.
- Segui, P., Aubert, J. E., Husson, B., & Measson, M. (2012). Characterization of wastepaper sludge ash for its valorization as a component of hydraulic binders. *Applied Clay Science*, 57, 79-85.
- Sen, S., Patil, S., & Argyropoulos, D. S. (2015a). Thermal properties of lignin in copolymers, blends, and composites: a review. *Green Chemistry*, 17(11), 4862-4887.
- Sen, S., Patil, S., & Argyropoulos, D. S. (2015b). Thermal properties of lignin in copolymers, blends, and composites: a review. *Green Chemistry*. 00(1-3), 1-29.
- Serjun, V. Z., Mladenovič, A., Mirtič, B., Meden, A., Ščančar, J., & Milačič, R. (2015). Recycling of ladle slag in cement composites: Environmental impacts. *Waste Management*, 43, 376-385.
- Shaheen, S. M., & Rinklebe, J. (2015). Impact of emerging and low cost alternative amendments on the (im) mobilization and phytoavailability of Cd and Pb in a contaminated floodplain soil. *Ecological Engineering*, 74, 319-326.
- Shi, C. (2004). Steel slag-its production, processing, characteristics, and cementitious properties. *Journal of Materials in Civil Engineering*, 16(3), 230-236.
- Shi, H., & Kan, L. (2009). Leaching behavior of heavy metals from municipal solid wastes incineration (MSWI) fly ash used in concrete. *Journal of Hazardous Materials*, 164(2), 750-754.
- Shi, X., Fay, L., Peterson, M. M., Berry, M., & Mooney, M. (2011). A FESEM/EDX investigation into how continuous deicer exposure affects the chemistry of Portland cement concrete. *Construction and Building Materials*, 25(2), 957-966.

- Shi, Y., Chen, H., Wang, J., & Feng, Q. (2015). Preliminary investigation on the pozzolanic activity of superfine steel slag. *Construction and Building Materials*, 82, 227-234.
- Shuit, S. H., Tan, K. T., Lee, K. T., & Kamaruddin, A. (2009). Oil palm biomass as a sustainable energy source: A Malaysian case study. *Energy*, 34(9), 1225-1235.
- Siddique, R., & Bennacer, R. (2012). Use of iron and steel industry by-product (GGBS) in cement paste and mortar. *Resources, Conservation and Recycling*, 69, 29-34.
- Siew, H. S., Kok, T. T., & Keat, T. L. (2008). Oil Palm Biomass As A Sustainable Energy Source: A Malaysian Case Study, *Energy*, 34(9), 1225-1235.
- Singh, J., & Kalamdhad, A. S. (2013). Assessment of bioavailability and leachability of heavy metals during rotary drum composting of green waste (water hyacinth). *Ecological Engineering*, 52, 59-69.
- Singh, J., & Lee, B. (2015). Reduction of environmental availability and ecological risk of heavy metals in automobile shredder residues. *Ecological Engineering*, 81, 76-81.
- Singh, N. B., Singh, V. D., & Rai, S. (2000). Hydration of bagasse ash-blended portland cement. *Cement and Concrete Research*, 30(9), 1485-1488.
- Smith, R. D., Campbell, J. A., & Nielson, K. K. (1979). Characterization and formation of submicron particles in coal-fired plants. *Atmospheric Environment*, 13(5), 607-617.
- Snellings, R., Salze, A., & Scrivener, K. L. (2014). Use of X-ray diffraction to quantify amorphous supplementary cementitious materials in anhydrous and hydrated blended cements. *Cement and Concrete Research*, 64, 89-98.
- Snels, M., Stefani, S., Grassi, D., Piccioni, G., & Adriani, A. (2014). Carbon dioxide opacity of the Venus' atmosphere. *Planetary and Space Science*, 103, 347-354.
- Soares, L. W. O., Braga, R. M., Freitas, J. C. O., Ventura, R. A., Pereira, D. S. S., & Melo, D. M. (2015). The effect of rice husk ash as pozzolan in addition to cement Portland class G for oil well cementing. *Journal of Petroleum Science and Engineering*, 131, 80-85.
- Solak, S., Turhan, Ş., Uğur, F. A., Gören, E., Gezer, F., Yeğingil, Z., & Yeğingil, İ. (2015). Evaluation of potential exposure risks of natural radioactivity levels emitted from building materials used in Adana, Turkey. *Indoor and Built Environment*, 23(4), 594-602.
- Souri, A., Golestani-Fard, F., Naghizadeh, R., & Veisheh, S. (2015). An investigation on pozzolanic activity of Iranian kaolins obtained by thermal treatment. *Applied Clay Science*, 103, 34-39.
- Sow, M., Hot, J., Tribout, C., & Cyr, M. (2015). Characterization of Spreader Stoker Coal Fly Ashes (SSCFA) for their use in cement-based applications. *Fuel*, 162, 224-233.

- Standard, ASTM. (2000). *C 151: Autoclave Expansion of Portland Cement*. Annual Book of ASTM standards: USA.
- Standard, ASTM. (2004). *C187: Standard test methods for normal consistency of hydraulic cement*. Annual Book of ASTM Standards: USA.
- Standard, ASTM. (2008). C191: Standard test methods for setting time of hydraulic cement by Vicat needle. Annual Book of ASTM Standards: USA.
- Standard, ASTM. (2009). *C118: Standard Test Method for Density of Hydraulic Cement*. Annual Book of ASTM Standards: USA.
- Standard, ASTM. (2011a). C204: Standard Test Methods for Fineness of Hydraulic Cement by Air-Permeability Apparatus. Annual Book of ASTM Standards; USA.
- Standard, ASTM. (2011b). C-209: Standard Test Methods for Fineness of Hydraulic Cement by Air-Permeability Apparatus. Annual Book of ASTM Standards: USA.
- Standard, ASTM (2013). *C114: Standard Test Methods for Chemical Analysis of Hydraulic Cement*. Annual Book of ASTM Standards: USA.
- Stroeven, Piet, & Stroeven, Martijn. (1999). Assessment of packing characteristics by computer simulation. *Cement and Concrete Research*, 29(8), 1201-1206.
- Sun, Y., Xie, Z., Li, J., Xu, J., Chen, Z., & Naidu, R. (2006). Assessment of toxicity of heavy metal contaminated soils by the toxicity characteristic leaching procedure. *Environmental Geochemistry and Health*, 28(1-2), 73-78.
- Sushil, S., & Batra, V. S. (2006). Analysis of fly ash heavy metal content and disposal in three thermal power plants in India. *Fuel*, 85(17), 2676-2679.
- Tangchirapat, W., Saeting, T., Japitakkul, C., Kiattikomol, K., & Siripanichgorn, A. (2007). Use of waste ash from palm oil industry in concrete. *Waste Management*, 27(1), 81-88.
- Tangpagasit, J., Cheerarot, R., Jaturapitakkul, C., & Kiattikomol, K. (2005). Packing effect and pozzolanic reaction of fly ash in mortar. *Cement and Concrete Research*, 35(6), 1145-1151.
- Tantawy, M. A. (2015). Characterization and pozzolanic properties of calcined alum sludge. *Materials Research Bulletin*, 61, 415-421.
- Thomas, C., Rolls, J., & Tennant, T. (2000). *The GHG indicator: UNEP guidelines for calculating greenhouse gas emissions for businesses and non-commercial organisations*: UNEP: USA.
- Tiwari, M. K., Bajpai, S., Dewangan, U. K., & Tamrakar, R. K. (2015). Suitability of leaching test methods for fly ash and slag: A review. *Journal of Radiation Research and Applied Sciences*, 8(4), 523-537.
- Trevisi, R., Risica, S., D'Alessandro, M., Paradiso, D., & Nuccetelli, C. (2012). Natural radioactivity in building materials in the European Union: a database and an

estimate of radiological significance. *Journal of Environmental Radioactivity*, 105, 11-20.

- Trevisi, R., Nuccetelli, C., & Risica, S. (2013). Screening tools to limit the use of building materials with enhanced/elevated levels of natural radioactivity: analysis and application of index criteria. *Construction and Building Materials*, 49, 448-454.
- Turanli, L., Uzal, B., & Bektas, F. (2004). Effect of material characteristics on the properties of blended cements containing high volumes of natural pozzolans. *Cement and Concrete Research*, 34(12), 2277-2282.
- Uchima, J. S., Restrepo, O. J., & Tobón, J. I. (2015). Pozzolanicity of the material obtained in the simultaneous calcination of biomass and kaolinitic clay. *Construction and Building Materials*, 95, 414-420.
- Vegas, I., Urreta, J., Frías, M., Rodríguez, O., Ferreiro, S., Nebreda, B., & Vigil, R. (2009). *Engineering properties of cement mortars containing thermally activated paper sludge*. Sustainable management of waste and recycled materials in concrete (WASCON 2009): Lyon, Itali.
- Wang, F. H., Zhang, F., Chen, Y., Gao, J., & Zhao, Bin. (2015). A comparative study on the heavy metal solidification/stabilization performance of four chemical solidifying agents in municipal solid waste incineration fly ash. *Journal of Hazardous Materials*, 300, 451-458.
- Wang, Q., Yan, P., & Feng, J. (2011). A discussion on improving hydration activity of steel slag by altering its mineral compositions. *Journal of Hazardous Materials*, 186(2), 1070-1075.
- Wang, Q., Yan, P., & Mi, G. (2012). Effect of blended steel slag–GBFS mineral admixture on hydration and strength of cement. *Construction and Building Materials*, 35, 8-14.
- Wang, ., Shao, Y., Matovic, M. D., & Whalen, J. K. (2014). Recycling of switchgrass combustion ash in cement: Characteristics and pozzolanic activity with chemical accelerators. *Construction and Building Materials*, 73, 472-478.
- Wu, S., Xu, Y., Sun, J., Cao, Z., Zhou, J., Pan, Y., & Qian, G. (2015). Inhibiting evaporation of heavy metal by controlling its chemical speciation in MSWI fly ash. *Fuel*, 158, 764-769.
- Xie, Y., & Zhu, J. (2013). Leaching toxicity and heavy metal bioavailability of medical waste incineration fly ash. *Journal of Material Cycles and Waste Management*, 15(4), 440-448.
- Yılmaz, B., & Ediz, N. (2008). The use of raw and calcined diatomite in cement production. *Cement and Concrete Composites*, 30(3), 202-211.
- Yılmaz, B., Uçar, A., Öteyaka, B., & Uz, V. (2007). Properties of zeolitic tuff (clinoptilolite) blended Portland cement. *Building and Environment*, 42(11), 3808-3815.

- Yılmaz, H. (2015). Characterization and comparison of leaching behaviors of fly ash samples from three different power plants in Turkey. *Fuel Processing Technology*, 137, 240-249.
- Yusoff, S. (2006). Renewable energy from palm oil–innovation on effective utilization of waste. *Journal of Cleaner Production*, 14(1), 87-93.
- Zeyad, A Johari, M., Bunnori, N. M., Ariffin, K. S., & Altwair, N. M. (2013). Characteristics of Treated Palm Oil Fuel Ash and its Effects on Properties of High Strength Concrete. *Advanced Materials Research*, 626, 152-156.
- Zhang, T., Yu, Q., Wei, J., Li, J., & Zhang, P. (2011). Preparation of high performance blended cements and reclamation of iron concentrate from basic oxygen furnace steel slag. *Resources, Conservation and Recycling*, 56(1), 48-55.
- Zhou, Y., Ning, X., Liao, X., Lin, M., Liu, J., & Wang, J. (2013). Characterization and environmental risk assessment of heavy metals found in fly ashes from waste filter bags obtained from a Chinese steel plant. *Ecotoxicology and Environmental Safety*, 95, 130-136.

## LIST OF PUBLICATIONS

1. **Karim M. R.**, Hashim H., & Razak H. A. (2016). Thermal activation effect on palm oil clinker properties and their influence on strength development in cement mortar. *Construction and Building Materials*, 125, 670–678.
2. . **Karim M. R.**, Hashim H., & Razak H. A. (2016), Assessment of pozzolanic activity of palm clinker powder. *Construction and Building Materials*, 127, 335–343.
3. **Karim M. R.**, Hashim H., Razak H. A., & Yusoff, S. (2017). Characterization of palm oil clinker powder for utilization in cement-based applications, *Construction and Building Materials*, 135, 21-29.
4. **Karim M.R.**, Khandaker, M. U., Asaduzzaman, Kh., Razak, H. A., & Yusoff, S. (2017). Radiological risk assessment of building materials ingredients: Palm Oil Clinker and Fuel Ash, *Indoor and Built Environment*. (Accepted)
- 5 **Karim M. R.**, Hashim H., Razak H. A., & Yusoff, S. (2017). Effect of palm oil clinker powder characteristics on setting and hardening properties of cement. *Construction and Building Materials*. (Under review)
6. **Karim M. R.**, Hashim H., Razak H. A., & Yusoff, S. (2017). Heavy metal levels and potential leaching risk assessment of palm oil clinker, *Arabian Journal of Science and Engineering*. (Under review)